A NETWORK-FUNCTION SIMULATOR

A Thesis
Presented to
the Faculty of Graduate Studies
and Research
The University of Manitoba

In Partial Fulfillment
of the Requirements for the Degree
Master of Science
in
Electrical Engineering

---

by
Ernest Bridges
October 1958

PREFACE

The study presented in this thesis on the application of the potential analog to circuit theory was initiated by the Department of Electrical Engineering at the University of Manitoba in 1956. The first use of the analog was in network analysis for the presentation of a physical picture of the logarithmic modulus and phase characteristics of an immittance function. The next step of study led to the application of the analog to network synthesis problems and in order to facilitate this study it was decided to construct an automatic scanning and display system. The unit produced is similar to one developed at Stanford University and described in a research memorandum (SF).

The material is divided into the following five chapters. Chapter 1 presents the fundamental theory of the potential analog. Chapter 2 describes the Network-Function Simulator and gives its construction and performance details. Chapter 3 outlines the calibration and operating procedures. Chapter 4 presents a series of tests which serve to determine the operating characteristics of the analog. Chapter 5 contains a discussion of the results and the conclusions.

The appendix of this thesis contains much important material which could have been included in the main body of the thesis; however, it was felt that to maintain continuity an arrangement of this type would be preferable.

The studies conducted in this thesis were made possible by a research grant (NRC G584-1956) from the National Research Council of Canada. Appreciation for this support is extended to the Council. Thanks are also extended to Siemens Brothers for their kind donation of equipment.

Finally, the author wishes to express his gratitude to Professor R. A. Johnson for his able supervision of this project, his invaluable suggestions and technical assistance, without which the completion of this thesis would have been difficult.

ABSTRACT

This thesis is an investigation into the application of the potential analog to circuit theory. A dry type of electrolytic tank with a carbon-impregnated paper was used. The fundamental theory and the description of a device for automatically scanning the analog is presented. Tests were performed to determine the characteristics of the conducting sheet and the analog.

TABLE OF CONTENTS

LIST OF FIGURES

LIST OF TABLES

CHAPTER 1

FUNDAMENTAL THEORY

1.1 INTRODUCTION

The two dimensional potential field may be represented by the theory of functions of a complex variable and is indeed one of the earliest applications of this theory (CH)#. Network immittance functions are all functions of a complex variable (DA) which suggests their representation by a potential field model. The characteristic behaviour of any immittance function is specified by its pole-zero distribution just as the characteristic of the potential field is determined by its charge distribution. Thus, if the complex planes of the potential field and the immittance function are identified and the charge distributions and pole-zero locations equated, an analog relationship is created.

This analog relationship serves two fundamental purposes with respect to circuit theory : a) it gives a physical picture of the response of networks, and b) it provides a powerful tool in determining the immittance function characteristics for a given type of response. The latter application is the first stage of a network synthesis procedure and is accomplished by manipulating the charge distributions until the desired response characteristic is obtained.

Various conformal transformations may also be applied to the two dimensional potential field in order to expand the required response region.

1.2 THE IMMITTANCE FUNCTION

All immittance functions (let us define them as F(s)) have the form of a quotient of polynomials such as

$$F(s)= \frac{a_o s^n + a_1 s^{n-1} + \ldots\ldots + a_{n-1} s + a_n}{b_o s^m + b_1 s^{m-1} + \ldots\ldots + b_{m-1} s + b_m} \qquad 1.1$$

The letters in parentheses refer to the Bibliography

They are all rational functions of the complex variable $s=\alpha+j\omega$ which is defined as the complex frequency (VA).

Factoring each polynomial yields the following equation:

$$F(s)=\frac{H\,(s-s_1)(s-s_3).....(s-s_n)}{(s-s_2)(s-s_4).....(s-s_m)} = \frac{H\prod(s-s_x)}{\prod(s-s_y)} \qquad 1.2$$

The roots of the numerator are called the zeros of the immittance function, the roots of the denominator the poles and H is a scale factor. Let us now express the immittance as a phasor quantity:

$$F(s)= |F(s)|\ e^{j\ \text{Argument}\ F(s)} \qquad 1.3$$

or
$$F(s)= H\,\frac{\prod |s-s_x|\ e^{j\theta_x}}{\prod |s-s_y|\ e^{j\theta_y}} \qquad 1.4$$

if
$$s-s_i= |s-s_i|\ e^{j\theta_i} \qquad 1.5$$

Consider now the logarithmic transform of this immittance function:

$$\ln F(s)= \ln \left(|F(s)|\ e^{j\ \text{Argument}\ F(s)} \right) = W(s) \text{ say}, \qquad 1.6$$

thus
$$W(s) = \ln |F(s)| + j\ \text{Argument}\ F(s) \qquad 1.7$$

In terms of the poles and zeros, where it is understood that in the algebraic summations the zeros contribute positive valued terms and the poles negative valued terms, we may write:

$$W(s) = \ln H + \Sigma \ln |s-s_i| + j\Sigma\,\theta_i \qquad 1.8$$

In general we have:

$$W(s) = M(s) + j\Theta(s) \qquad 1.9$$

a function of the complex variable s with M(s) giving the logarithm of the immittance magnitude and $\Theta(s)$, the immittance phase.

1.3 THE TWO DIMENSIONAL POTENTIAL FIELD

Let us consider a sheet of homogeneous isotropic conducting paper as a two dimensional plane of the complex variable $z=x+jy$. Unit currents are injected at the points $z_o, z_1, z_2 \ldots\ldots z_n$. The electric field produced in the sheet is given by:

$$\underline{E}(z) = -\nabla \phi(z) \qquad 1.10$$

where it is understood that:

$$\nabla \phi(z) = i \frac{\partial \phi(z)}{\partial x} + j \frac{\partial \phi(z)}{\partial y}$$

The current flow in the sheet is given by:

$$\underline{I}(z) = \sigma \, \underline{E}(z) \qquad 1.11$$

where σ is the surface conductivity of the conducting sheet.

The divergence of the current must be zero everywhere in the sheet except at the points of current injection and if the divergence at these points of discontinuity is represented by a Dirac delta function (ST) we have:

$$\nabla \cdot \underline{I}(z) = K \Sigma \delta (z-z_i) \qquad 1.12$$

Using equation 1.11 we may write:

$$\nabla \cdot \underline{E}(z) = \frac{K}{\sigma} \Sigma \delta (z-z_i) \qquad 1.13$$

and substituting from equation 1.10, there results:

$$-\nabla \cdot \nabla \phi(z) = -\nabla^2 \phi(z) = \frac{K}{\sigma} \Sigma \delta (z-z_i) \qquad 1.14$$

This is Poisson's equation for the two dimensional field having a driving function

$$\rho(z) = \frac{K}{\sigma} \Sigma \delta (z-z_i).$$

The solution of this well known equation (WE) is:

$$\phi(z) = C_1 \Sigma \ln (z-z_i) + C_o \qquad 1.15$$

where C_o is some arbitrary constant. If polar co-ordinates are introduced such that:

$$z-z_i = |z-z_i| \, e^{j \psi i} \qquad 1.16$$

then $$\phi(z) = C_o + C_1 \Sigma \ln |z-z_i| + jC_1 \Sigma \psi_i \qquad 1.17$$

where it is understood that at points of current source negative terms are contributed to the summations and at points of current sink positive terms (or vice versa if it is so defined).

If we identify:

$$V(z) = C_o + C_1 \Sigma \ln |z-z_i| \qquad 1.18$$

and $$\psi(z) = C_1 \Sigma \psi_i \qquad 1.19$$

we may write $$\phi(z) = V(z) + j\,\psi(z) \qquad 1.20$$

a function of the complex variable, z, where V(z) is the potential function and $\psi(z)$ the stream function.

1.4 THE POTENTIAL ANALOG

We have shown that the potential field of a two dimensional conducting sheet is a function of a complex variable, z , and has the form:

$$\phi(z) = C_o + C_1 \Sigma \ln |z-z_i| + j\,C_1 \Sigma \psi_i \qquad 1.17$$

where the z_i are the points of current source and sink.

Also it has been shown that any immittance function as a rational function of a complex variable s has the general logarithmic form:

$$W(s) = \ln H + \Sigma \ln |s-s_i| + j \Sigma \theta_i \qquad 1.8$$

where the s_i are the pole and zero locations.

With the identification of the plane of the potential field with the complex frequency plane, s=z, and the location of the current sinks at the zero positions and current sources at the pole positions, the potential field becomes the analog of the immittance function.

Thus $$\phi(s) = K_o + K_1 W(s) \qquad 1.21$$

where K_o is a reference constant and K_1 a scale factor.

Rewriting equation 1.21 we have:

$$V(s) + j\psi(s) = K_o + K_1 \ln F(s)$$
$$= K_o + K_1 \ln |F(s)| + j\,K_1 \text{ Argument } F(s) \qquad 1.22$$

Identifying real and imaginary parts yields:

$$V(s) = K_o + K_1 \ln |F(s)| \qquad 1.23$$

and $$\psi(s) = K_1 \text{ Argument } F(s) \qquad 1.24$$

Any point s_o on the plane may be used as a reference potential and at this point:

$$V_o = K_o + K_1 \ln |F(s_o)| \qquad 1.25$$

also at any other point, say s_1

$$V_1 = K_o + K_1 \ln |F(s_1)|$$

The potential difference between the reference point and the arbitrarily selected point yields the logarithm of the ratio of the ~~impedance~~ immittance magnitudes at the two points.

Thus $$V_1 - V_o = K_1 \ln \frac{|F(s_1)|}{|F(s_o)|} \qquad 1.26$$

or $$\ln \left| \frac{F(s)}{F(s_o)} \right| = \frac{V}{K_1} \qquad 1.27$$

where V is the potential measured at s with respect to the potential at s_o.

Consider now the stream function

$$\psi(s) = K_1 \text{ Argument } F(s) \qquad 1.24$$

Rewriting $$\text{Argument } F(s) = \frac{\psi(s)}{K_1}$$

The stream function at any point may be determined by a line integration.

Thus $$\psi(s) = \int \frac{d\psi(s)}{ds} ds \qquad 1.28$$

or $$\psi(s) = \int \left[\frac{\partial \psi(s)}{\partial \alpha} d\alpha + \frac{\partial \psi(s)}{\partial \omega} d\omega \right] \qquad 1.29$$

From the Cauchy-Riemann conditions the following relations must hold for any analytic function (DA):

$$\frac{\partial \psi(s)}{\partial \alpha} = -\frac{\partial V(s)}{\partial \omega} \qquad 1.30$$

and $$\frac{\partial \psi(s)}{\partial \omega} = \frac{\partial V(s)}{\partial \alpha} \qquad 1.31$$

Substituting into equation 1.29 we now have:

$$\psi(s) = \int \left[-\frac{\partial V(s)}{\partial \omega} d\alpha + \frac{\partial V(s)}{\partial \alpha} d\omega \right] \qquad 1.32$$

In particular, if the line integration is performed up the real frequency axis and started at the origin, since $d\alpha = 0$, we have the following:

$$\psi(0,\omega) = \int_0^{\omega} \frac{\partial V(0,\omega)}{\partial \alpha} d\omega \qquad 1.33$$

That is $\psi(0) \equiv 0$ for any immittance function. Now substituting equation 1.33 into equation 1.24 gives:

$$\text{Argument } F(\omega) = \frac{1}{K_1} \int_0^{\omega} \frac{\partial V(0,\omega)}{\partial \alpha} d\omega \qquad 1.34$$

which may be written in summation form as:

$$\text{Argument } F(\omega) = \frac{1}{K_1} \sum_0^{\omega} \frac{\Delta V(0,\omega)}{\Delta \alpha} \Delta\omega \qquad 1.35$$

We may also use an alternate symbol to represent immittance phase, that is Argument $F(\omega) = \Theta(\omega)$. The immittance time delay or phase slope is defined as $\frac{d\,\Theta(\omega)}{d\omega}$. Differentiating equation 1.34 yields the immittance time delay as:

$$\frac{d\,\Theta(\omega)}{d\omega} = \frac{1}{K_1} \frac{\partial V(0,\omega)}{\partial \alpha} = \frac{1}{K_1} \frac{\Delta V(0,\omega)}{\Delta \alpha} \qquad 1.37$$

Let us again consider equation 1.32 which may be recognized as:

$$\psi(s) = \int \left[\underline{E}(s) \cdot \underline{n} \right] ds \qquad 1.38$$

where $\underline{n}$ is a unit vector normal to the path of integration. Substituting from equation 1.11 we have:

$$\psi(s) = \frac{1}{\sigma} \int \left[\underline{I}(s) \cdot \underline{n} \right] ds \qquad 1.39$$

That is, the phase is proportional to the total current crossing the path of integration.

1.5 SYMMETRICAL PROPERTIES OF THE ANALOG

The coefficients of the polynomials describing any immittance function must be real, which results in all the roots being real or occurring in complex conjugate pairs (ST). Because of this property the immittance function is symmetrical about the α or attenuation axis.

Thus $$F(s) = F(\alpha,\omega) = F(\alpha,-\omega) \qquad 1.40$$

which implies that $$\frac{\partial F(s)}{\partial \omega}\bigg|_{\omega=0} = 0 \qquad 1.41$$

In the potential analog this corresponds to the fact that the α axis is a current flow line. The implication is that only that half of the plane with the positive frequency axis need be simulated, the other being represented as a reflection product.

Let us now consider a quarter plane which has its real and imaginary axis open-circuited. The poles and zeros of this quarter plane are reflected into the other three quadrants of the plane so as to set up a function having quadrantal symmetry.

That is $$F(s) = F(\alpha,\omega) = F(-\alpha,\omega) = F(\alpha,-\omega) = F(-\alpha,-\omega) \qquad 1.42$$

Now if $F(s)$ is representative of an immittance function then $F(s)F^{*}(s)$ will possess quadrantally symmetrical properties, where $F^{*}(s)$ is the complex conjugate function, and it may be shown (ST,GU) that along the real frequency axis:

$$F(\omega)F^{*}(\omega) = |F(\omega)|^{2} \qquad 1.43$$

that is $$\ln F(\omega)F^{*}(\omega) = 2 \ln |F(\omega)| \qquad 1.44$$

Again consider a quarter plane but in this case having the imaginary axis short-circuited and the real axis open. The poles and zeros of this plane are reflected into the other three quadrants so as to create a function having dissymmetric properties.

That is $$F(\alpha,\omega) = -F(-\alpha,\omega) \qquad 1.45$$

If $F(s)$ is an immittance function then $\frac{F(s)}{F^{*}(s)}$ is a function which is dissymmetric and it may be shown (ST,GU) that along the real frequency axis:

$$\frac{F(\omega)}{F^{*}(\omega)} = e^{j\ 2\ \text{Argument}\ F(\omega)} \qquad 1.46$$

that is $$\ln \frac{F(\omega)}{F^{*}(\omega)} = j\ 2\ \text{Argument}\ F(\omega) \qquad 1.47$$

It is also of interest to note that if the immittance function is an impedance then the interchange of poles for zeros and zeros for poles yields the admittance response (or vice versa).

1.6 CONFORMAL TRANSFORMATIONS

Once the immittance function is shown to be an analytic function of a complex variable the applicability of the potential analog to a conformal transformation is apparent. Many transformations are possible (CH), namely, exponential, logarithmic, orthogonal circle (Smith diagram), the Schwartz-Christoffel transformations etc. The logarithmic transformation was selected as being of particular interest since it has the property of presenting the immittance attenuation in a logarthmic scale versus the frequency, also in a logarithmic scale.

The complex frequency plane s is now identified with a new plane, say $w=u+jv$, by the transformation

$$w = \ln s \qquad 1.47$$

If the polar co-ordinate system is used to define the s plane, namely:

$$s = |s| e^{j\phi} \qquad 1.48$$

then a mapping of significant axes may be performed as follows:

a) for the positive attenuation axis

$$w = \ln (|s| e^{j0}) = \ln |s| + j0$$

b) for the positive frequency axis

$$w = \ln (|s| e^{j \pi/2}) = \ln |s| + j \pi/2$$

c) for the negative attenuation axis

$$w = \ln (|s| e^{j \pi}) = \ln |s| + j \pi$$

This mapping is illustrated in figure 1.1 .

The properties of the quarter plane may be applied as well to this transformed plane when the proper boundaries are left open or short-circuited. This transformed plane does not lend itself to phase measurement techniques utilizing the voltage gradient method since the incremental sampling distance $\Delta\alpha$ changes along the real frequency axis.

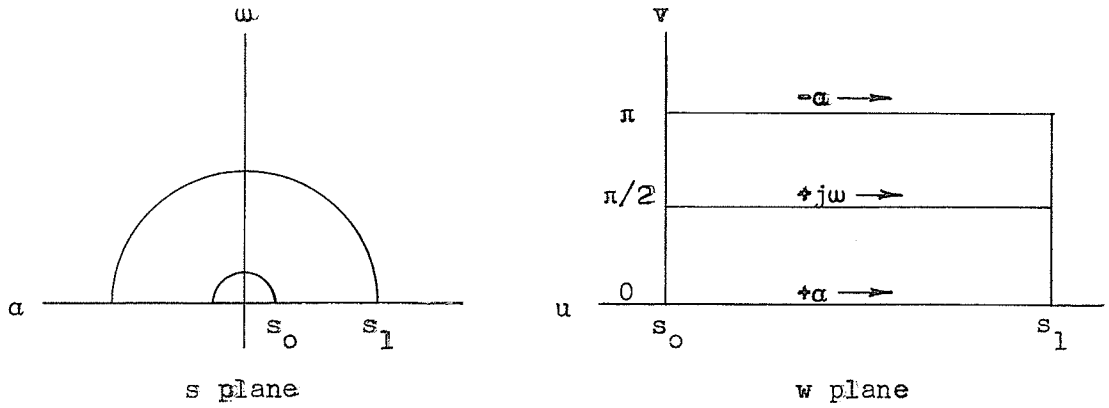

FIGURE 1.1

THE LOGARITHMIC TRANSFORMATION

CHAPTER 2

THE POLE-ZERO NETWORK FUNCTION SIMULATOR

2.1 GENERAL DESCRIPTION

The pole-zero network function sumulator is basically a device for simulating and scanning the complex frequency plane. A dry type of electrolytic tank using a carbon-impregnated paper and excited from several movable probes serves as the potential analog. The automatic or manual scanning is accomplished by a series of mounted probes which feed a motor driven rotary switch.

The equipment layout is illustrated in figure 2.1 and consists of a) a portable rack mounting the electronic units and b) a work table carrying the conducting sheet, probe chassis, transposition frame, movable probes, a distribution unit and a plane reference bias circuit. The portable rack holds, from top to bottom, a monitor oscilloscope, an operational unit consisting of d.c. amplifiers, a constant current pole-zero supply, a set of manual selector switches, a regulated power supply for the d.c. amplifiers and the panel for the motor-driven rotary switch.

Figure 2.2 is a block diagram which illustrates the functional operation of the unit. A set of movable probes supply d.c. current to the conducting sheet and create a two-dimensional potential field. The d.c. supply is a constant current device having six current outputs and six current inputs. Thus, by using a half plane an immittance function having up to 12 poles and 12 zeros may be simulated. Each probe is plugged into the distribution unit which in turn is connected to the pole-zero supply.

A probe chassis consisting of 208 probes is located on the real frequency axis of the analog plane. The potential created by the electric field is sampled by the probes and passed through the transposition frame to either the manual selector switch or the rotary switch. The manual selector switch permits an individual selection of any one probe, the signal of which may be fed directly or through the d.c. amplifier to a metering system. A rotary switch scans the probes in sequence and supplies a

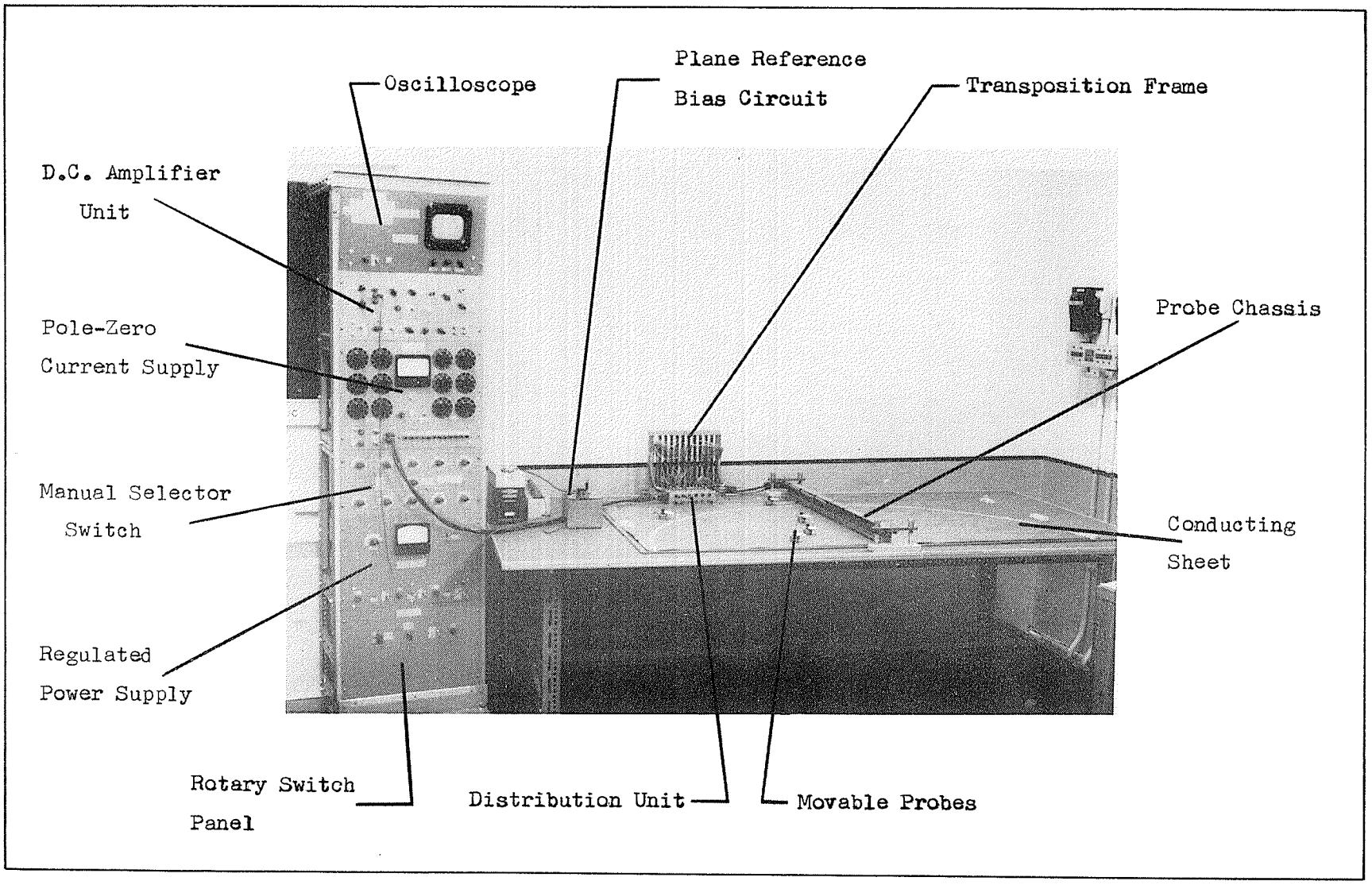

FIGURE 2.1 THE NETWORK-FUNCTION SIMULATOR

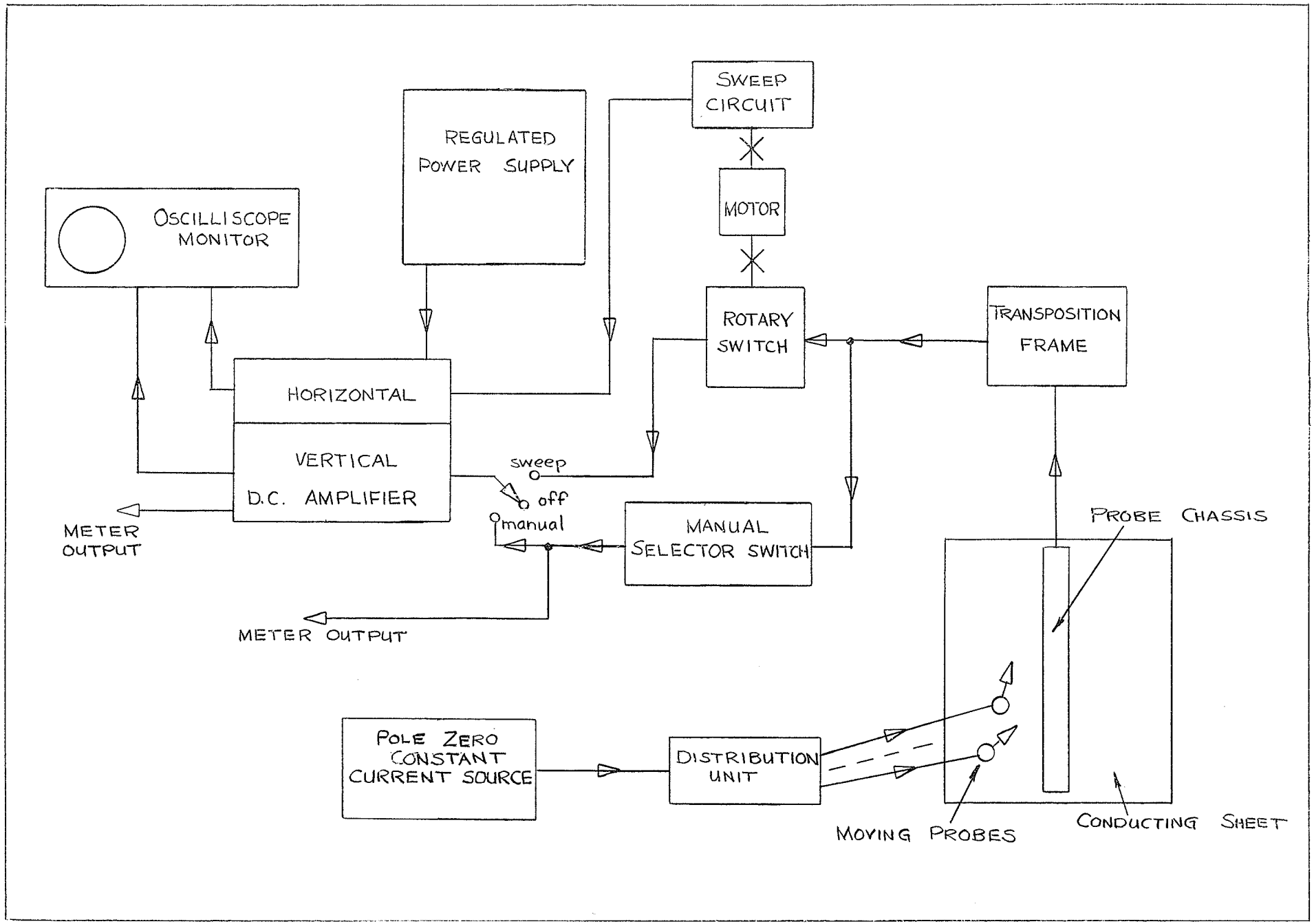

FIGURE 2.2 A BLOCK DIAGRAM OF THE NETWORK-FUNCTION SIMULATOR

synchronized sweep signal to the d.c. amplifier. The probe chassis has two sets of probes, called A and B, spaced 1/4 inch between centers. The rotary switch at any instant has two outputs, one from the A probe and one from the adjacent B probe, which are fed to the d.c. amplifier unit and subsequently to the monitor oscilloscope.

The d.c. amplifier unit may operate on these two signals in a number of ways. The two signals may be taken separately directly to the deflection amplifier; the observed signal being proportional to the logarithm of the modulus of the immittance function. The difference of the signals may be obtained to give a display of the immittance phase slope or time delay. This difference signal may also be integrated with respect to ω (which is proportional to time) and then displayed which yields the immittance phase response.

The conducting plane and the amplifier are connected through a biasing circuit which adjusts the d.c. level of the plane and allows any equipotential on the plane to be made a point of reference potential.

2.2 THE ELECTROLYTIC TANK

The electrolytic tank is a dry type utilizing a conducting paper called Teledeltos type L-48 which is manufactured by the Western Union Telegraph Company. The sheet is a carbon-impregnated paper having a specified resistance of from 1500 to 4000 ohms per square and an anisotropic property of less than 10 percent of a mean value.

It was decided to investigate thoroughly the properties of this conducting paper and to apply compensating measures wherever possible. The conductivity in the direction of rolling was found to be 12 percent greater than the conductivity across the paper. Appendix A.1 gives the test results. This error was corrected for by a transformation of the horizontal and vertical co-ordinates and is outlined in Appendix A.2 . Briefly, the correction involves stretching the axis in the direction of rolling by 6 percent to keep the potential gradient along the sheet the same as that across the sheet for the same current density.

The conductivity in the direction of rolling was found to be fairly constant while across the sheet it varied by an average of 6 percent. Appendix A.3 gives the test data. It was decided that a correction for non-linearity would not be practical since the region to which the correction must be applied is close to the infinity circle and subject to distortion due to that proximity.

It was anticipated that the current density in the conducting sheet at the probe inputs would be high and prompted an investigation to determine the effect of current density on conductivity. For normal current probe inputs up to 5 milliamperes the conductivity increases by not more than 4 percent for any point at least 1/8 inch from the probe center and not more than 1 percent for any point at least 1/4 inch from the probe center. The current density in the sheet as a whole is very low and the effects thus introduced may be neglected. Appendix A.4 gives the test results. The resistivity of the silver paint, used for drawing lines of equipotential (such as the infinity circle), was found to be approximately one ohm per square. This indicates a necessity for painting the equipotential simulating infinity by a strip at least 1/2 inch wide and periodically parallelling sections with copper leads.

2.3 THE PROBE CHASSIS

The probe chassis is a frame assembly mounting two rows of probes spaced 1/4 inch apart with a total of 104 probes in each row spaced 1 cm. between centers. The function of this probe assembly is to make an electrical contact with the conducting sheet at points along the real frequency axis. The frame is clamped to the table and a pressure contact is made with the sheet by means of a set of adjustable clamps. To ensure electrical contact between all probes and the conducting paper a quarter inch thick sponge rubber sheet is laid between the table and the paper. Figure 2.1 illustrates the frame assembly as it appears when mounted on the conducting sheet.

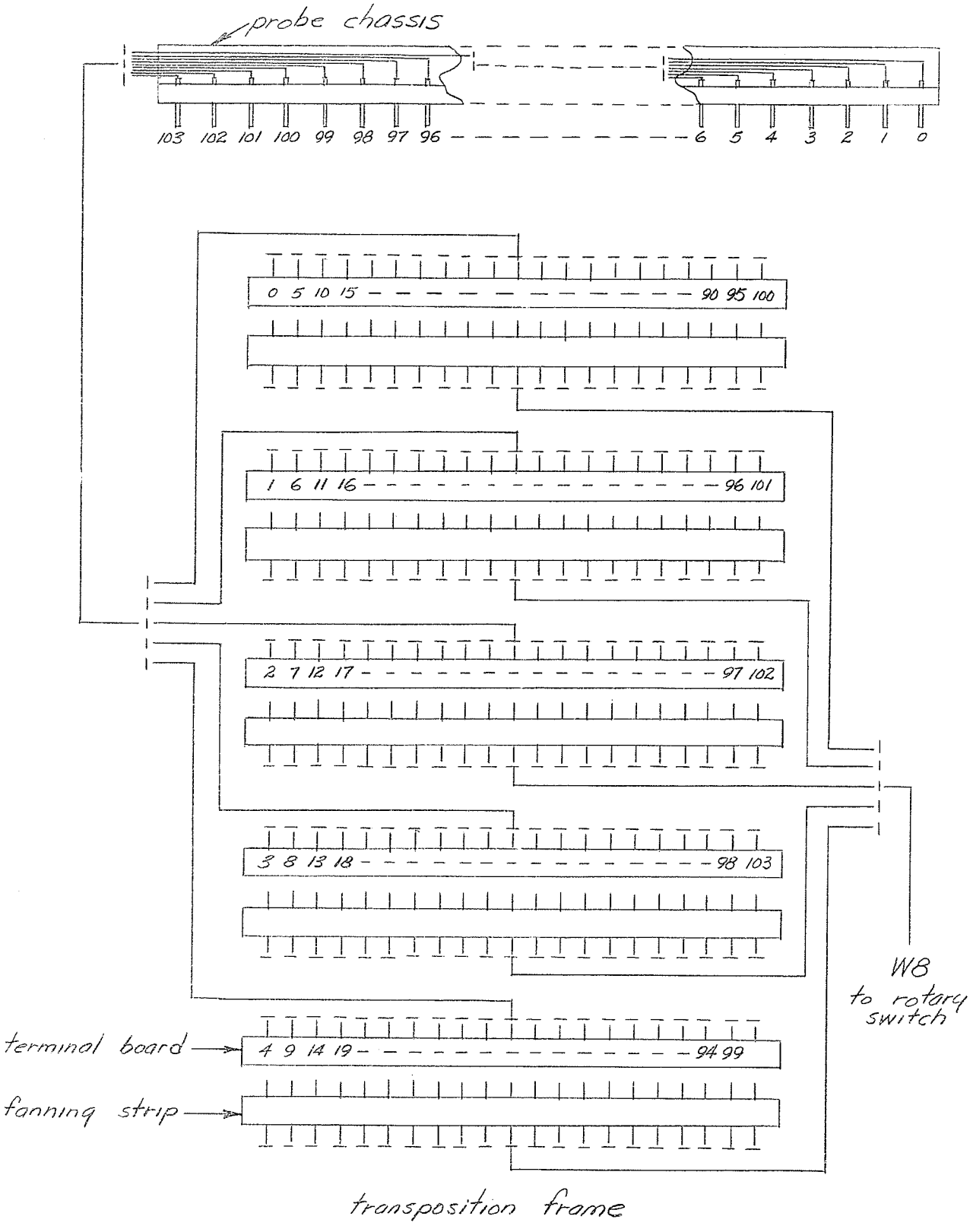

FIGURE 2.3 THE PROBE CHASSIS AND TRANSPOSITION FRAME

2.4 THE TRANSPOSITION FRAME, ROTARY SWITCH AND MANUAL SELECTOR SWITCH

The signal from each probe is fed through a cable first to the motor driven switch and then to a set of wafer switches. Between the probe chassis and the switch assemblies there is a transposition frame holding 10 terminal strips each having 21 contacts. This unit permits the interconnection of the switch contacts to the probes in any desired sequence. Figure 2.3 is a schematic diagram showing the connection of the probe chassis to the transposition frame.

The rotary switch is a modified Siemens Brothers High Speed Motor Uniselector with 16 banks of contacts at 52 contactors per bank. Six banks of contacts are used, two for each probe set and two for the sweep circuit. Figure 2.8 is a photograph of the unit.

The rotary switch is driven by a single phase 110 volt induction motor having a speed of 1800 rpm . A gear train reduces the rotor speed to 360 rpm. or 6 cps . The stator connections are made so that the rotor scans the output of every 5th probe, that is in the first 1/5 of a revolution the rotor sweeps through 21 points and scans the 0, 5, 10.... ... 100th probe outputs while in the next 1/5 of a revolution another 21 points are scanned consisting of probe outputs 1, 6, 11,....101st, etc. This system was devised to obtain a waveform presentation 30 times per second for effective oscilloscope display. Figure 2.4 is a schematic diagram of the rotor circuit.

This probe scanning method necessitated the construction of a horizontal sweep generator which not only supplied 5 sweeps per rotor revolution but shifted the origin by one unit for each consecutive sweep. A method was devised whereby two banks of contacts on the rotary switch were used as the contact points of a fixed potential divider. Precision resistors provide the high resolution required. A six volt battery supplies the potential divider and is switched on and interlocked with the sweep motor input. A schematic diagram of the sweep circuit is found in figure 2.5.

A bank of manually operated switches enables the potential from any one probe to be selected at a set of output jacks or fed to the amplifier.

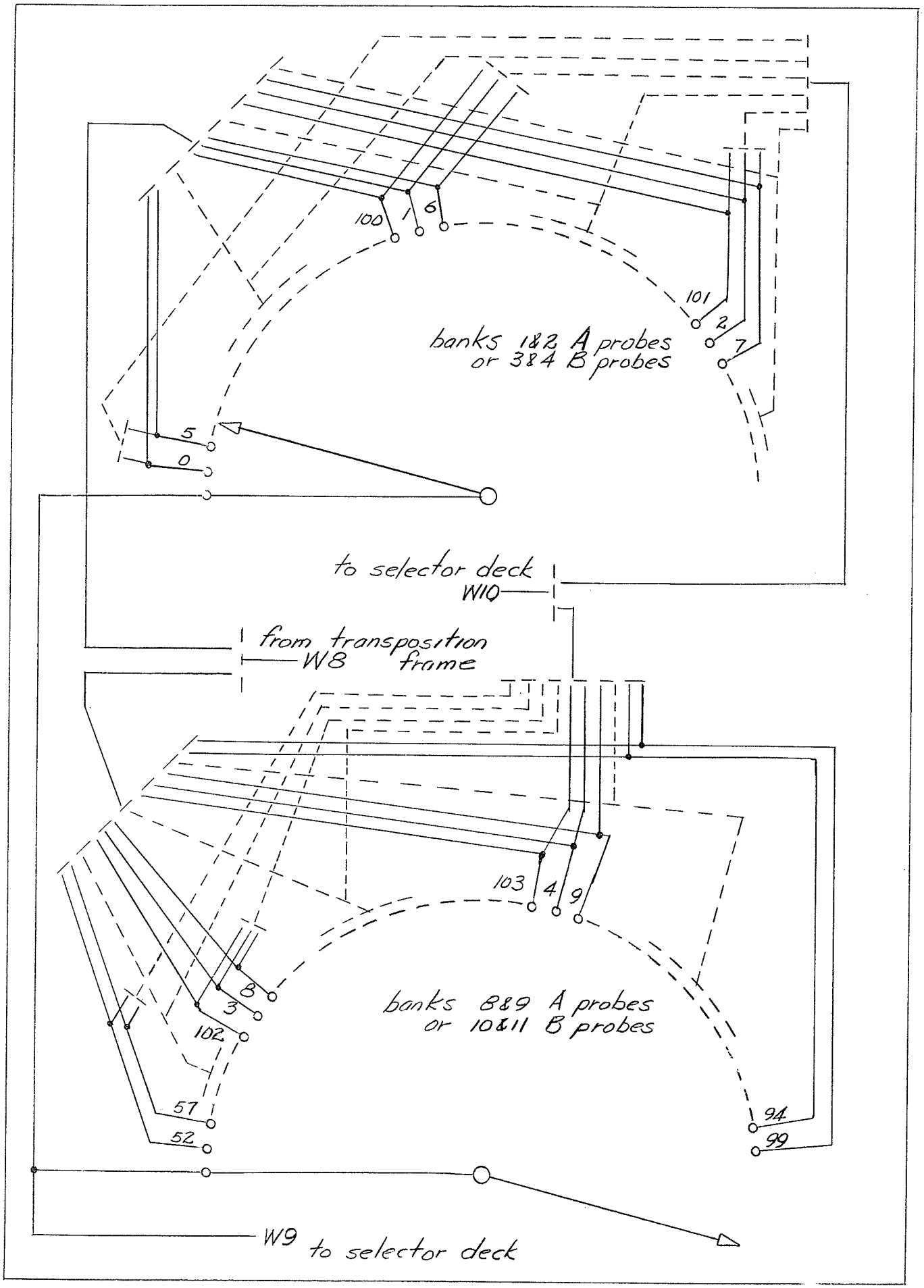

FIGURE 2.4 THE ROTARY SWITCH

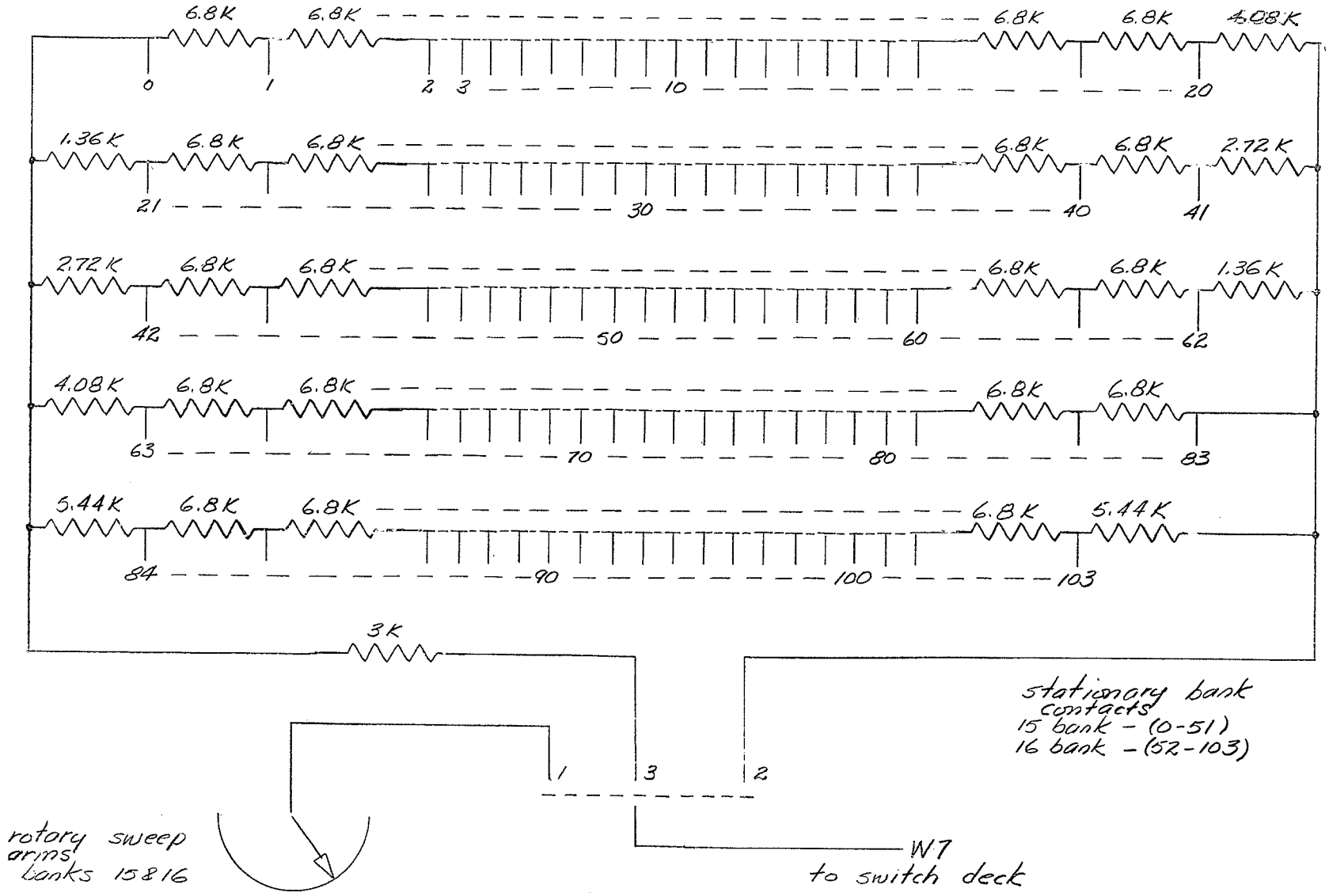

FIGURE 2.5 THE SWEEP CIRCUIT

The unit consists of eleven, ten position, two section wafer switches the electrical interconnection of which is given in the schematic diagram of figure 2.6 . A manual-sweep toggle switch, connected to the d.c. amplifier unit, selects either the rotary switch or manual switch output.

Figure 2.7 is a schematic diagram of the ancillary equipment located on the same deck as the rotary switch. This equipment includes a power input panel, a bank of batteries for the d.c. amplifiers and a terminal strip.

2.5 THE POLE-ZERO SUPPLY

The pole-zero unit was designed to supply six current sources and six current sinks at any value of current up to 8 milliamperes and maintain these currents at a constant value.

The current sources are fed through six regulator units from a +400 volt d.c. supply while the current sinks have six regulator units supplied by a -400 volt d.c. supply. Both power supplies are standard LC filter type units, a schematic diagram of which is shown in figure 2.11 . The regulator unit uses a series connected triode which is biased in such a manner as to have an almost flat bias line. The tube maintains a constant current through the probe. The operation of this unit is unique and a full description is given in appendix B.1 . Figure 2.12 is a schematic diagram of the regulator unit. The current sink supply requires a special isolated bias supply; see the schematic of figure 2.13 .

The regulator units are connected by a cable to a distribution unit which serves as the switching and terminating point for the travelling probes. See figure 2.9 for an illustration of the unit and figure 2.14 for the schematic diagram. Figure 2.9 also illustrates the movable probes; their basic construction being a spring contactor mounted on a circular metal base insulated with sponge rubber.

A milliammeter for measuring the probe current may be inserted in series with any probe by means of a twelve position push-button switch. The probe current may be adjusted to any value between 1.5 and 8.0 milli-

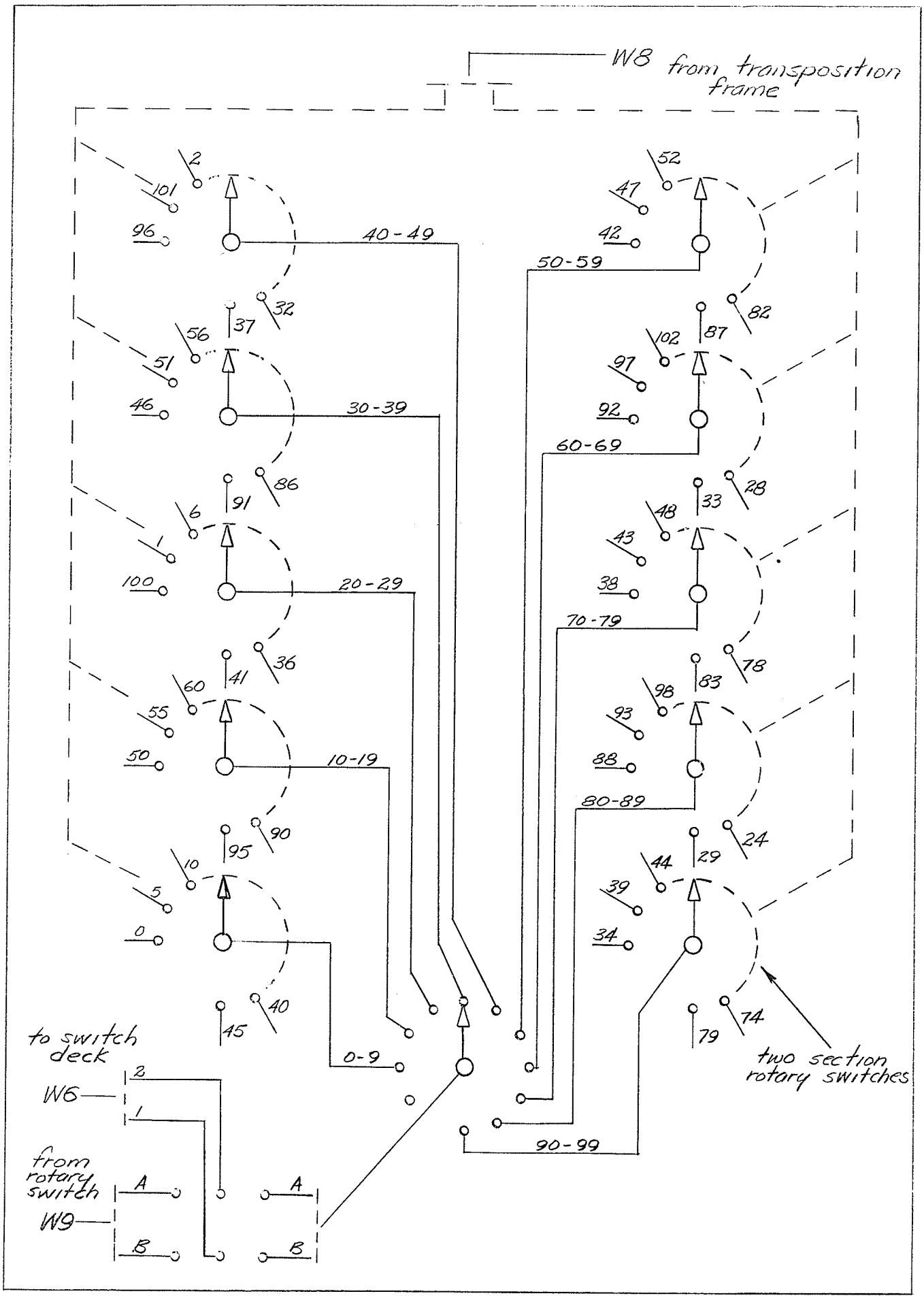

FIGURE 2.6 THE MANUAL SELECTOR SWITCHES

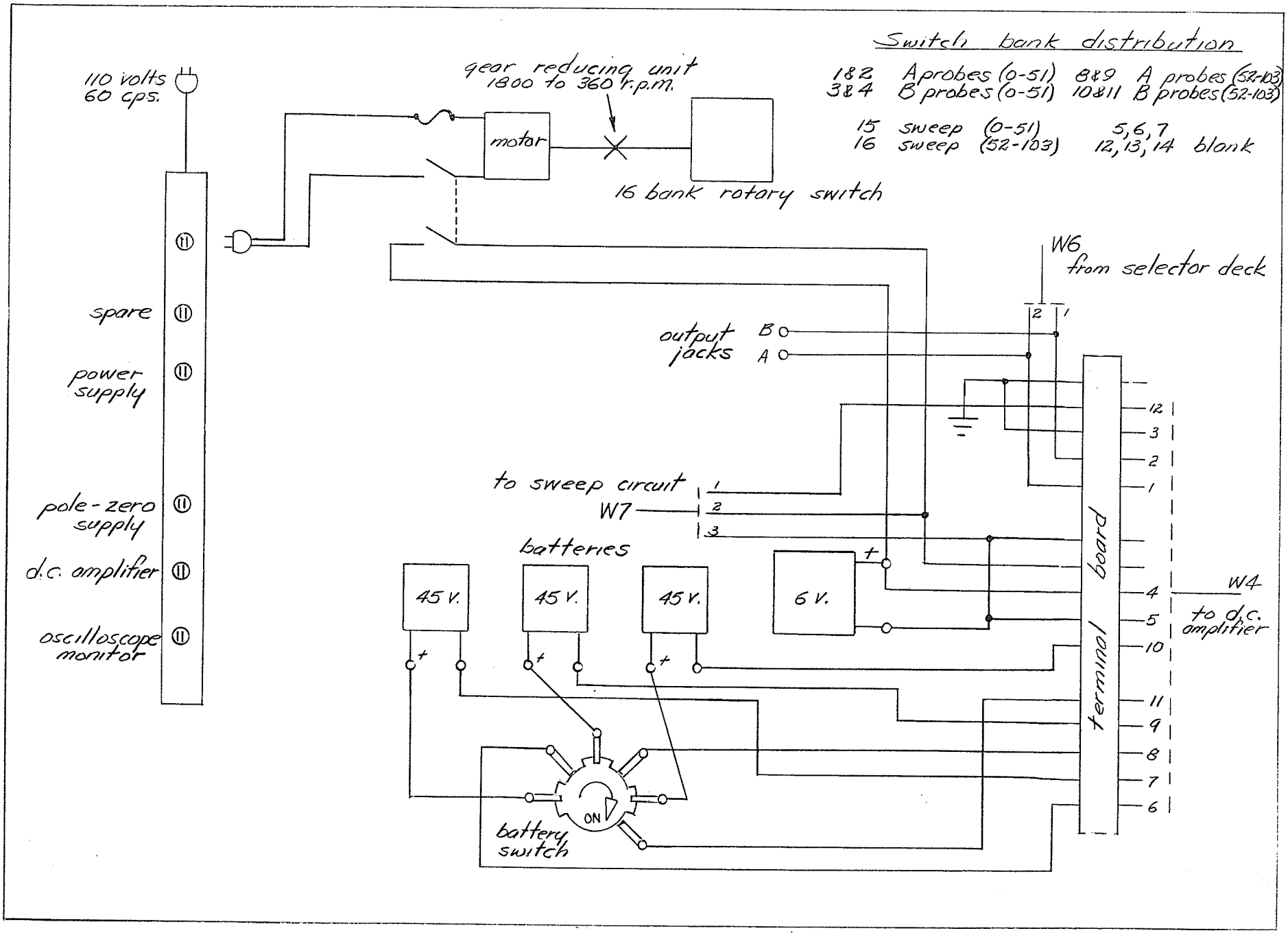

FIGURE 2.7 THE ROTARY SWITCH-DECK

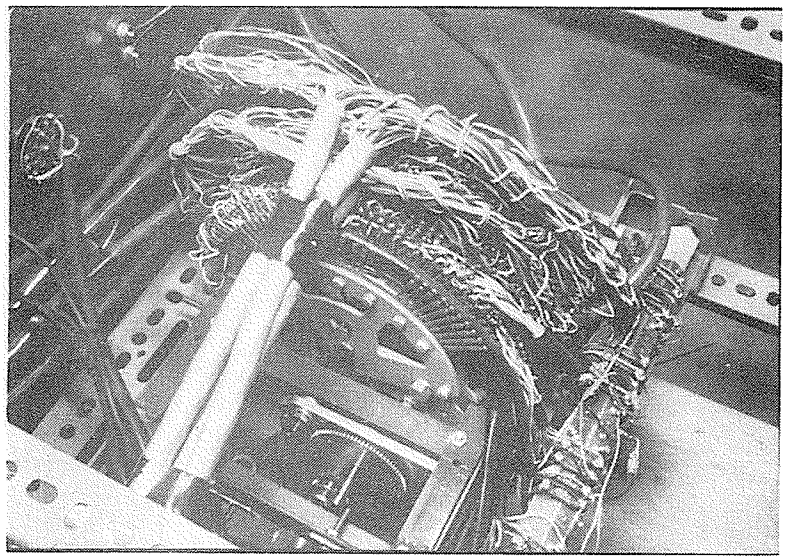

FIGURE 2.8 THE MOTOR DRIVEN ROTARY SELECTOR SWITCH

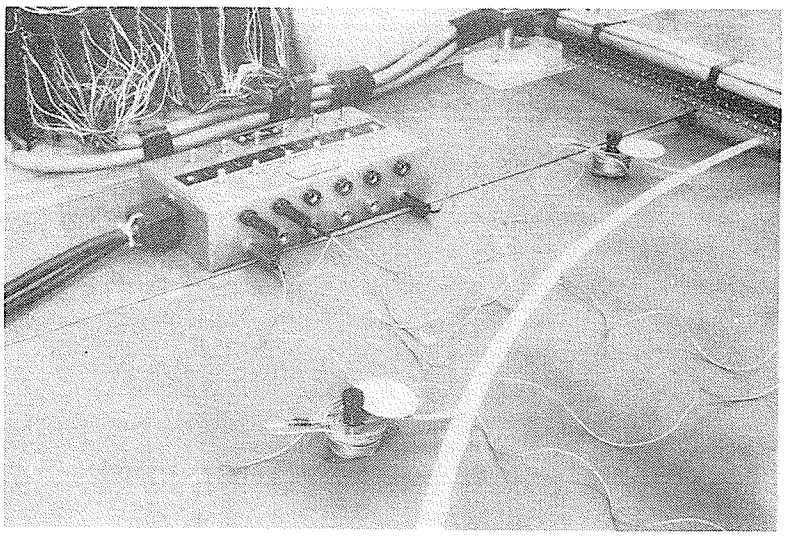

FIGURE 2.9 THE DISTRIBUTION UNIT, MOVABLE PROBES, PROBE CHASSIS AND TRANSPOSITION FRAME

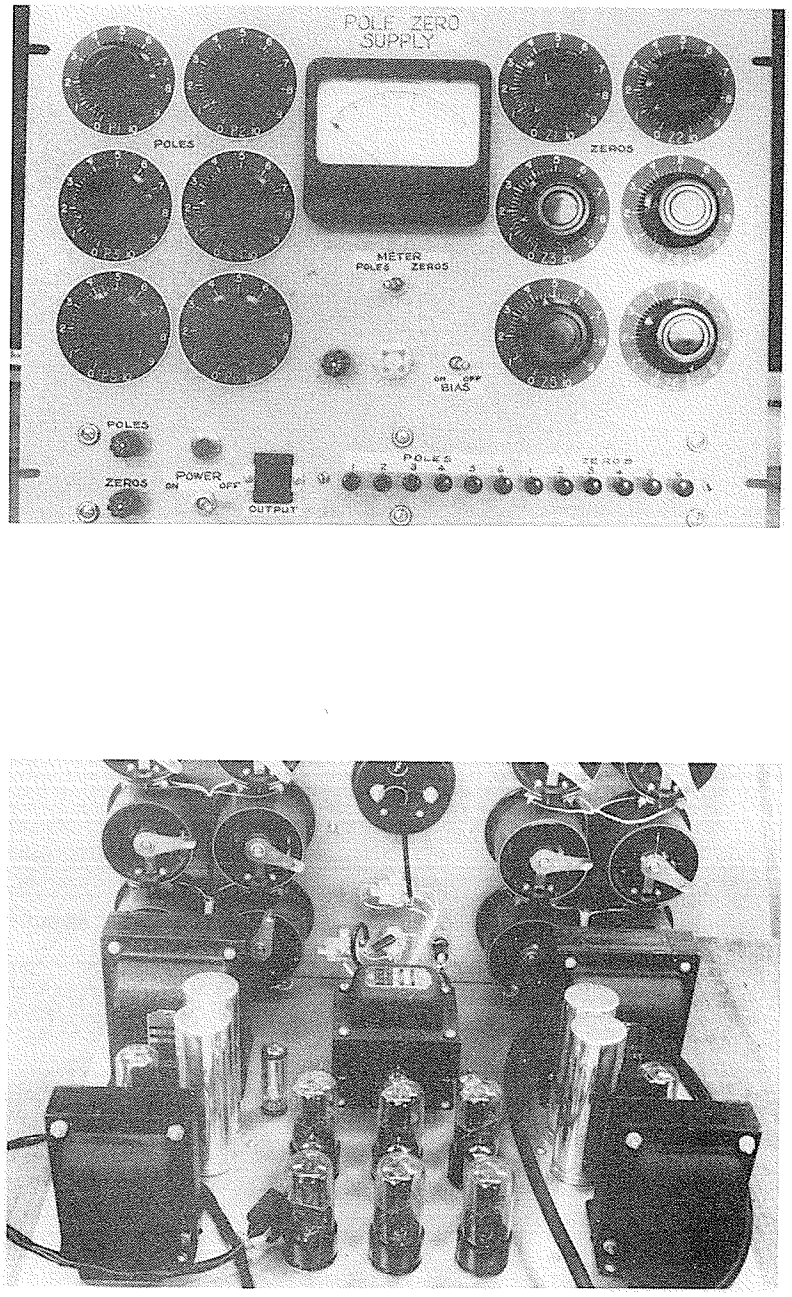

FIGURE 2.10 THE POLE-ZERO CONSTANT CURRENT SUPPLY

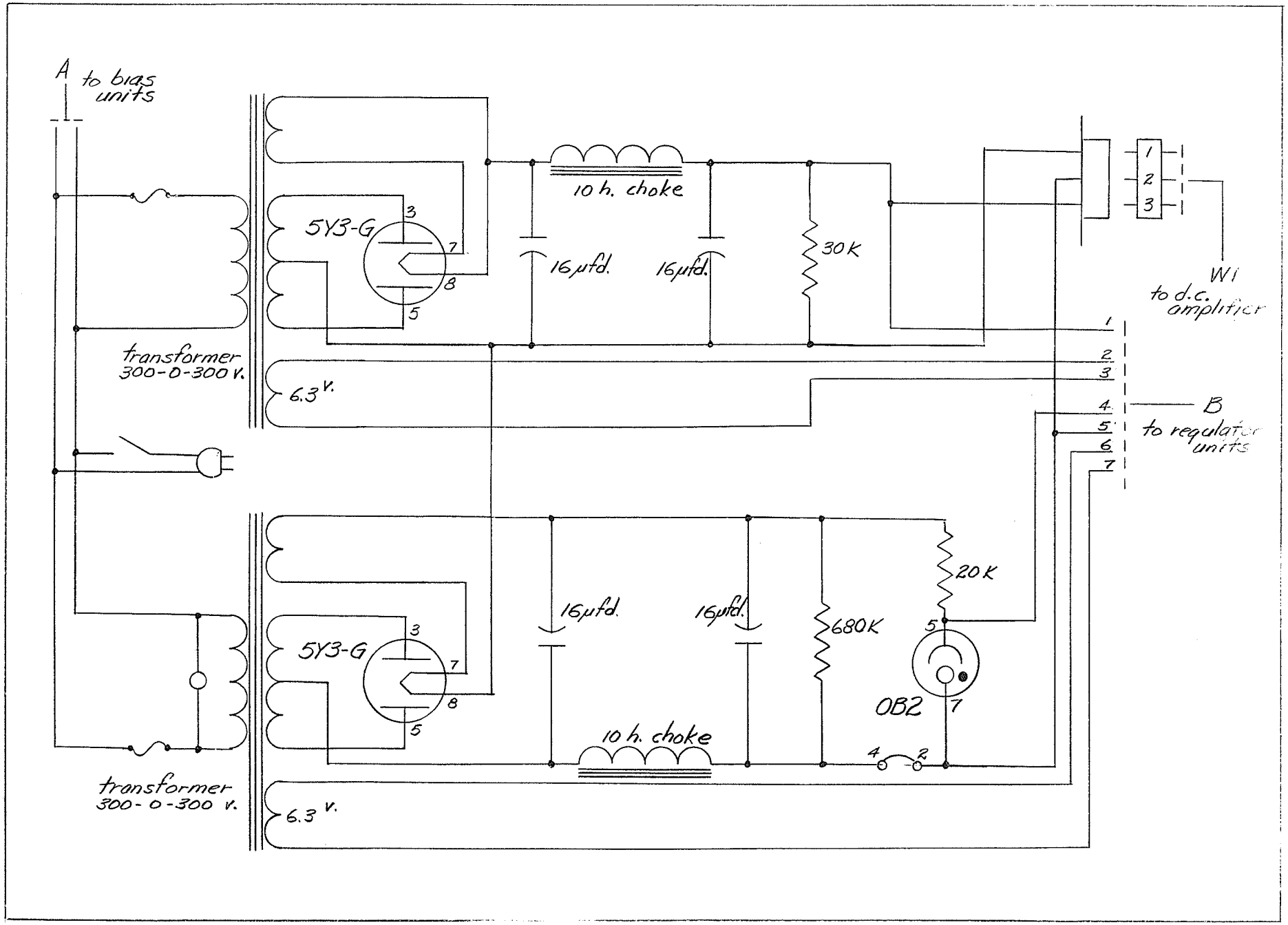

FIGURE 2.11 THE POLE-ZERO POWER SUPPLY

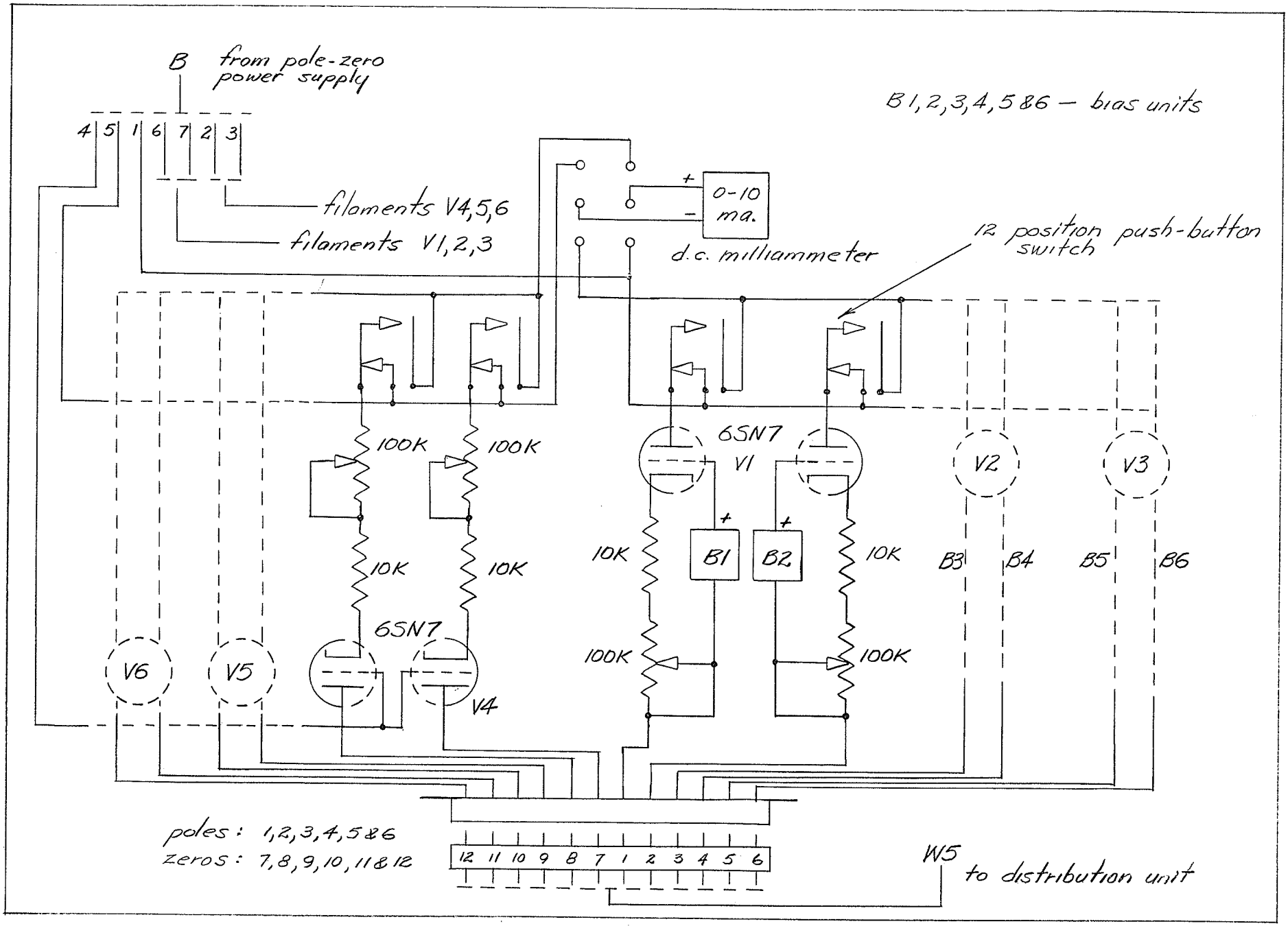

FIGURE 2.12 THE POLE-ZERO REGULATOR UNIT

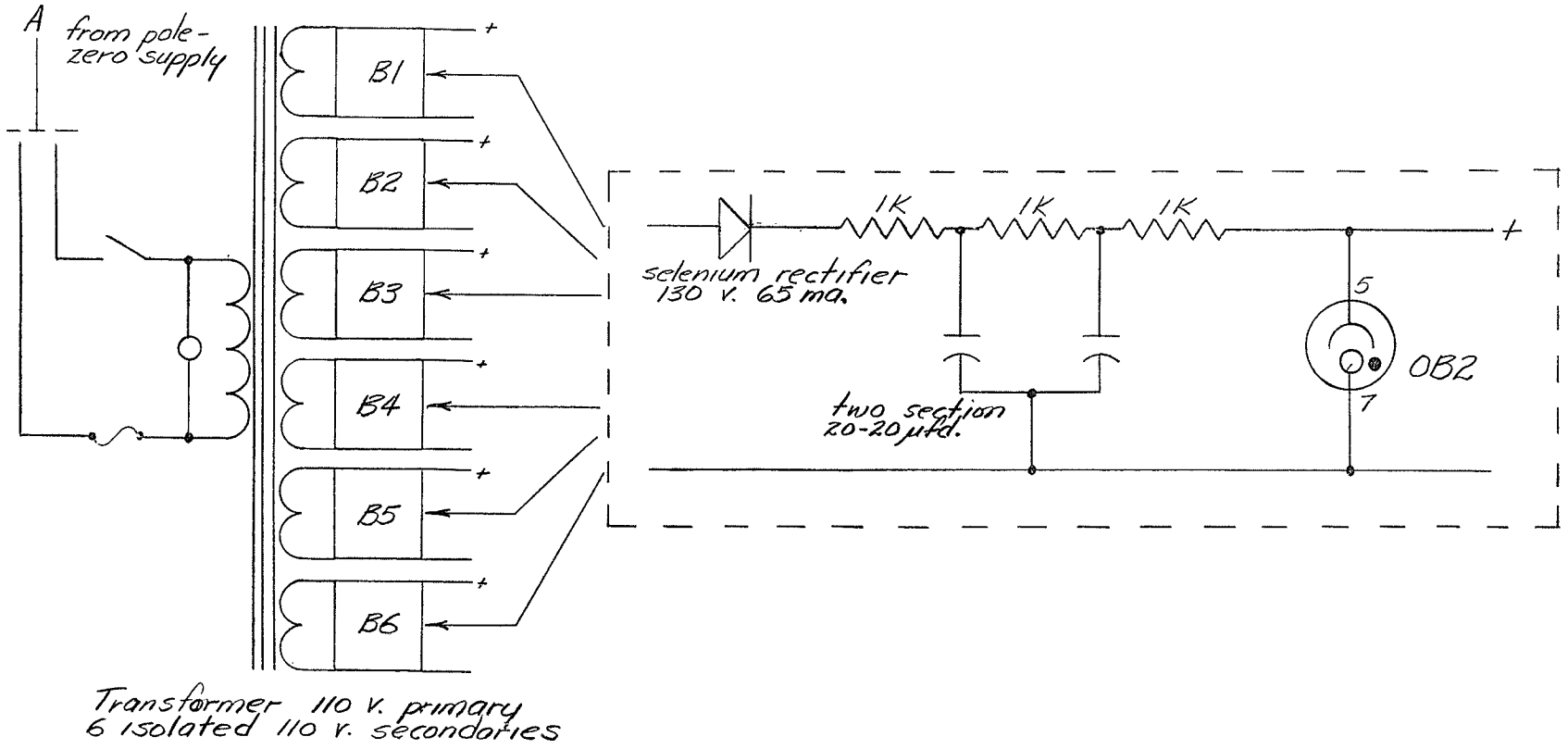

FIGURE 2.13 THE POLE-ZERO BIAS UNIT

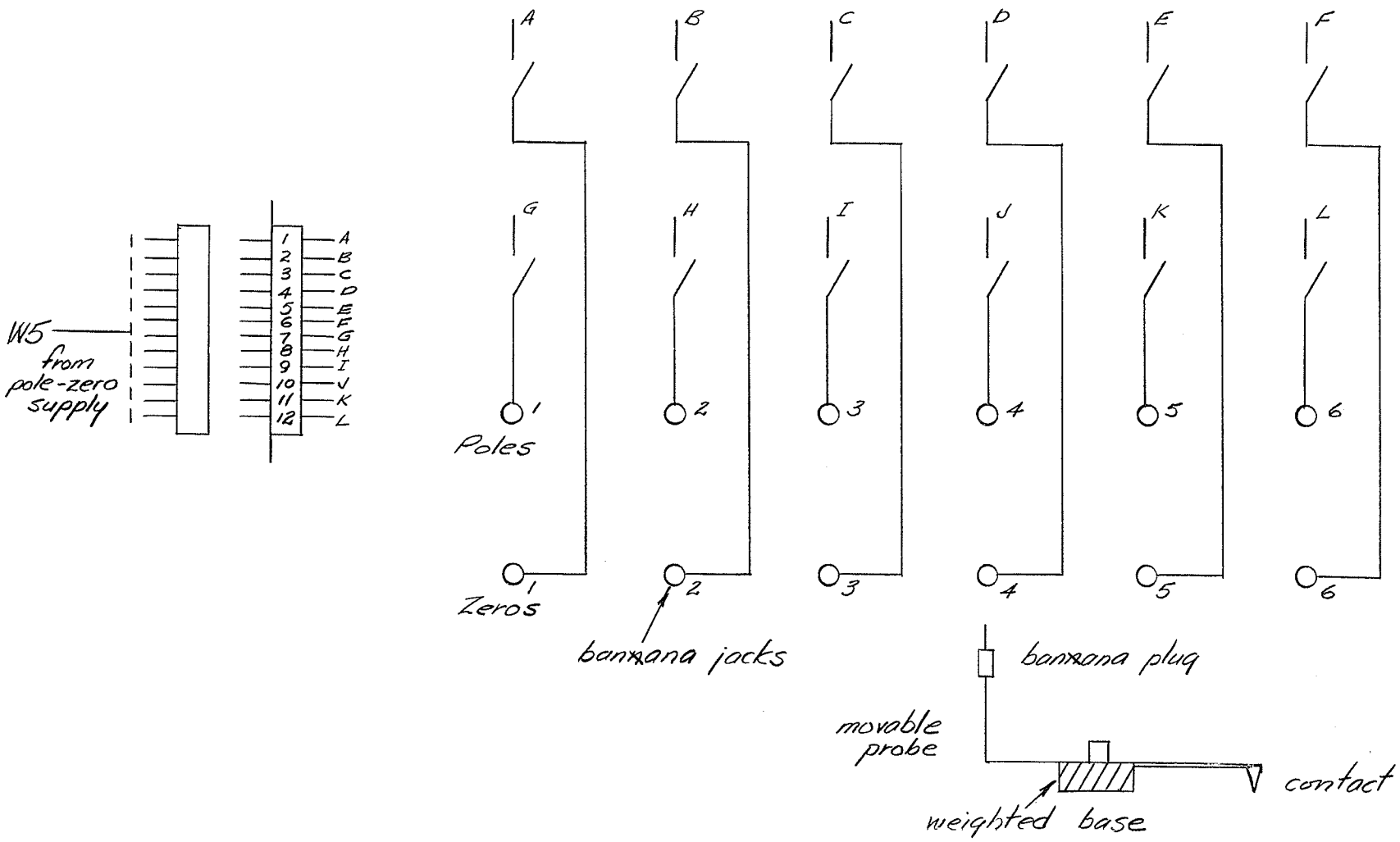

FIGURE 2.14 THE POLE-ZERO DISTRIBUTION UNIT

amperes with a 5 percent accuracy. Current regulation is maintained to within one percent for a 10 kilohm impedance change from a short-circuit. Performance and test results are given in appendix B.2. A calibration chart for the milliammeter is supplied with the unit.

In practice the probes may be located to within one millimeter of their theoretical position. This causes negligible error in the case of a probe location distant from the real frequency axis and a considerable error for one near the axis. The amount of error cannot be estimated in general since it is dependent upon the pole-zero configuration in each case. The error due to any pole or zero is dependent not only on the positioning error but also on the distance to the point of measurement and the proximity of other poles and zeros. In all cases the function error introduced on the real frequency axis in the vicinity of a probe is at least as great as the error in positioning the probe. Thus, for a probe located 1 cm. from the frequency axis the ~~positioning~~ error is at least 10 percent.

2.6 THE D.C. AMPLIFIER UNIT

The d.c. amplifier unit was designed to operate on the A and B probe outputs and supply a signal to the monitor oscilloscope which will display either the immittance magnitude, phase slope or phase response. A block diagram of the amplifier unit is given in figure 2.15 illustrating the circuit operation.

The A and B probe outputs are each coupled to the amplifier unit by a cathode follower stage which provides a high input and low output impedance. The B channel input has a potentiometer in the grid circuit so that any fraction of the B signal may be selected. This control is called the inverter gain. A schematic diagram of this section is given in figure 2.16.

Basically the d.c. amplifier unit has two sections, one an operational section and the other a vertical and horizontal deflection system for the oscilloscope. The operational unit is controlled by a ganged four section, five position rotary wafer switch. This switch interconnects three operational circuits in a number of different manners.

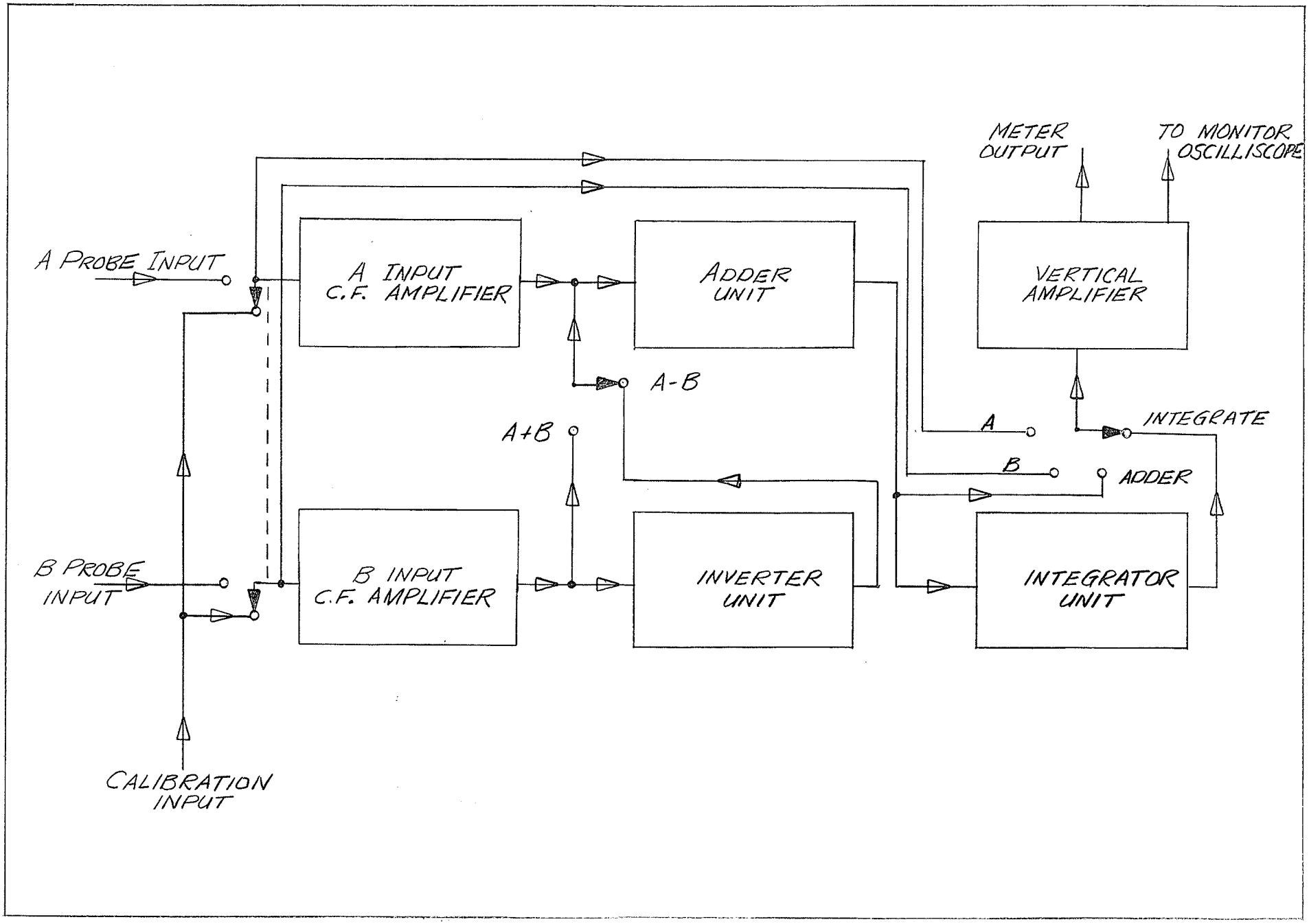

FIGURE 2.15 BLOCK DIAGRAM OF THE D.C. AMPLIFIER UNIT

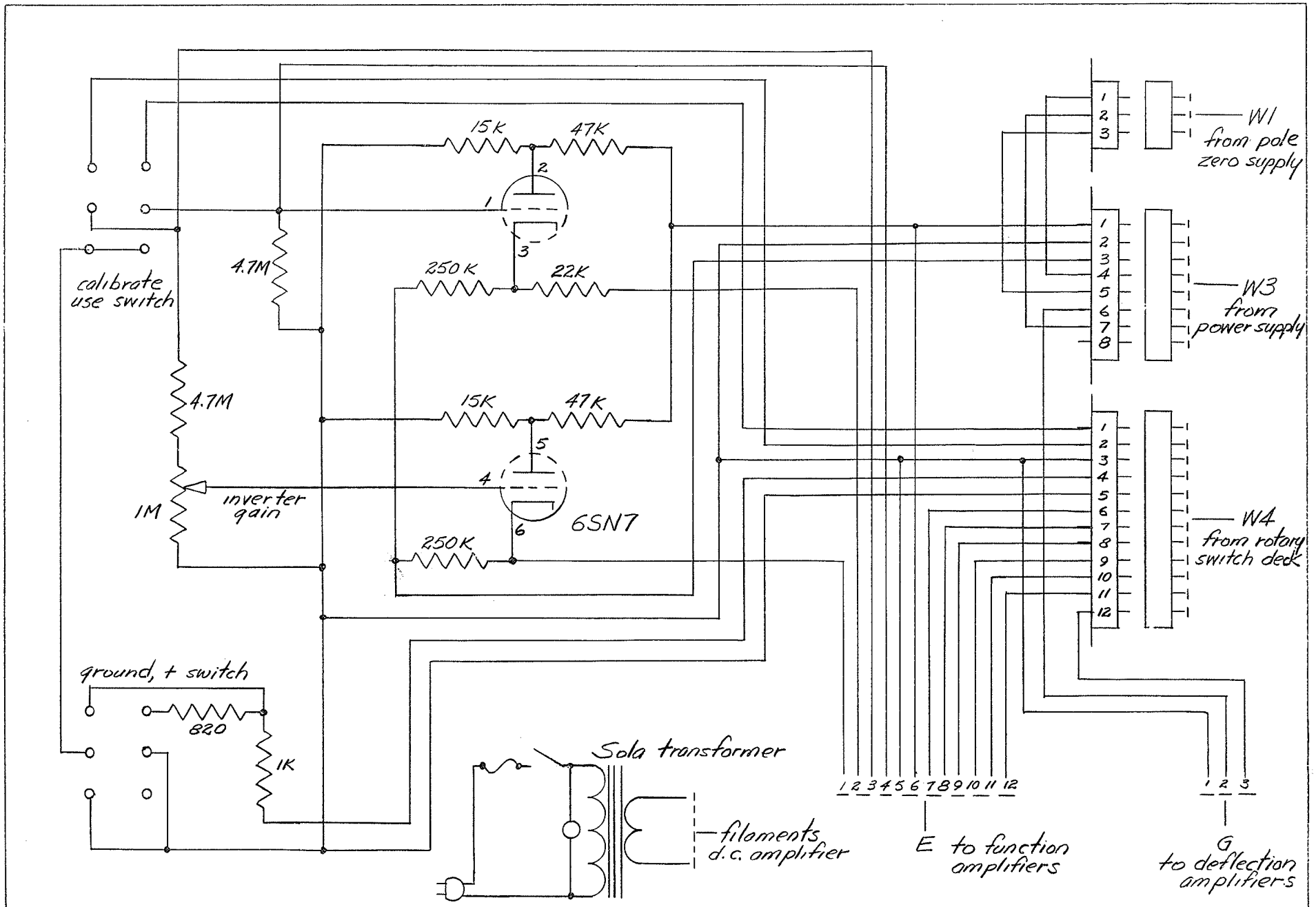

FIGURE 2.16 THE D.C. AMPLIFIER UNIT INPUT SECTION

The three circuits are as follows; an adder circuit, an inverter circuit and an integrator circuit.

Each circuit employs an elementary operational amplifier consisting of a triode section driving a cathode follower. The amplifier output may be zeroed by adjusting a potentiometer in the cathode circuit of the triode stage. This controls the d.c. output level of the cathode follower and "bucks" out a 45 volt battery potential. A schematic diagram of the circuit is shown below in figure 2.17.

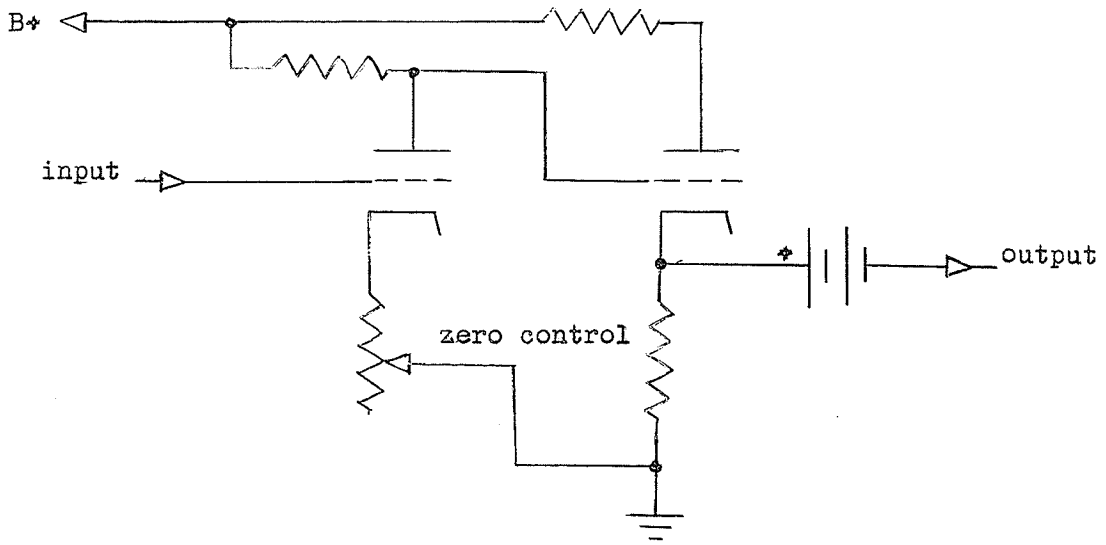

FIGURE 2.17

THE ELEMENTARY OPERATIONAL AMPLIFIER

The adder circuit employs the operational amplifier together with a resistive feedback loop and an input mixing circuit. Figure 2.18 below illustrates this circuit.

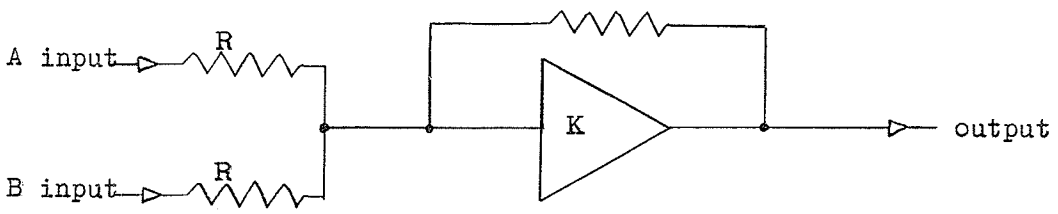

FIGURE 2.18

THE ADDER CIRCUIT

The inverter circuit uses an operational amplifier to shift the B signal through 180 degrees.

For the integrator circuit the operational amplifier is modified by a regenerative feedback loop in the cathode circuit. This modified amplifier is used as a Miller type integrator and is illustrated in figure 2.19 below.

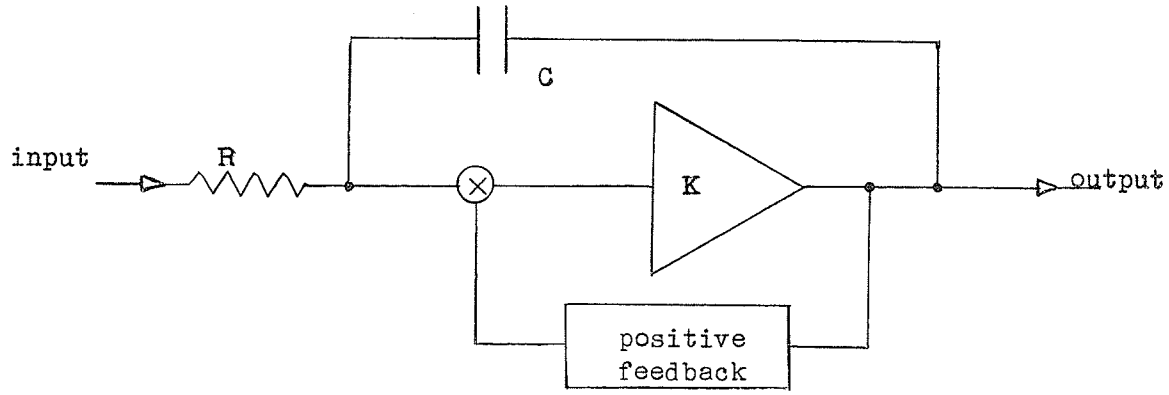

FIGURE 2.19
THE INTEGRATOR CIRCUIT

The schematic diagram of the complete operational section is given in figure 2.20. The wafer switch has five positions and in each position the operational units are interconnected to perform a different signal operation. The first switch position connects the A and B cathode follower outputs to give the sum of the two signals. The B input in this connection is used only as a buffer stage for calibration purposes. The second switch position feeds the output of the B cathode follower section to the inverter circuit and then to the adder circuit to give the difference of the A and B signals. This signal is proportional to the voltage gradient across the real frequency axis and thus also proportional to the phase slope of the immittance function as is described in section 1.4. The third switch position takes the difference signal from the adder circuit and feeds it through the integrator circuit. The resulting signal is proportional to the phase of the immittance function as is shown in section 1.4. For the last two switch positions the operational

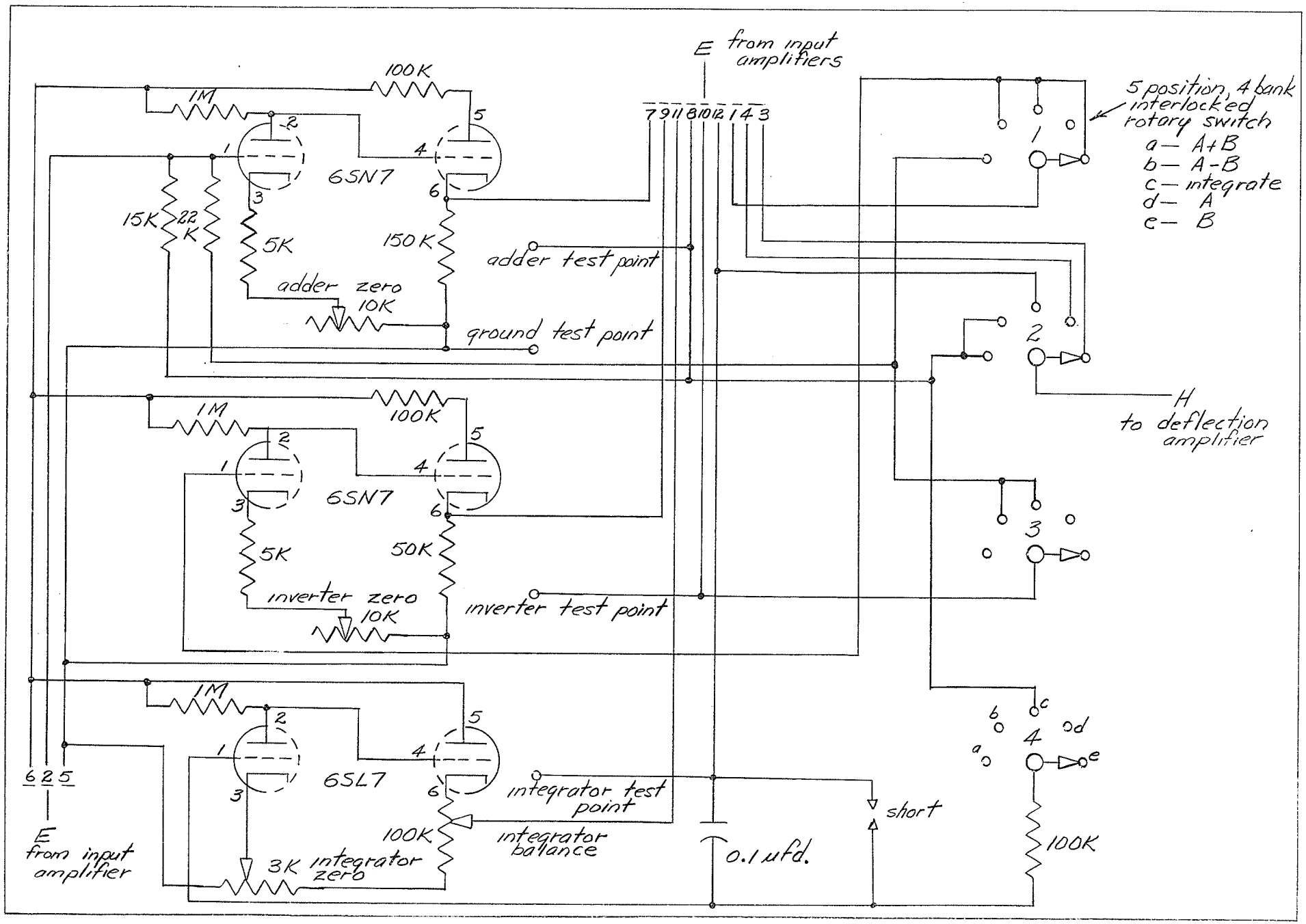

FIGURE 2.20 THE D.C. AMPLIFIER UNIT OPERATIONAL SECTION

units are not used, the probe signals being fed directly to the deflection section with position four yielding the A signal and position five the B signal.

The resultant signal from each of the five switch positions is applied to the vertical deflection amplifier. The response is available at a set of output jacks or is observable on the oscilloscope. The d.c. amplifier unit also has a horizontal deflection amplifier which receives the synchronized signal from the sweep potentiometer circuit.

The horizontal and vertical deflection amplifiers are almost identical in design differing only in their operating range. Each unit consists of a cathode follower input driving two triode sections in a differential manner. In the one triode stage the signal is injected at the grid while in the other stage the signal injection is made at the cathode. The signal is taken off between the plates of these two sections. The output is balanced and the levels are controlled by two potentiometer bias controls. A schematic diagram of this unit is given in figure 2.21. Figure 2.22 (a) and (b) illustrate the d.c. amplifier unit.

The oscilloscope monitor has a 5UP1A long persistence cathode-ray tube supplied by a 2.5 kilovolt power supply. Several potentiometers in the power supply control the beam focus, intensity and astigmatism. Figure 2.22 (c) and (d) illustrate the unit while figure 2.23 is a schematic diagram.

The amplifier unit power supply has a regulated +400 volt output for the deflection amplifiers and a regulated as well as balanced plus and minus 250 volt output for the operational units. The +400 volt supply is a standard regulated unit having a capacitor input filter section, a 6AS7 series loss tube, a 12AX7 control tube and an OD3 reference tube. The ± 250 volt supply is unique in that only one reference tube is used for both sections. A change in reference potential causes both sections to change equally and in ~~the~~ opposite directions. The two outputs may be balanced to within 0.1 volt of each other by means of a potential divider setup. The d.c. outputs change by less than 2 percent and the ripple stays below 20 millivolts rms. for an a.c.

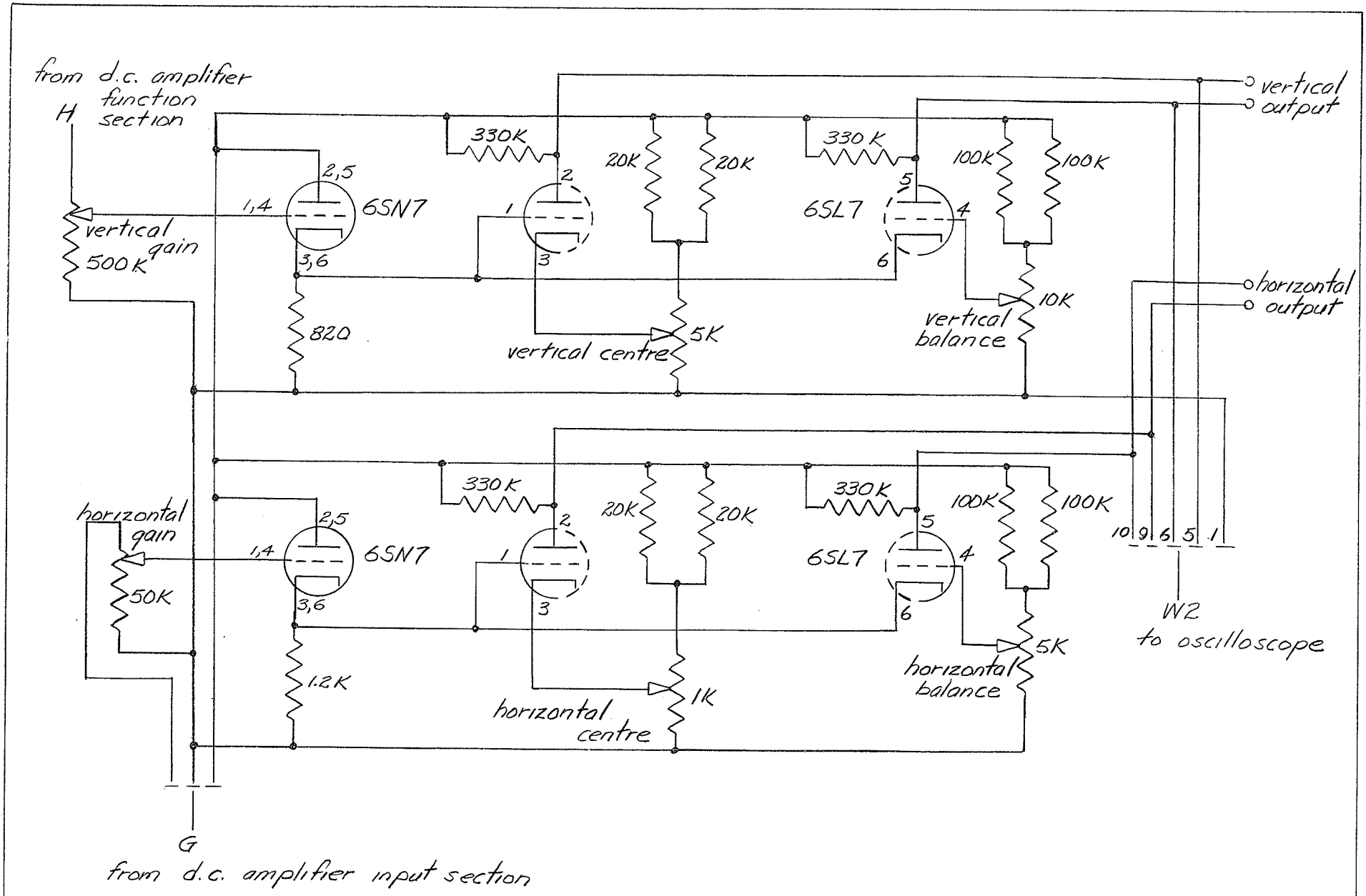

FIGURE 2.21 THE DEFLECTION AMPLIFIERS

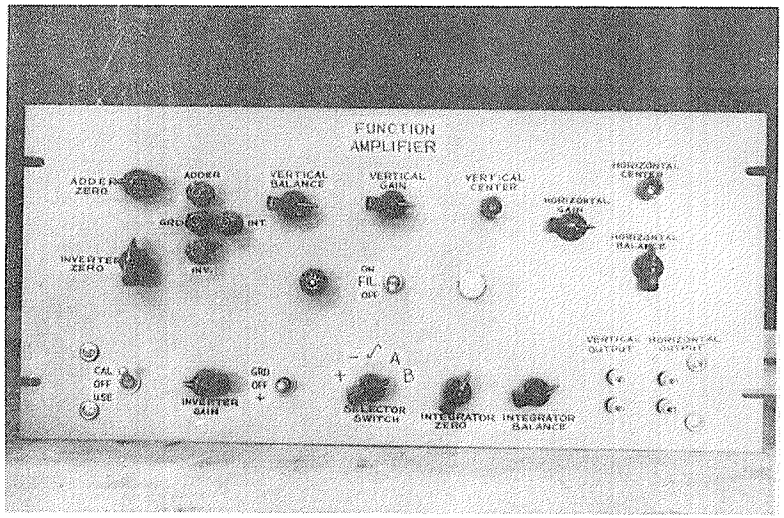

(a)

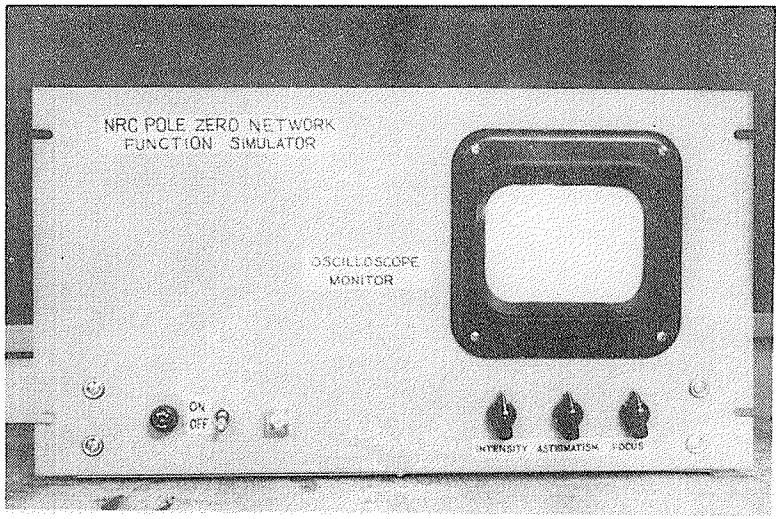

(c)

(b)

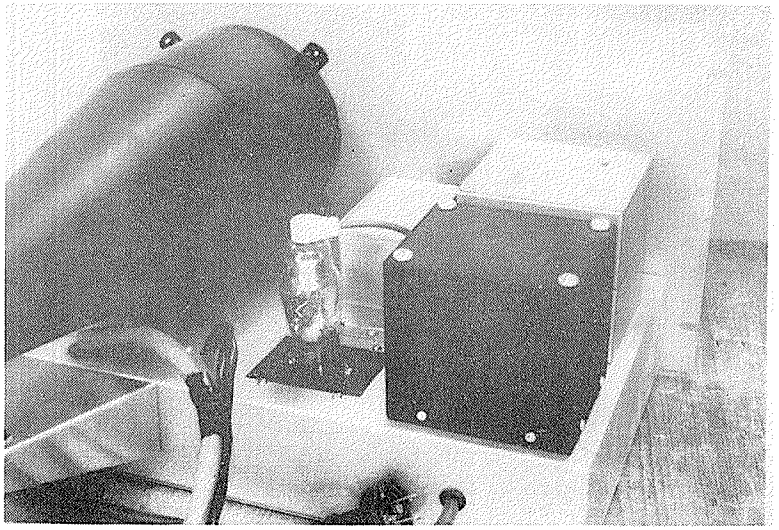

(d)

FIGURE 2.22 THE D.C. AMPLIFIER UNIT, (a) and (b). THE OSCILLOSCOPE MONITOR, (c) and (d)

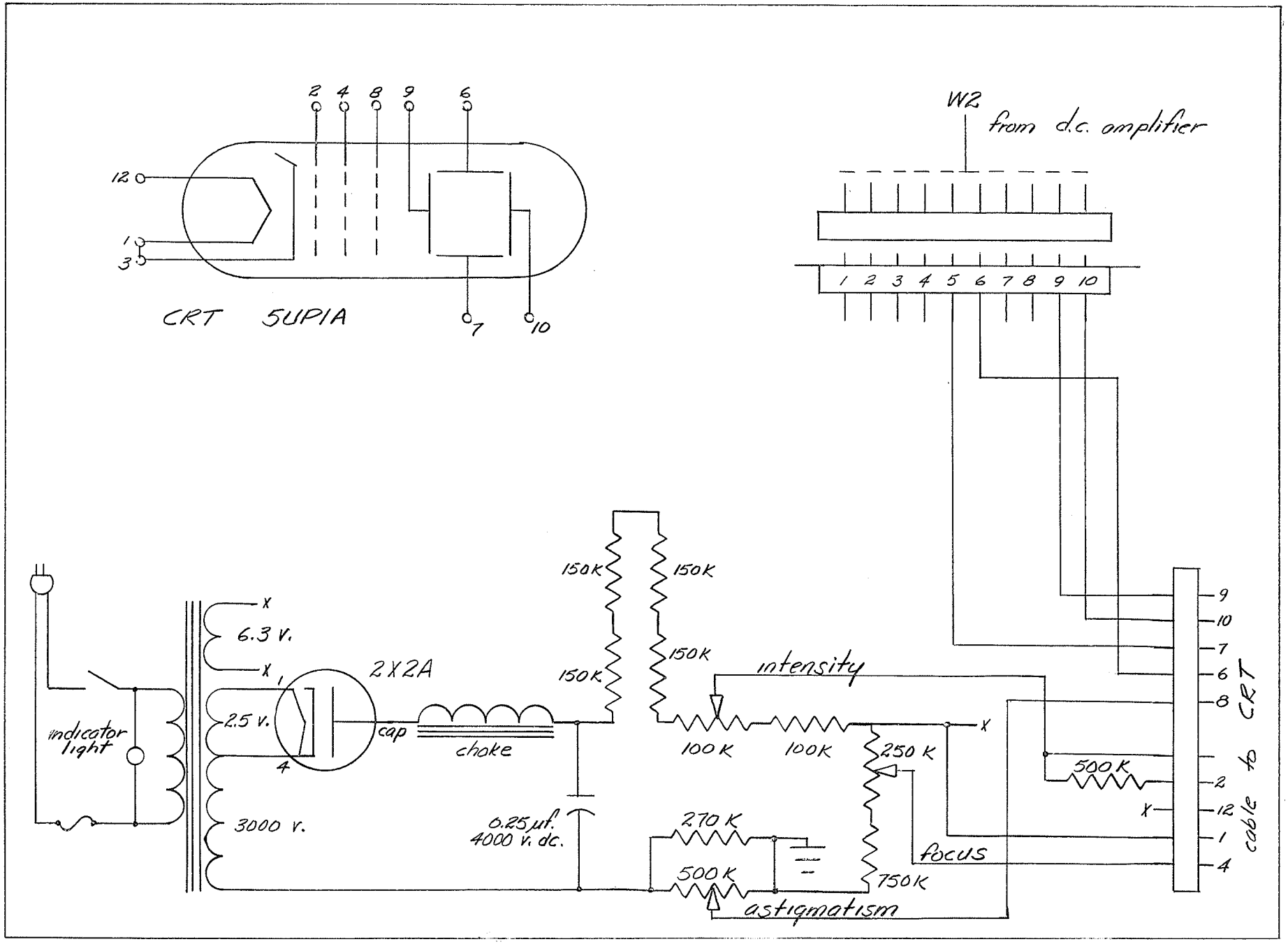

FIGURE 2.23 THE MONITOR OSCILLOSCOPE

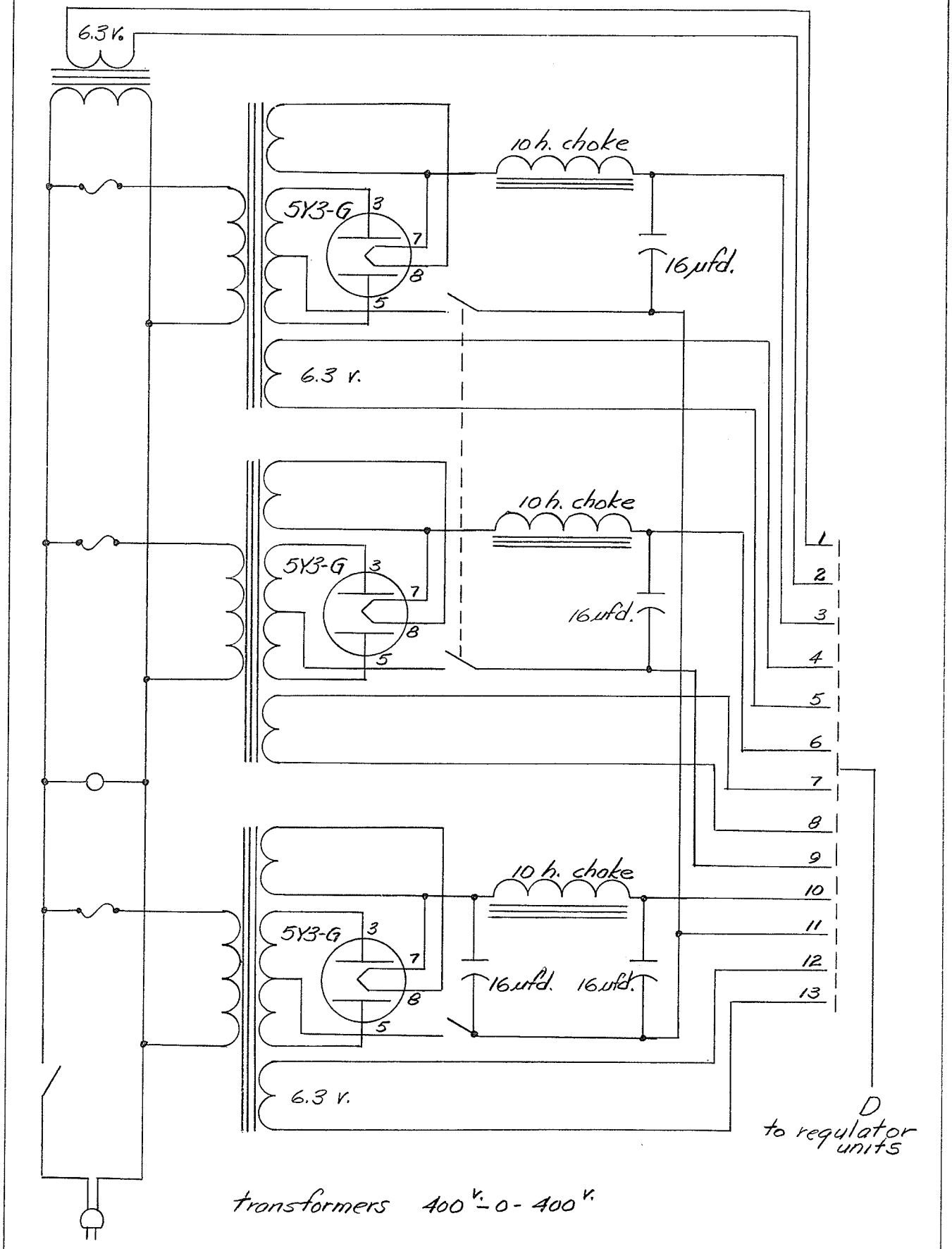

FIGURE 2.24 THE FILTER SECTION OF THE REGULATED POWER SUPPLY

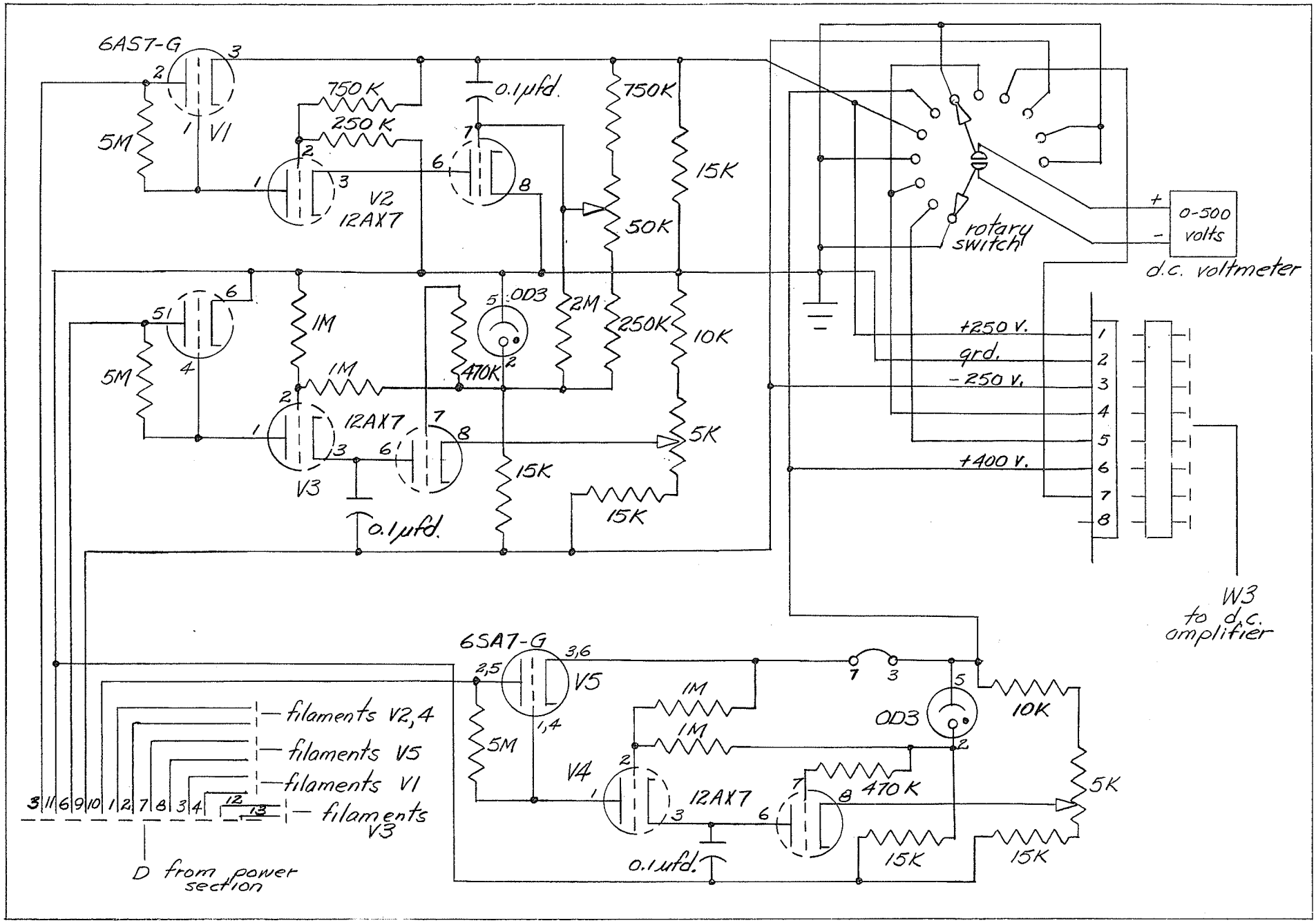

FIGURE 2.25 THE CONTROL SECTION OF THE REGULATED POWER SUPPLY

input range of from 105 volts to 125 volts. Figure 2.24 is a schematic diagram of the filter section while figure 2.25 gives the regulator section.

The test data of appendix C.1 shows that the operational and deflection units perform linearly over a wide range.

The neutral of the d.c. amplifier unit may be made a reference point on the plane by a potentiometer and battery setup illustrated below in figure 2.26.

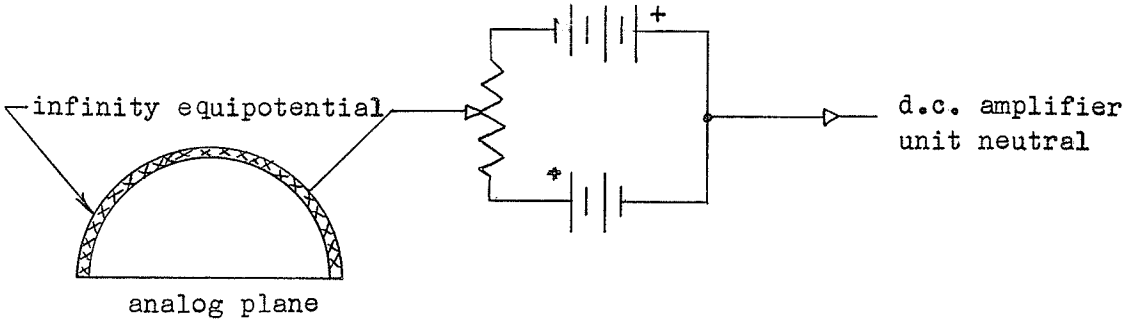

FIGURE 2.26

THE REFERENCE POTENTIAL BIAS CIRCUIT

CHAPTER 3

CALIBRATION AND OPERATION OF THE NETWORK-FUNCTION SIMULATOR

3.1 THE ELECTROLYTIC SHEET

Each electrolytic sheet is prepared by marking a 10 cm. grid on a strip of conducting paper andthen painting on the infinity circle. The sheet is oriented so that the real frequency axis falls across the full width of the paper. The linearity correction discussed in appendix A.2 is applied to the co-ordinate system in laying out the infinity circle.

The frequemcy scale for each immittance pole-zero configuration must be chosen so that each pole and zero is located within a circle having a radius of half the distance to the infinity circle. Also all measurements must be made on the first half of the frequency axis. These two restrictions are due to the finite location of infinity on the plane. This forced equipotential has the effect of producing an image zero for each pole and an image pole for each zero which contribute errors to the value of the actual immittance function.

Appendix D.1 illustrates that the error for a single real pole with the maximum above specifications is less than 2 percent. Each pole and each zero causes an error, but with opposite sign, the net effect being a partial error cancellation.

If a smaller error due to this infinity ring is desired, then the region of probe location and measurement must be made even smaller.

It was also found that a unit current strength of approximately 4 milliamperes produced a sufficiently large signal in the sheet and did not cause the paper to burn with probe movement.

3.2 SCALE FACTOR (K_1) CALIBRATION

A single zero is located at the origin and a pole at infinity both with half unit current strength and the resulting potential measured point-by-point along the real frequency axis.

Previously we had:

$$V(s) = K_o + K_1 \ln |F(s)| \qquad 1.23$$

and for this particular case

$$F(s) = s \tag{3.1}$$

If we consider values along the real frequency axis then:

$$F(j\omega) = d \tag{3.2}$$

where d is the distance along the real frequency axis.

We now have:

$$V_d = K_o + K_1 \ln d \tag{3.3}$$

The slope of the line obtained in plotting the measured potential versus the distance gives the scale factor or plane coefficient K_1.

3.3 CALIBRATION METHODS FOR THE AUTOMATIC SWEEP

(A) MAGNITUDE

A single zero is placed at s = -1 and a pole at infinity, both of half unit current strength. This represents the following immittance function.

$$F(s) = s + 1 \tag{3.4}$$

For real frequencies

$$F(j\omega) = j\omega + 1 \tag{3.5}$$

the magnitude of which is:

$$|F(j\omega)| = \sqrt{\omega^2 + 1} \tag{3.6}$$

Thus at $\omega = 0$

$$|F(0)| = 1 \tag{3.7}$$

and at $\omega = 1$

$$|F(j1)| = \sqrt{2} \tag{3.8}$$

We see that the impedance magnitude at $\omega = 1$ is 3 db. above the impedance magnitude at $\omega = 0$. The information in table 3.1 was compiled in a similar manner. The db. scale chosen depends on the range of the immittance magnitude.

The frequency point $\omega = a$ may be marked on the oscilloscope trace by lifting the probe at $\omega = a$ and connecting a battery between this probe and ground.

TABLE 3.1

CALIBRATION CHART FOR IMPEDANCE MAGNITUDE

db.	ratio a/b	where: $F(s) = s + b$ $db. = 20 \log_{10} \frac{\lvert F(ja) \rvert}{\lvert F(0) \rvert}$
1	0.52	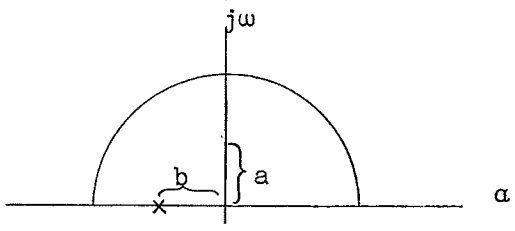
2	0.77	
3	1.00	
5	1.49	
10	3.00	

(B) PHASE SLOPE

The same immittance pole-zero configuration is used as in part (A). We had for real frequencies:

$$F(j\omega) = j\omega + 1 \qquad 3.5$$

The phase of this function is:

$$\text{Argument } F(j\omega) = \theta = \tan^{-1} \frac{\omega}{1} \qquad 3.9$$

and the phase slope $$\frac{d\theta}{d\omega} = \frac{1}{1 + \omega^2} \qquad 3.10$$

Table 3.2 gives the computed phase slope at a number of real frequency values.

TABLE 3.2

CALIBRATION CHART FOR PHASE SLOPE

ω radians	$\frac{d\theta}{d\omega}$ seconds	where: $F(s) = s+1$ $\frac{d\theta}{d\omega} = \frac{1}{1 + \omega^2}$
0.00	1.00	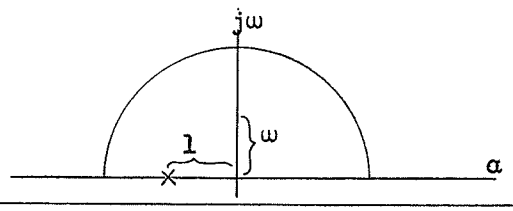
1.00	0.50	
3.00	0.10	
4.36	0.05	

(C) PHASE

Again the same immittance pole-zero configuration is used as in part (A). The phase was found to be:

$$\theta = \tan^{-1} \frac{\omega}{1} \qquad 3.9$$

Table 3.3 gives the computed phase for a number of frequency values.

TABLE 3.3

CALIBRATION CHART FOR PHASE

ω radians	θ degrees	where: $F(s) = s + 1$ $\theta = \tan^{-1} \frac{\omega}{1}$
0.000	0	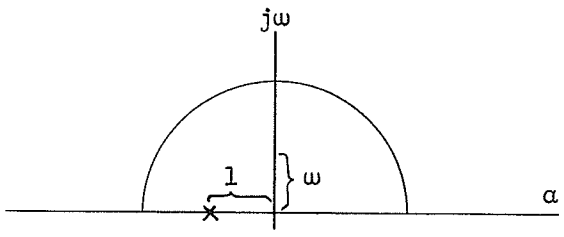
0.176	10	
0.364	20	
1.000	45	
1.192	50	

3.4 OPERATING PROCEDURE

A summary of the actual procedure will be outlined, the exact step-by-step routine appears in appendix D.2.

A frequency scale must be chosen so that the requirements outlined in section 3.1 are met. The probes are positioned at the pole and zero locations; the non-linearity correction being taken into account. The probe currents are turned on by means of the switches on the distribution unit and then adjusted with the meter and appropriate potentiometer control. Appendix D.2A outlines this procedure in detail.

The sweep motor is started, the d.c. amplifier unit calibrated and the oscilloscope trace adjusted. For observation of the impedance magnitude the operational switch is turned to either the A or B input position and the calibration procedure of section 3.3A applied. The phase slope

is obtained with the A-B switch position and the calibration method of section 3.3B. The INTEGRATE switch position and the calibration outlined in section 3.3C gives the immittance phase response. Appendices D.2B, C and D are a step-by-step outline of the exact operating procedure.

3.5 CALIBRATION OF THE LOGARITHMIC TRANSFORMED PLANE (HU)

A single zero is placed at the origin and a pole at infinity of the transformed sheet discussed in section 1.6. This now represents the immittance function:

$$F(s) = s \tag{3.11}$$

For real frequencies

$$|F(j\omega)| = d$$

where d is the distance along the imaginary axis of the complex frequency plane.

In the transformed plane:

$$\log |F(j\omega)| = \log d \tag{3.12}$$

In particular at d = 1

$$\log |F(j1)| = \log 1 = 0 \tag{3.13}$$

and at d = 10

$$\log |F(j10)| = \log 10 = 1 \tag{3.14}$$

The immittance magnitude changes by 20 db. in passing through a frequency decade. If the probe currents are adjusted so that the potential measured by a meter between the points s = j1 and s = j10 (or across any other decade) is 20 divisions then the meter is calibrated with one division being equal to one db. of change in immittance magnitude.

CHAPTER 4

TEST APPLICATIONS

4.1 TEST OUTLINE

The network simulator unit was applied to the solution of several specific problems using only the manual selector system. The interlaced scanning of the automatic sweep prevented the phase measuring system from operating because of the long sampling interval. The impedance magnitude response was observed on the oscilloscope but data was not obtained due to a lack of development in recording facilities.

The specific problems attempted all used one particular pole-zero configuration called the Mark II circuit. This configuration was representative of an impedance function for which the magnitude, time delay and phase response were calculated. The analog result in each case was then compared with the computed result.

The first problem involved determining the impedance magnitude, phase shift and phase response of the Mark II circuit using the half plane analog. In the next problem the magnitude response of the Mark II circuit was determined with the logarithmically transformed plane. The third problem was a mapping of the Mark II circuit impedance magnitude by means of potential cross-sections taken over the half plane analog.

4.2 THE TEST CIRCUIT

The following impedance function, called the Mark II circuit, was used to illustrate the use of the analog unit.

$$Z(s) = \frac{(s + 20) (s + 10 - j40) (s + 10 + j40)}{(s + 10 - j20) (s + 10 + j20)} \qquad 4.1$$

This impedance function has a zero on the real axis, a pair of conjugate zeros, a pair of conjugate poles and a pole at infinity. Table E.1 in

appendix E gives the solution of this function for magnitude, phase slope and phase for a range of real frequencies from $\omega = 0$ to $\omega = 80$ radians. The calculations were performed with the use of a Bendix G-15 General Purpose Digital Computer.

4.3 CALIBRATION OF THE PLANE COEFFICIENT (K_1)

A single pole with a half unit current strength of 1.8 milliamperes was placed at the origin and a zero with the same current strength at infinity. The potential along the real frequency axis was taken point-by-point using the manual selector switch and the infinity as reference. This potential was measured with a VTVM connected to the probe output jacks on the switch deck panel. The resulting test data is given in table E.2 of appendix E.

The potential was plotted against the logarithm of the distance from the origin. See figure 4.1. The slope of the resulting straight line was computed to be 2.288 which is the plane coefficient K_1 for a unit current strength of 3.60 milliamperes.

4.4 HALF PLANE ANALOG RESULTS FOR THE MARK II CIRCUIT

(A) IMPEDANCE MAGNITUDE (UNCORRECTED PROBE POSITIONS)

A set of zeros and poles were located at the following positions on the half plane analog (prepared according to section 3.1) with a unit current strength of 3.60 milliamperes.

1) A zero at -20 cm. at half unit current strength.

2) A pole at $-10 + j20$ cm. at unit current strength.

3) A zero at $-10 + j40$ cm. at unit current strength.

4) A pole on the infinity circle at half unit current strength.

The above pole-zero configuration is the analog representation of the Mark II circuit. No correction for conductivity non-isotropy was made in the location of the poles and zeros.

The potential, using the origin as reference, was measured point-by-point with a VTVM along the real frequency axis. Table E.3 in appendix E gives the test results and the computed impedance values. The resulting magnitude response is plotted along with the computed response in figure 4.2.

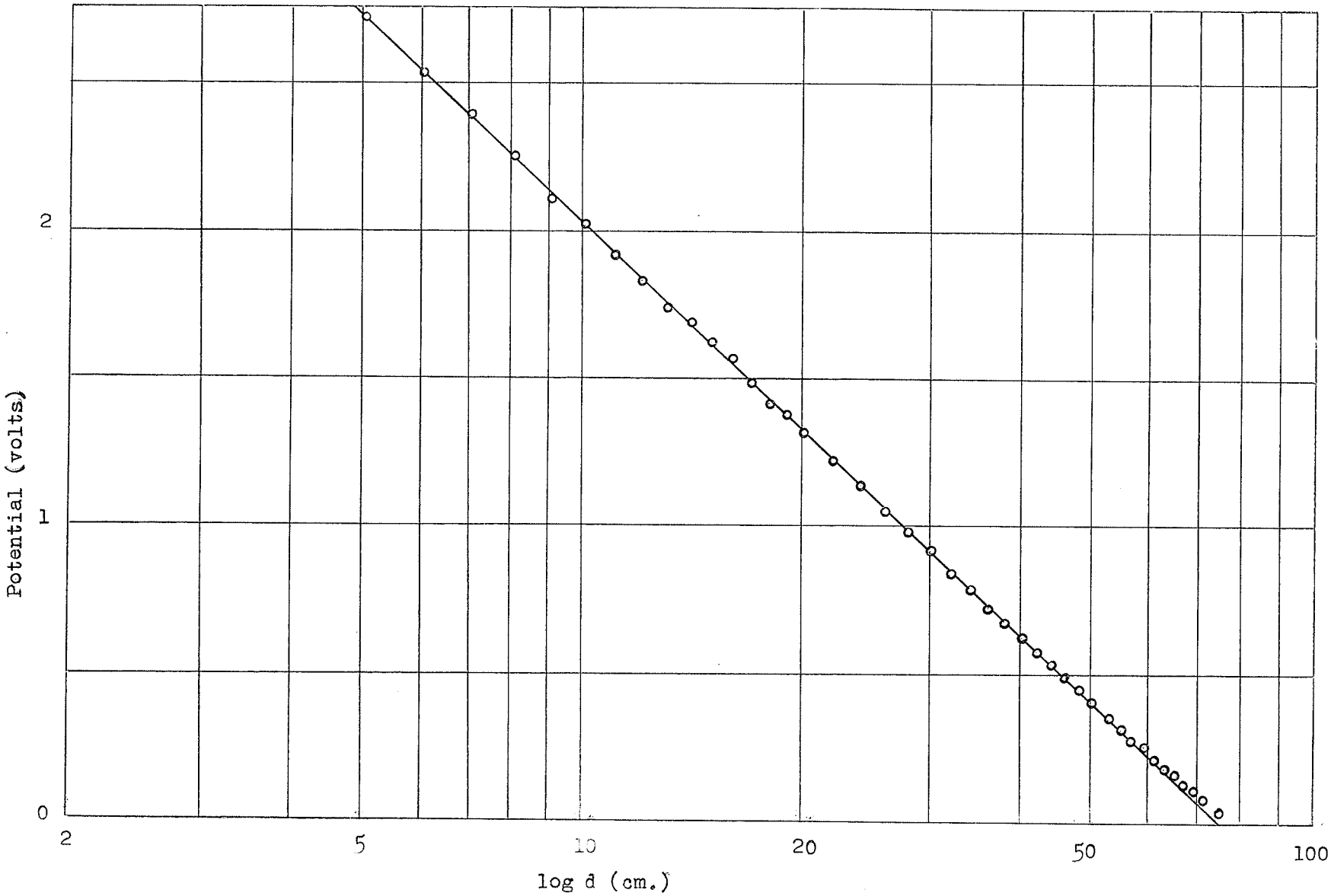

FIGURE 4.1 CALIBRATION CURVE FOR DETERMINING THE HALF PLANE SCALE COEFFICIENT K_1

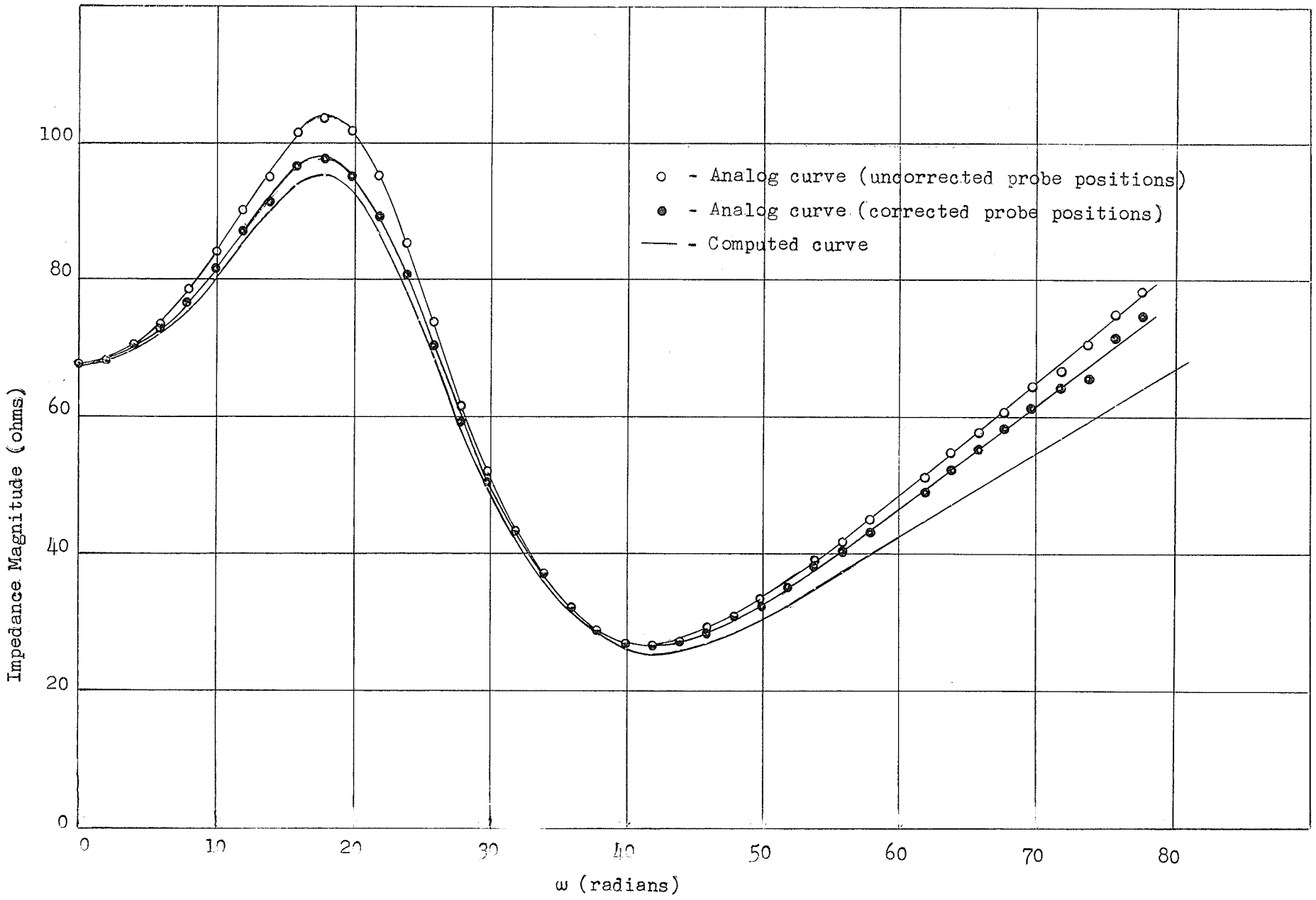

FIGURE 4.2 IMPEDANCE MAGNITUDE RESPONSE OF THE MARK II CIRCUIT

(B) IMPEDANCE MAGNITUDE (CORRECTED PROBE POSITIONS)

The zeros and poles of part (A) were relocated to correct for the conductivity non-isotropy of the sheet by increasing the real component of each probe position by a factor of $\sqrt{1.12}$. See appendix A.2. The test procedure of part (A) was repeated and the results are tabulated in table E.4 of appendix E. A curve of the resulting magnitude response is given in figure 4.2.

(C) PHASE SLOPE (TIME DELAY)

The pole-zero configuration of part (B) was used but with a unit current strength of 3.45 milliamperes. The experimental setup which was used to measure the voltage gradient across the real frequency axis is shown in figure 4.3. The potential across the helipot was adjusted to 0.1 volts so that each division of the 1000 division dial was representative of 0.1 millivolts. The voltage across each set of probes was metered by nulling the microammeter.

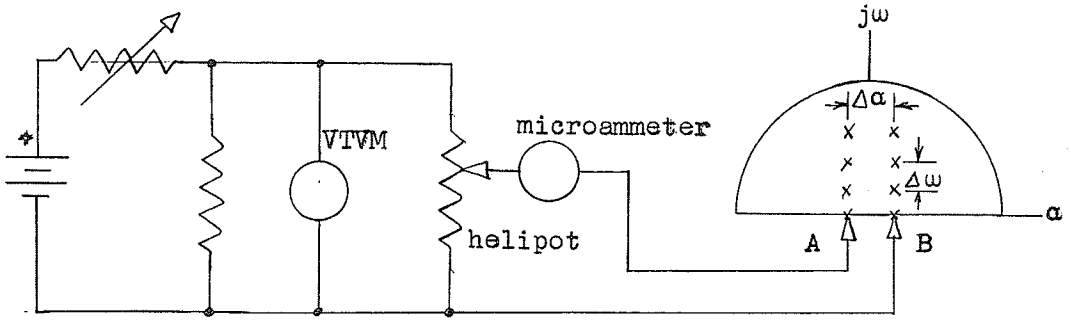

FIGURE 4.3
PHASE SLOPE METERING SYSTEM

The test results and computed values are given in table E.5 of appendix E . Figure 4.4 is a plot of the experimentally determined phase slope along with the computed curve.

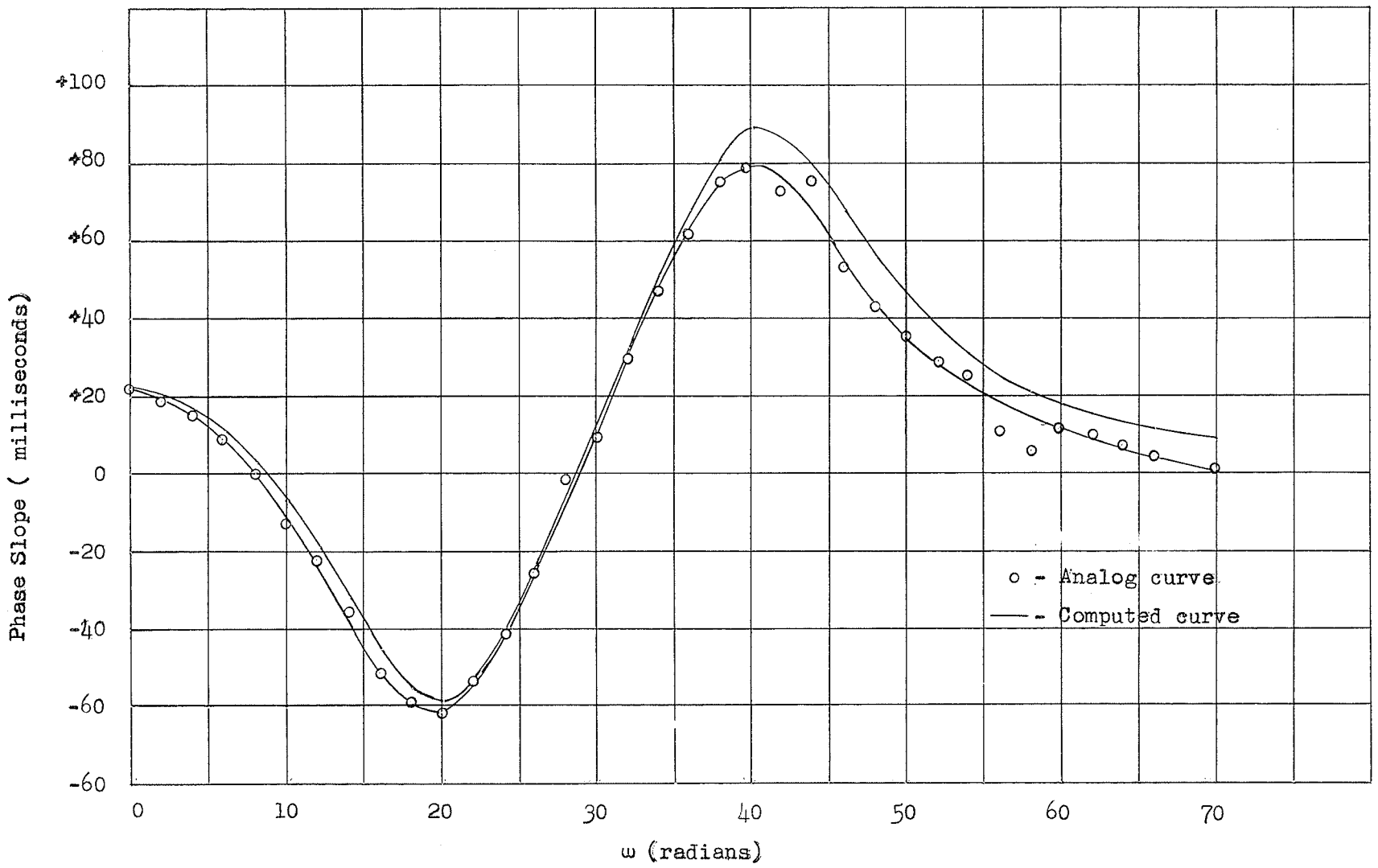

FIGURE 4.4 PHASE SLOPE RESPONSE OF THE MARK II CIRCUIT

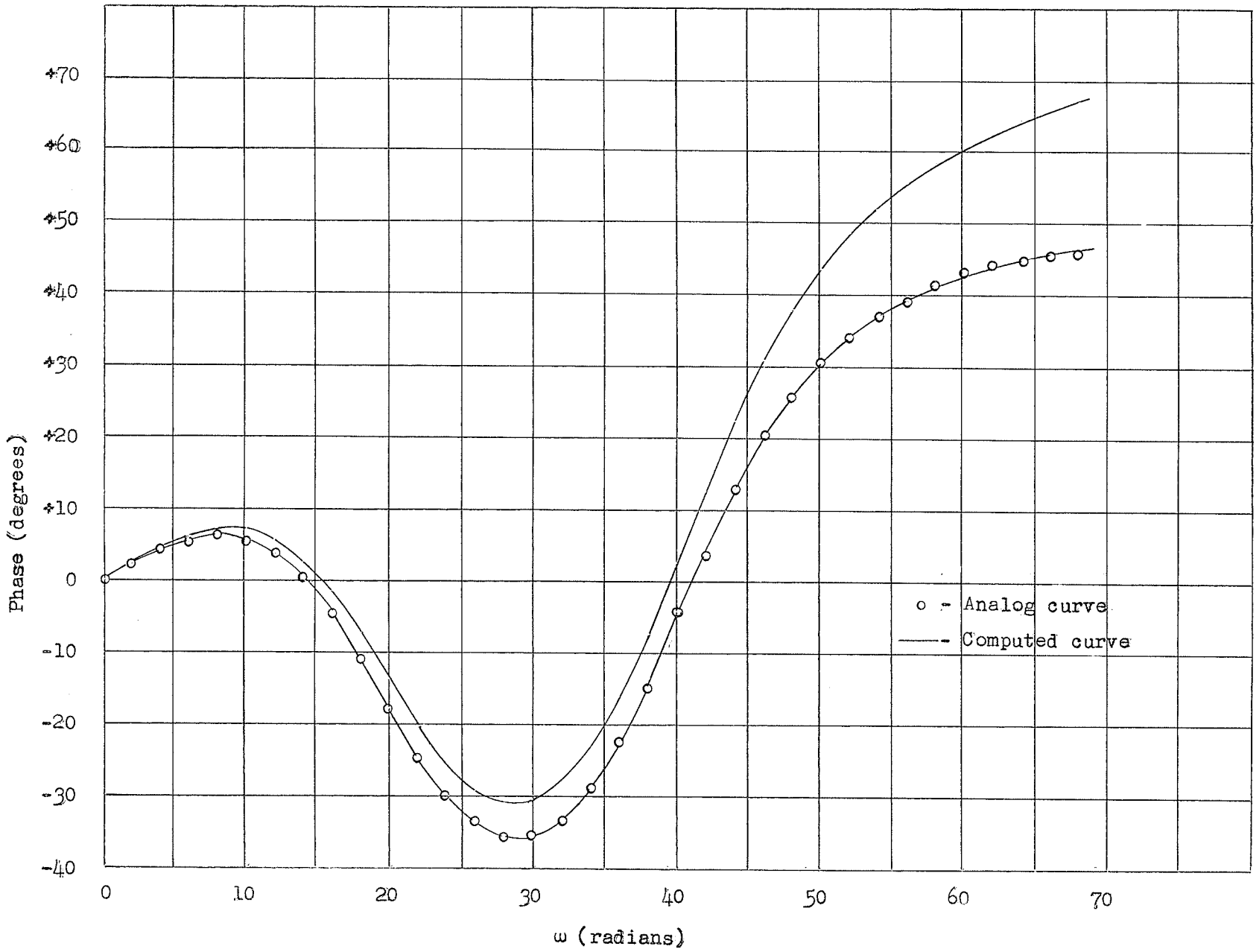

FIGURE 4.5 PHASE RESPONSE OF THE MARK II CIRCUIT

(D) PHASE RESPONSE

The phase response of the Mark II circuit was determined by performing a graphical integration with a planimeter of the time delay curve. The resulting computed phase is given in table E.6 of appendix E and plotted along with the actual phase response in figure 4.5 .

4.5 CALIBRATION OF THE LOGARITHMICALLY TRANSFORMED PLANE

A conducting sheet was prepared as is shown in figure 4.6 using the specifications outlined in section 1.6 .

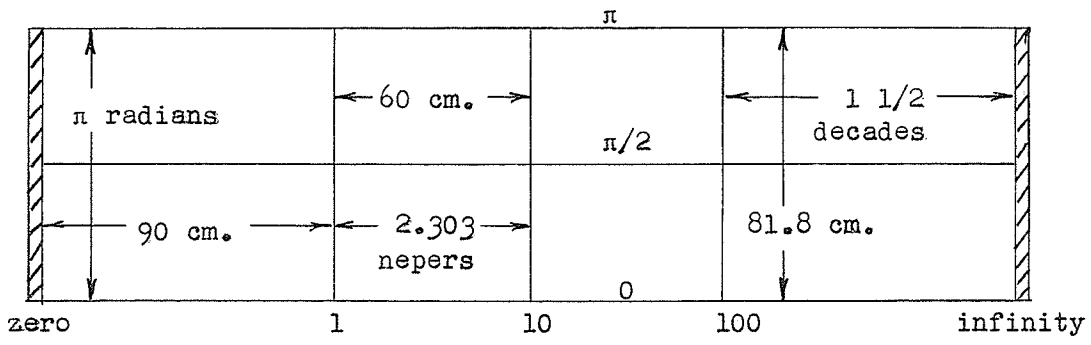

FIGURE 4.6

THE LOGARITHMICALLY TRANSFORMED PLANE

A zero was placed at the origin and a pole at infinity using half unit current strength (unit current = 3.45 milliamperes). The potential with respect to infinity was read every 5 cm. over the two decades. Test data is given in table E.6 of appendix E . The potential was plotted against distance using a linear scale on two cycle semi-log paper and the slope of the resulting straight line computed. See figure 4.7 . The scale coefficient, K_1, of the transformed plane was thus determined to be 2.08 .

4.6 ANALOG MARK II CIRCUIT RESPONSE FOR THE LOGARITHMICALLY TRANSFORMED PLANE

The pole-zero locations of the Mark II circuit were calculated in terms of the transformed plane units and found to be as follows:

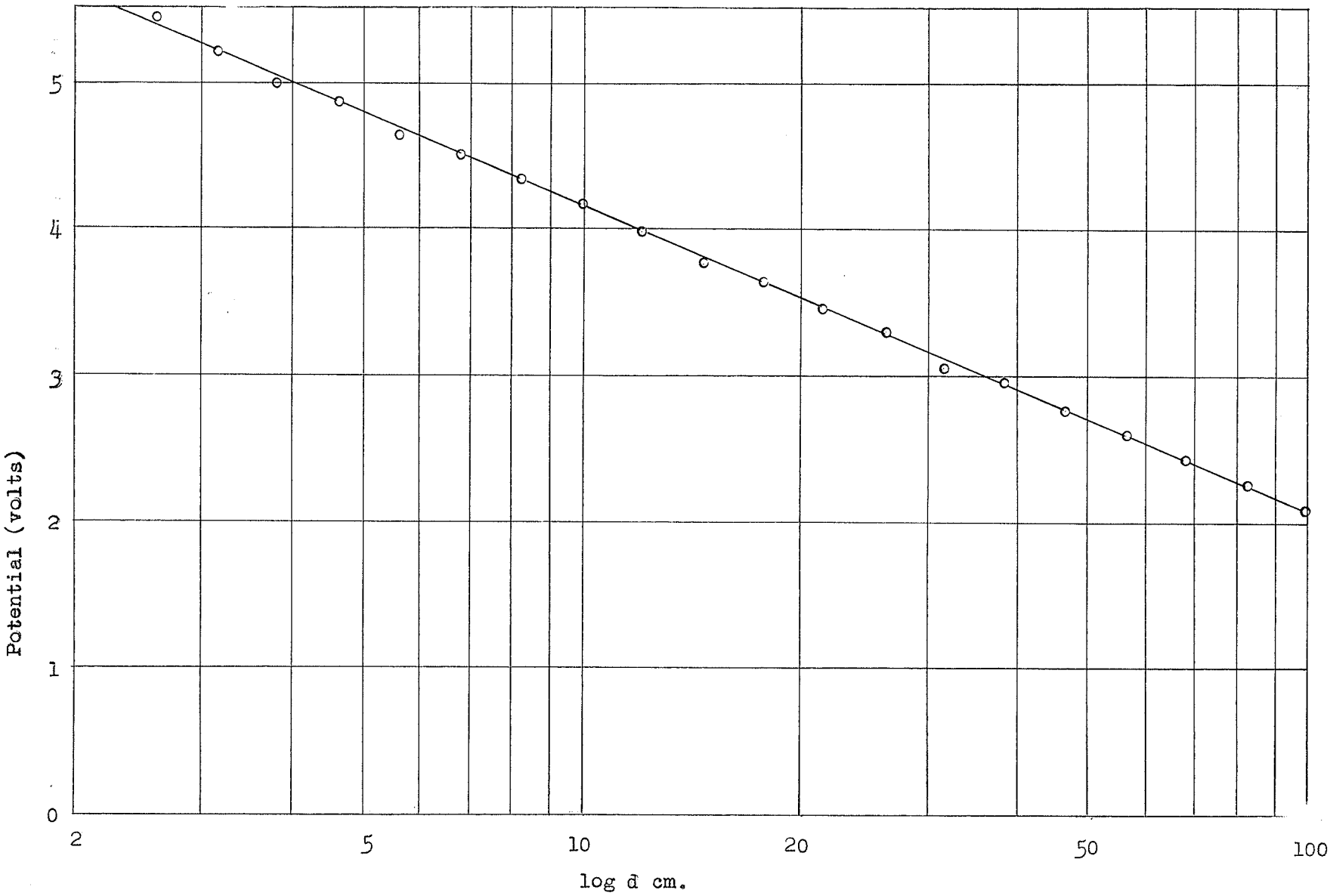

FIGURE 4.7 CALIBRATION CURVE FOR DETERMINING THE LOGARITHMICALLY TRANSFORMED PLANE COEFFICIENT K_1

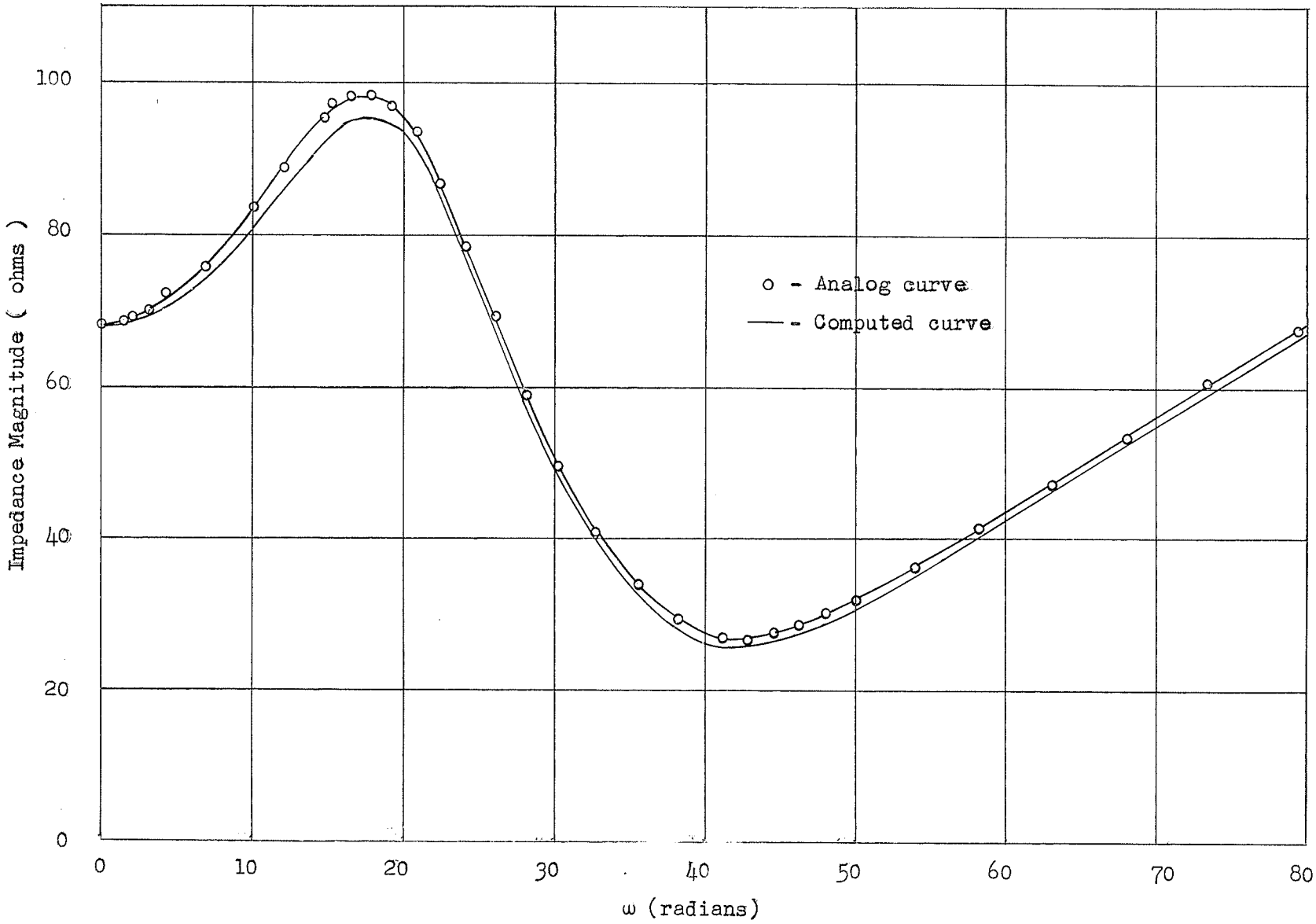

FIGURE 4.8 IMPEDANCE MAGNITUDE RESPONSE OF THE MARK II CIRCUIT AS DETERMINED BY THE LOGARITHMICALLY TRANSFORMED PLANE

$w_1 = 2.996 + j\,0$ ($s_1 = 20$)

$w_2 = 3.107 + j\,63.44^{\circ}$ ($s_2 = 10 + j\,20$)

$w_3 = 3.719 + j75.97^{\circ}$ ($s_3 = 10 + j\,40$)

In terms of the transformed plane scale these are:

$w_1 = (78.1 + j\,0)$ cm.

$w_2 = (81.0 + j\,28.8)$ cm.

$w_3 = (96.8 + j34.5)$ cm.

The unit current for the probes was 3.45 milliamperes. Potential readings were taken along the real frequency axis using a VTVM and the origin as reference. The results along with the computed impedance magnitudes is given in appendix E, table E.8 . A curve of the analog response along with the computed response is shown in figure 4.8 .

4.7 MAPPING OF THE MARK II IMPEDANCE FUNCTION

The pole-zero configuration of the Mark II circuit was set up on a half plane analog using a unit current of 3.45 milliamperes. The potential was measured in the jω direction for various fixed values of attenuation. Cross-sections of the potential distribution in the whole plane were in this manner determined. The impedance along the cross-sections was computed and a scale model of the cross-sections constructed. Table E.9 in appendix E gives the test data and calculations.

Locating these cross-sections in the proper sequence formed a three-dimensional model of the Mark II circuit impedance magnitude response over the complete plane. Figure 4.9 is a photograph of the resultant model. Figures 4.10 to 4.12 are a plot of the various cross-sections and illustrate the change of impedance across the plane.

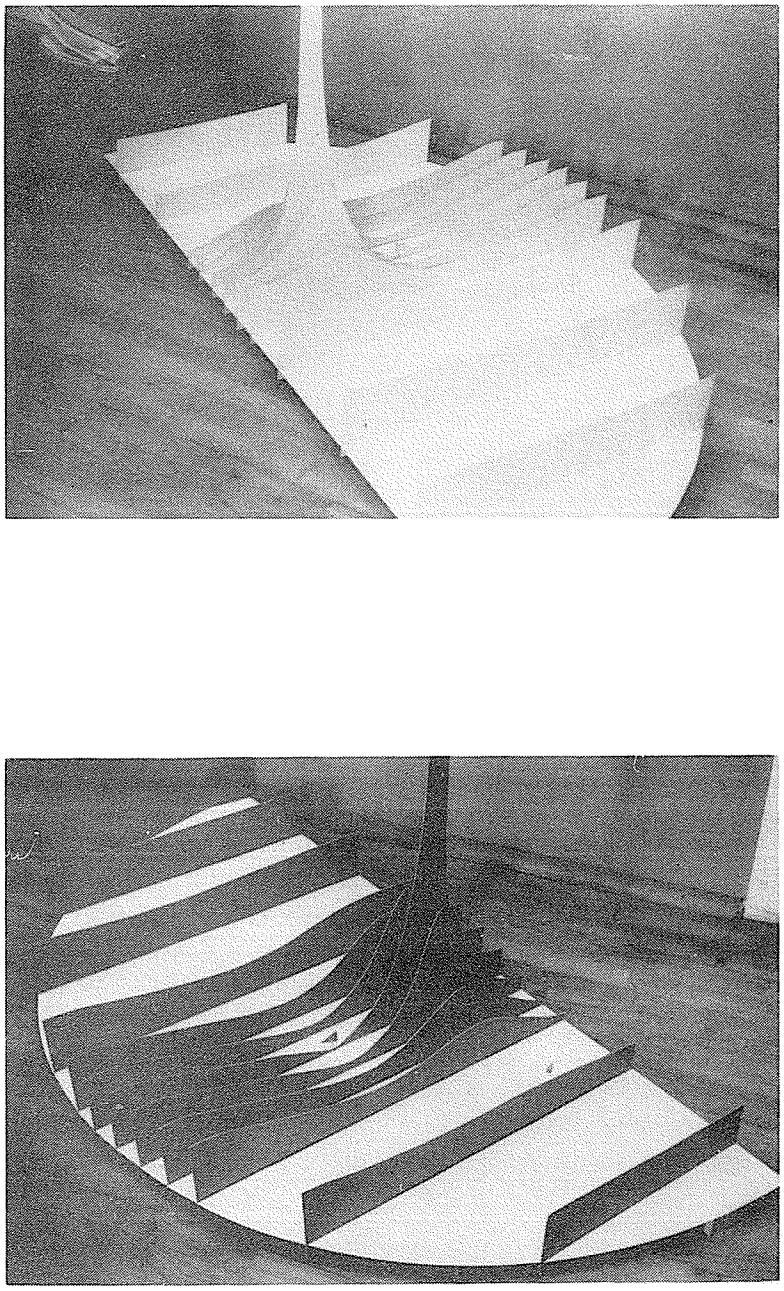

FIGURE 4.9 A MODEL OF THE MARK II CIRCUIT IMPEDANCE MAGNITUDE RESPONSE IN THE S PLANE

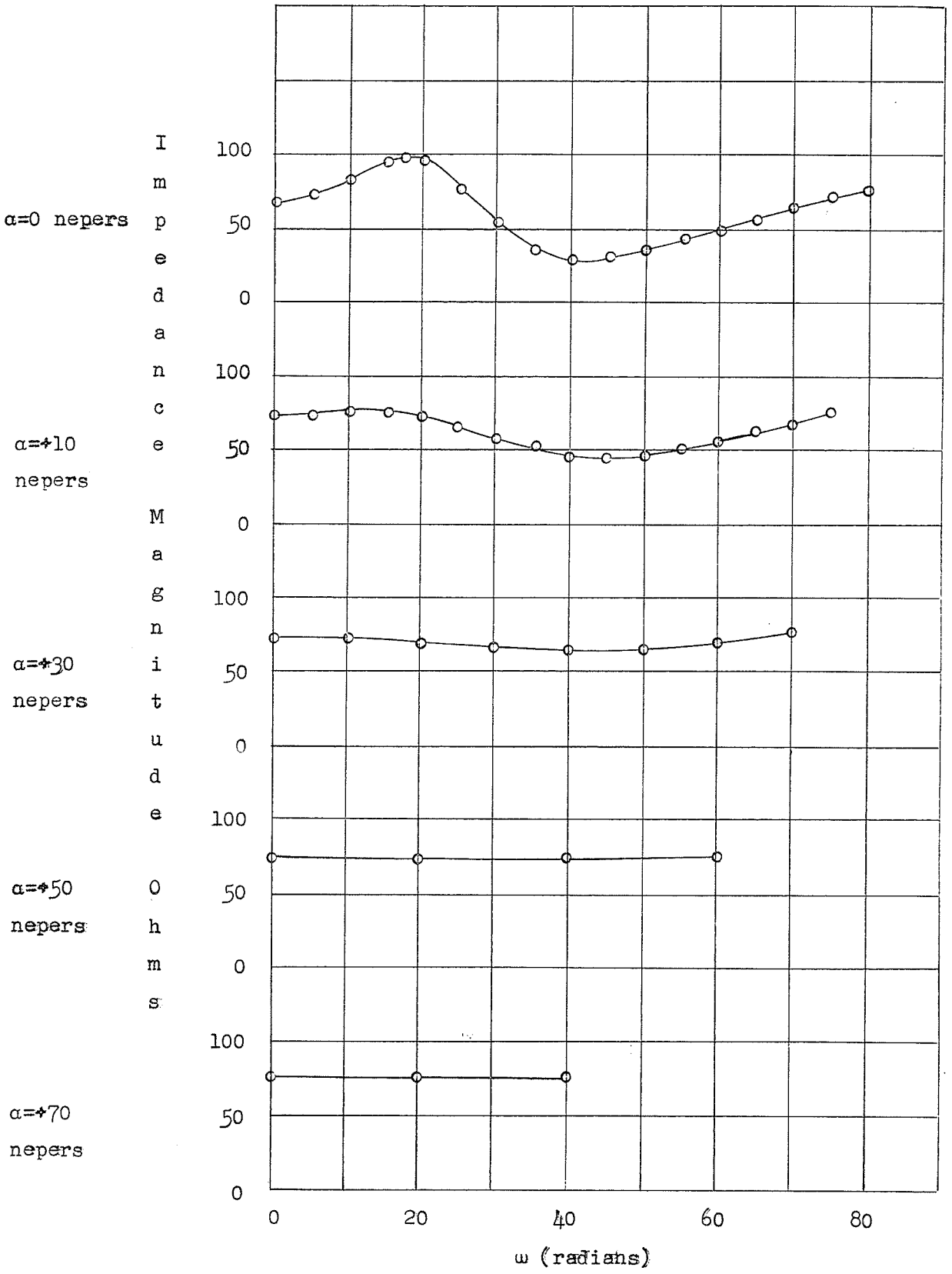

FIGURE 4.10 IMPEDANCE MAGNITUDE CROSS-SECTIONS OF THE MARK II CIRCUIT (α=+70 to α=0)

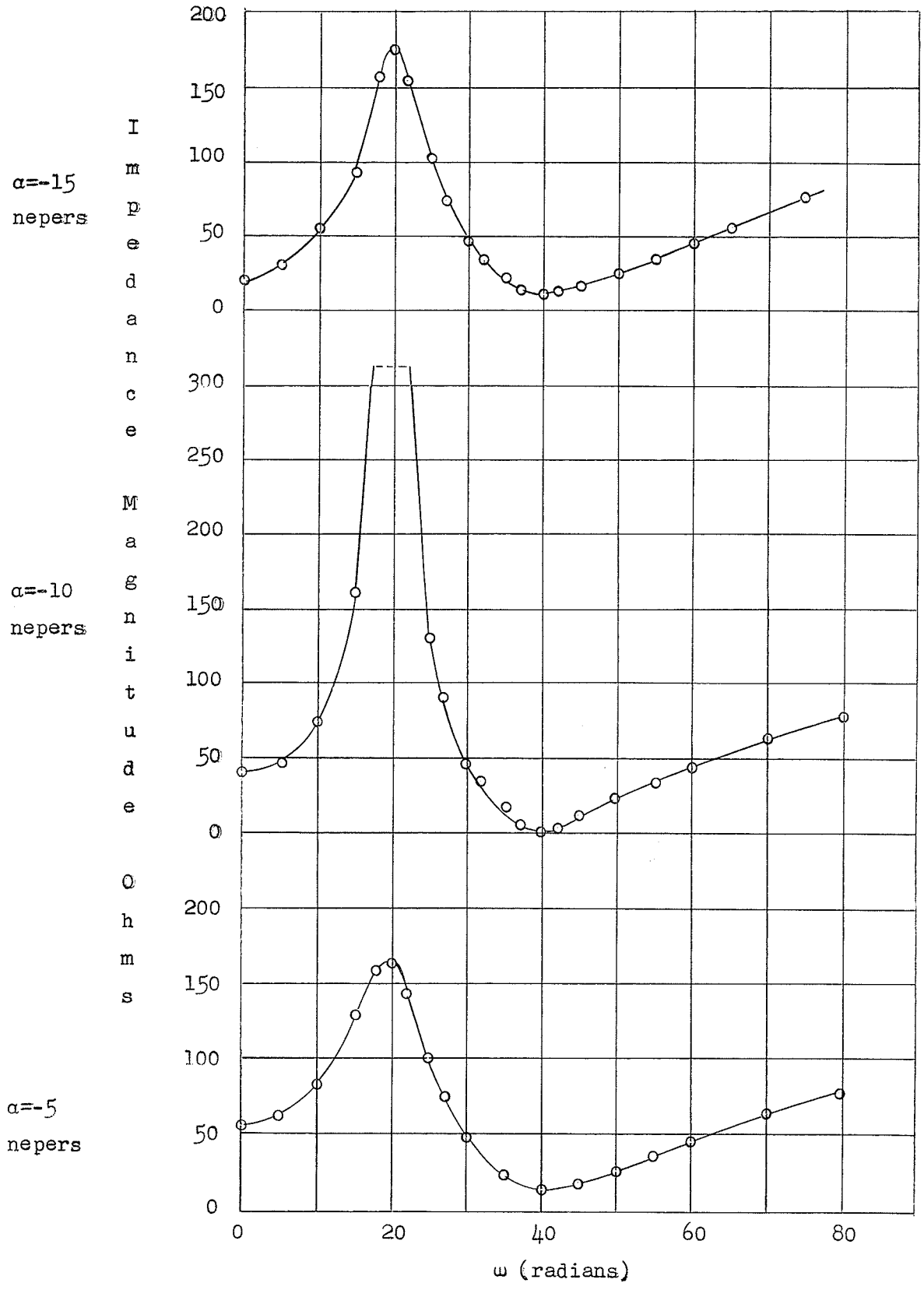

FIGURE 4.11 IMPEDANCE MAGNITUDE CROSS-SECTIONS OF THE MARK II CIRCUIT (α=-5 to α=-15)

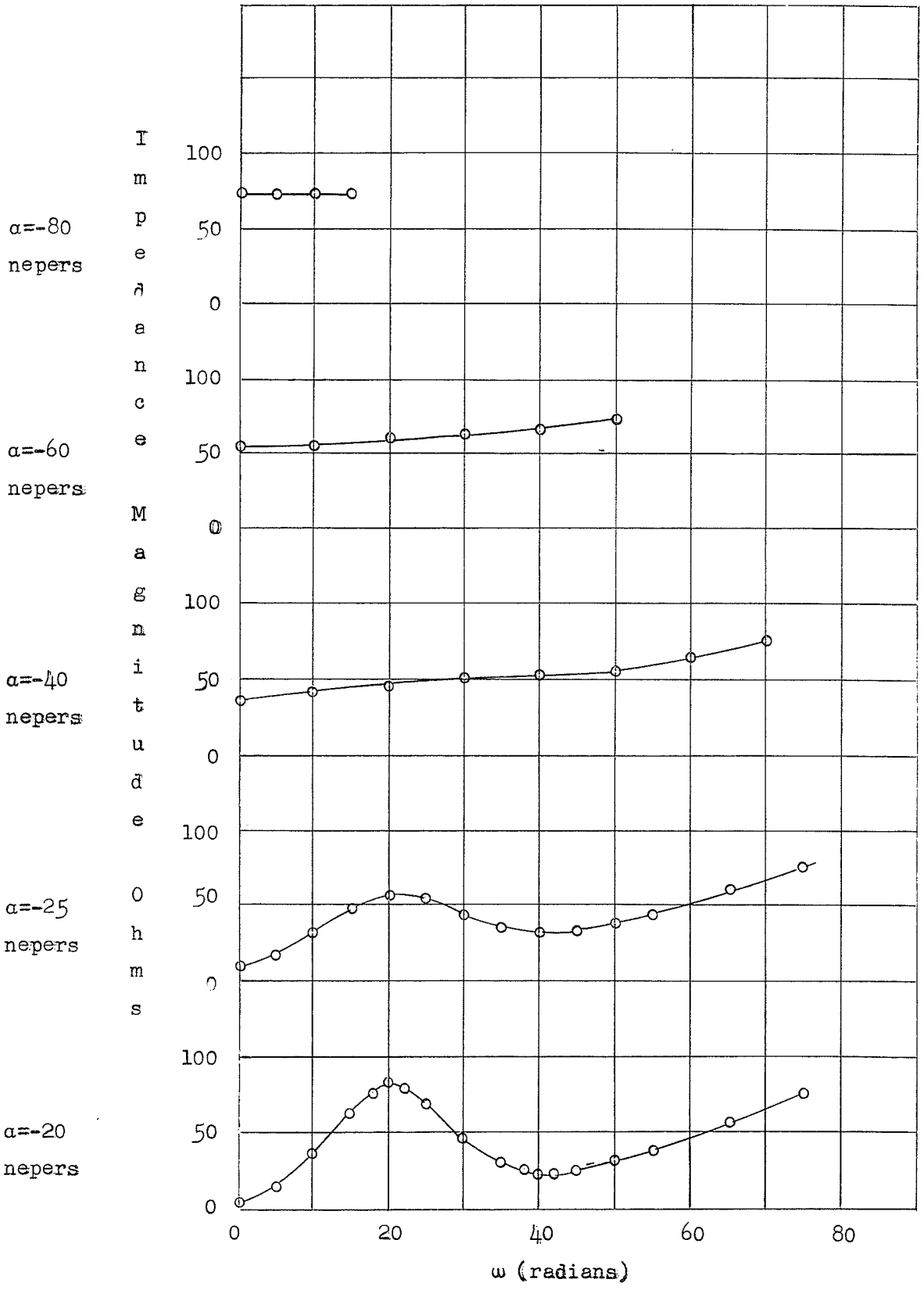

FIGURE 4.12 IMPEDANCE MAGNITUDE CROSS-SECTIONS OF THE MARK II CIRCUIT (α=-20 to α=-80)

CHAPTER 5

DISCUSSION AND CONCLUSIONS

5.1 TEST RESULTS

The experiments performed on the half plane verified that the potential analog may be used for determining the response characteristics of an immittance function to within an error of no more than 10 percent. The non-isotropic, non-linear properties of the conducting sheet along with the finite properties of the plane are the main source of error. The accuracy of probe location and the error in unit current strengths are contributing factors. Also, due to the small value of the potentials being measured, the error in the metering system for time delay and phase is not negligible.

Figure 4.2 illustrates the analog magnitude response as compared to the computed response and it is interesting to note the error reduction effect of the probe positioning correction. The uncorrected analog response has a maximum error of 10 percent while the corrected response error is 5 percent, that is, a 5 percent error reduction. The phase slope curve in figure 4.4 also closely follows the computed curve as does the phase curve in figure 4.5, the maximum error for both curves being 10 percent.

The transformed plane results agreed well within 10 percent of the computed data, the maximum error being 4 percent. The infinity effect was made negligible by locating the infinity equipotential 1 1/2 decades past the end of the second decade. This is equivalent to locating the infinity circle of the half plane at a point 50 times greater than the maximum point of frequency measurement. The transformed plane creates an origin error but this was also made negligible by locating the equipotential representing the origin 1 1/2 decades from the start of the first decade. The resulting equipotential when transformed into the half plane represents a circle having a diameter of 1 mm., that is an area which is normally covered by the first probe.

The plot of the immittance function over the complete half plane (figures 4.9, 4.10, 4.11 and 4.12) is an example of the feasability of applying the dry electrolytic tank to mapping problems. Three dimensional conditions cannot be simulated; however the quick determination of potential cross-sections is possible with the automatic scanning (tracking) system.

Lack of time did not permit an investigation into the performance of the tracking system.

5.2 SUGGESTED MODIFICATIONS

For the network function simulator to become a completely operational unit it is necessary to change the interlaced sweep system to a point-by-point scan of the real frequency axis. This will render the integration system operational. The sweep speed of the rotary switch should also be reduced to a rate which will permit the use of a pen recorder. The oscilloscope will still be capable of presenting the response as a trace.

The integrator circuit adjustments were found to be very critical and it is anticipated that with a slower sweep speed a higher gain operational amplifier will be required to perform a satisfactory integration. A suggestion is to redesign the d.c. amplifier unit using commercial plug-in operational amplifiers such as the type used in the Heathkit Analog Computer.

It is also suggested that all future measurements be carried out on a quarter plane analog. An additional tracking system should be devised for phase slope and phase measurements which will monitor the current crossing the real frequency axis directly rather than by the present potential gradient method. This would enable phase measurements to be carried out on the logarithmically transformed plane.

5.3 FURTHER APPLICATIONS

The test procedures used in this investigation were of the analysis type since it was desired to evaluate the performance of the unit as an analog. Digital computers solve analysis problems precisely and easily rendering the analog unpractical in this field. The essential value of the potential analog will be in applications to network and control system synthesis.

5.4 CONCLUSIONS

It is hoped that the material presented in this thesis will serve as the initial study in a program investigating the potential analog and its applications. The fundamental theory of the potential analog, the properties of the conducting sheet, the performance characteristics of the analog and a system for automatic scanning were presented. The future development of the tracking system and an evaluation of its characteristics should turn the study from the analog itself to its applications.

APPENDICES

APPENDIX A.1

NON-ISOTROPIC PROPERTIES OF THE CONDUCTING SHEET

A section of Teledeltos paper was cut into strips as shown in figure A.1.1 and the edge of each strip painted with silver paint to provide a good contact surface.

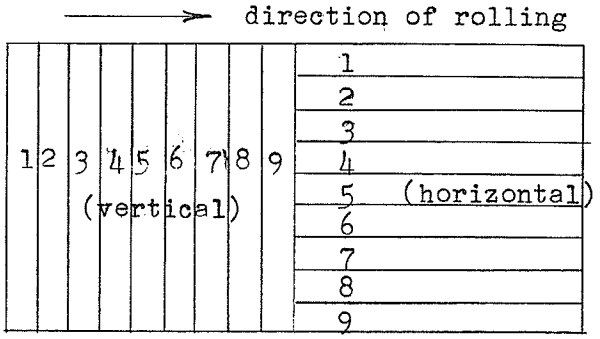

FIGURE A.1.1
TELEDELTOS SECTIONING DIAGRAM

A typical strip is illustrated below in figure A.1.2

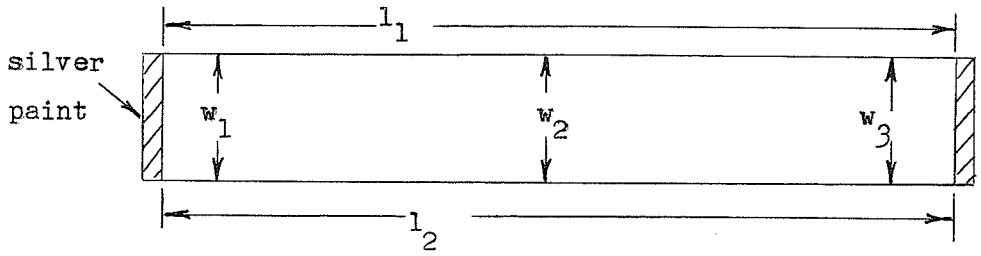

FIGURE A.1.2
TYPICAL TELEDELTOS SECTION

The resistance of each section was measured with a Wheatstone bridge and the dimensions outlined in figure A.1.2 taken and averaged.

It was found that the maximum error in the length of each strip was less than 1/3 percent and was thus negligible. The results are tabulated in table A.1.1 and indicate that the conductivity in the horizontal direction (direction of rolling) is 12 percent less than the conductivity in the vertical direction (across the width of the paper).

TABLE A.1.1

TEST DATA FOR THE TELEDELTOS SECTIONS

Section	Resistance ohms	Width (in.) w_1	w_2	w_3	Width average
1V	16024	3.774	3.768	3.771	3.771
2V	16090	3.689	3.716	3.712	3.706
3V	16077	3.740	3.735	3.757	3.744
4V	16147	3.755	3.758	3.757	3.757
5V	16050	3.742	3.763	3.775	3.760
6V	16296	3.735	3.745	3.751	3.744
7V	16168	3.766	3.749	3.740	3.752
8V	15935	3.753	3.748	3.733	3.745
9V	15845	3.798	3.772	3.773	3.781
	$V=\Sigma R \times w_{av.}$ = 5,425,227				
1H	14952	3.755	3.766	3.787	3.769
2H	15295	3.751	3.745	3.745	3.747
3H	15185	3.739	3.732	3.725	3.732
4H	15007	3.768	3.766	3.772	3.769
5H	14345	3.781	3.767	3.750	3.766
6H	14043	3.775	3.763	3.764	3.767
7H	13893	3.757	3.750	3.753	3.753
8H	13349	3.730	3.724	3.726	3.727
9H	12740	3.735	3.726	3.720	3.727
	$H=\Sigma R \times w_{av.}$ = 4,831,936				

then: $H/V = 0.8906$ $V/H = 1.1228$

A second experiment was performed which involved cutting the Teledeltos sheet into 11 inch squares as is shown in figure A.1.3 . Alternate squares were painted with silver paint on their vertical edges, the remaining squares were painted on their horizontal edges. The resistance of each square was measured with a Wheatstone bridge the results of which are indicated in figure A.1.3. The ratio of the mean vertical to mean horizontal resistance was found to be 1.14 $\pm$ 0.036 which confirms the results of the first test.

→ 1454 ohms A'	1650 ohms B' ↑	→ 1404 ohms A'	1584 ohms B' ↑
1773 ohms ↑	→ 1547 ohms	1753 ohms ↑	→ 1491 ohms
→ 1603 ohms A	1833 ohms B ↑	→ 1584 ohms A	1758 ohms B ↑

FIGURE A.1.3
TELEDELTOS SQUARE SECTIONS AND RESISTANCES

Figure A.1.3 was studied and it was noted that the conductivity remained fairly constant along the length of the sheet but changed across the width. Thus from figure A.1.3 it may be noted that A=A and B=B (approximately) but A≠A' and B≠B'. This observation prompted an investigation into the linearity of the sheet conductivity. The results are recorded in appendix A.3.

APPENDIX A.2

NON-ISOTROPIC SHEET CORRECTION (SM)

In the conducting sheet we have that:

$$\underline{I} = \underline{\underline{\sigma}}\,\underline{E} \qquad \text{A.2.1}$$

where $\underline{\underline{\sigma}}$ is the conductance dyadic.

Therefore:
$$I_x = \sigma_{xx} E_x$$
$$I_y = \sigma_{yy} E_y \qquad \text{A.2.2}$$

since the non-diagonal terms of $\underline{\underline{\sigma}}$ are zero due to the non-interaction of the two field components in current production.

Now everywhere in the sheet except at the probe positions:

$$\nabla \cdot \underline{I} = 0 \qquad \text{A.2.3}$$

so
$$\nabla \cdot (\underline{\underline{\sigma}}\,\underline{E}) = 0 \qquad \text{A.2.4}$$

or
$$\nabla \cdot (\underline{\underline{\sigma}} \nabla \phi) = 0 \qquad \text{A.2.5}$$

That is:
$$\frac{\partial}{\partial x} \left(\sigma_{xx} \frac{\partial \phi}{\partial x} \right) + \frac{\partial}{\partial y} \left(\sigma_{yy} \frac{\partial \phi}{\partial y} \right) = 0 \qquad \text{A.2.6}$$

Now assuming that σ_{xx} and σ_{yy} are independant of position equation A.2.6 becomes:

$$\sigma_{xx} \frac{\partial^2 \phi}{\partial x^2} + \sigma_{yy} \frac{\partial^2 \phi}{\partial y^2} = 0 \qquad \text{A.2.7}$$

that is
$$\frac{\partial^2 \phi}{\partial x^2} + \frac{\partial^2 \phi}{\partial y'^2} = 0 \qquad \text{A.2.8}$$

where
$$\partial y' = \sqrt{\frac{\sigma_{xx}}{\sigma_{yy}}}\, \partial y \qquad \text{A.2.9}$$

This states that Laplace's equation is satisfied in the x, y' co-ordinate system. We may also set up an x', y co-ordinate system to satisfy the specified conditions where:

$$x' = \sqrt{\frac{\sigma_{yy}}{\sigma_{xx}}}\ x \qquad \text{A.2.10}$$

The infinity point is simulated in this system by a circle

$$x^2 + y'^2 = R^2 \qquad \text{A.2.11}$$

But in the co-ordinates of the conducting sheet (x,y) this circle becomes:

$$\frac{x^2}{R^2} + \frac{y^2}{\frac{\sigma_{yy}}{\sigma_{xx}} R^2} = 1 \qquad \text{A.2.12}$$

which is an ellipse with semi-axes R and $\sqrt{\frac{\sigma_{yy}}{\sigma_{xx}}}\ R$ in the x and y directions respectively.

Now from the test results of appendix A.1 we have that:

$$\frac{\sigma_{xx}}{\sigma_{yy}} = 1.12 \pm 0.02$$

Hence the semi-axes of the ellipse are R and 0.944 R and

$$x' = \sqrt{1.12}\ x$$

APPENDIX A.3

LINEARITY OF THE SHEET CONDUCTIVITY

Three strips of Teledeltos paper 5 inches in width were cut out of the roll and the edge of each strip painted with silver paint. A current of 6 milliamperes was passed through the sheet and the potential along the strip measured using one end as the reference. Figure A.3.1 shows the experimental setup and sheet dimensions.

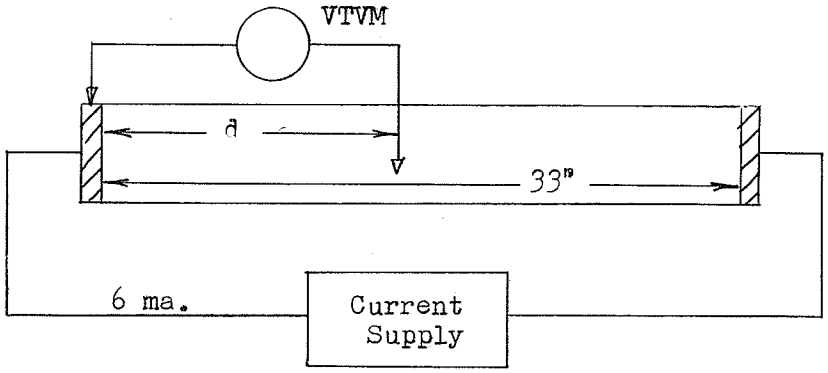

FIGURE A.3.1
EXPERIMENTAL SETUP FOR DETERMINING THE CONDUCTIVITY LINEARITY

The test results are given in table A.3.1 along with the computed deviation of the sheet conductivity.

The results of this test were plotted (figure A.3.2) and show that the conductivity changes across the sheet by 10 percent. No correction for non-linearity was applied since it was felt that a compensting transformation of co-ordinates would have been too involved and further that over the "working" region of the plane (region of probe location and potential measurement) the conductivity changes by less than 5 percent and the error thus introduced could be accepted.

The deviation at any point is the percentage change of V/d at that point as read from the curve with respect to the curve value at d=0.

TABLE A.3.1

TEST DATA FOR SHEET CONDUCTIVITY LINEARITY

d	Potential (volts)			Average V/d	Deviation
(inches)	sheet 1	sheet 2	sheet 3	(volts/in.)	(percent)
1	1.45	1.50	1.50	1.483	
2	3.00	2.92	3.01	1.488	
3	4.55	4.43	4.45	1.492	
4	6.00	6.00	6.00	1.500	
5	7.55	7.50	7.55	1.506	2.00
6	9.10	9.00	9.10	1.513	
7	10.65	10.60	10.60	1.519	
8	12.2	12.1	12.2	1.521	
9	14.0	13.9	13.9	1.548	
10	15.4	15.4	15.1	1.530	3.95
11	16.9	17.0	16.9	1.539	
12	18.5	18.4	18.4	1.536	
13	20.0	20.1	20.0	1.541	
14	21.8	21.8	21.7	1.555	
15	23.2	23.2	23.1	1.545	5.64
16	25.0	24.9	24.9	1.558	
17	26.5	26.5	26.4	1.557	
18	28.2	28.1	28.0	1.561	
19	29.9	29.5	29.7	1.564	
20	31.5	31.3	31.2	1.567	7.20
21	33.4	33.1	33.1	1.581	
22	35.1	34.8	34.9	1.588	
23	37.0	36.5	36.2	1.590	
24	38.8	38.1	38.2	1.598	
25	40.3	39.8	40.0	1.601	8.40
26	42.0	41.5	41.7	1.605	
27	43.8	43.1	43.3	1.607	
28	45.5	44.7	45.1	1.611	
29	47.0	46.2	46.7	1.609	
30	48.8	48.0	50.0	1.611	9.50
31	50.6	49.6	50.0	1.615	

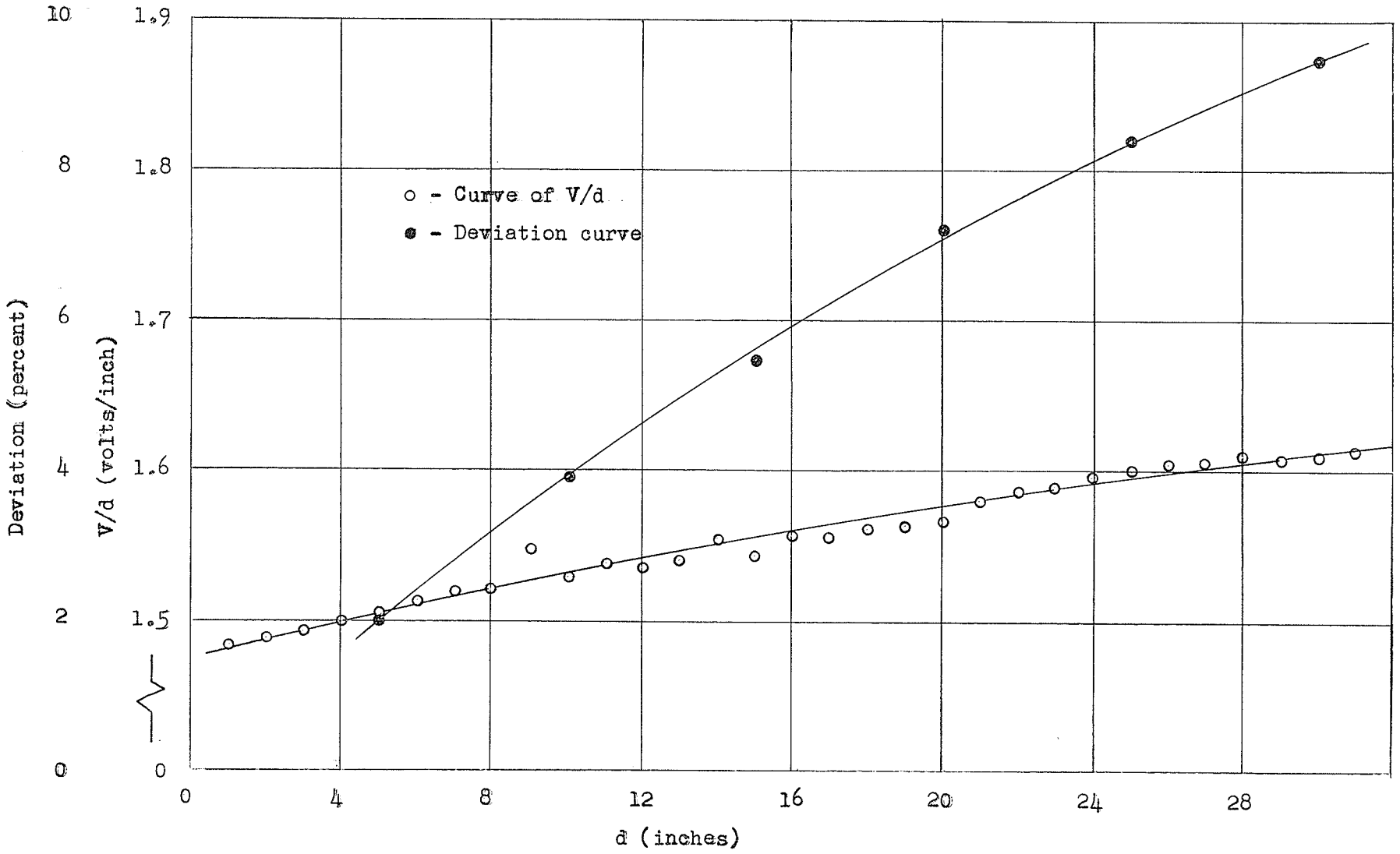

FIGURE A.3.2 CONDUCTIVITY LINEARITY OF THE TELEDELTOS SHEET

APPENDIX A.4

THE EFFECT OF CURRENT DENSITY ON SHEET CONDUCTIVITY

A strip of Teledeltos paper, painted with silver paint on its two edges, was prepared for test as shown in figure A.4.1.

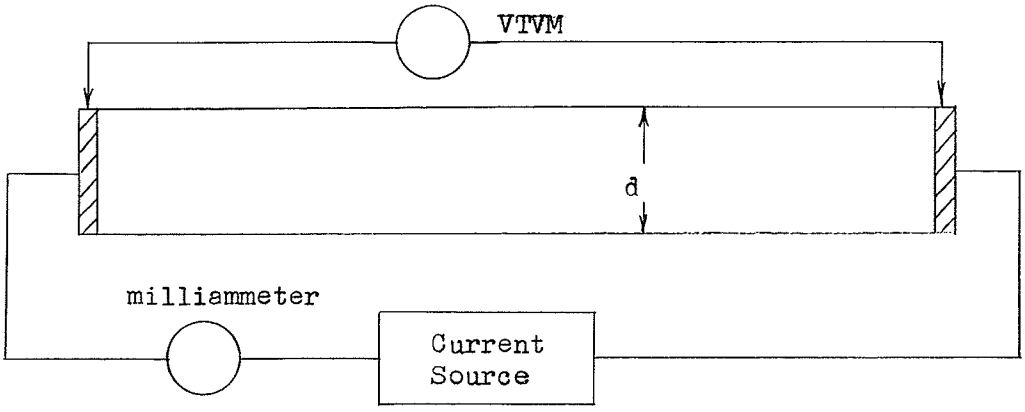

FIGURE A.4.1

TEST SETUP FOR DETERMINING CONDUCTIVITY CHANGE WITH CURRENT DENSITY

The potential across the sheet was determined for various values of current input. Data is given in table A.4.1. The sheet resistance was plotted against the current density. The resulting curve in figure A.4.2 then illustrates the change of sheet conductivity with current density.

The normal unit current strength of a probe is approximately 4 milliamperes. Thus at a distance of 1/8 inch from the probe center the current density is approximately 5 ma./in. and the conductivity 4 percent greater than that in a region of low current density. At 1/4 inch from the probe center the conductivity is greater by only 1 percent.

The error introduced by conductivity change due to current density is in general small and negligible.

The preceding data was computed in the following manner. At a distance of 1/8 inch from the probe center the current passes through a surface length of $2\pi \times 1/8$ or 0.785 inches which corresponds to a current of $\frac{11}{0.785} \times 4 = 56.0$ ma (5.09 ma/inch) for an 11 inch width. Now from figure A.4.2 the resistance change (and thus also the conductivity) was computed to be approximately 4 percent. The procedure for the 1/4 inch distance is similar.

TABLE A.4.1

CONDUCTIVITY CHANGE WITH CURRENT DENSITY

Current (ma.)	Potential (volts)	V/I (kilohms)	Current (ma.)	Potential (volts)	V/I (kilohms)
d= 11 inches					
2	3.48	1.740	32	55.0	1.718
4	6.95	1.737	34	58.5	1.720
6	10.55	1.760	36	61.5	1.707
8	13.95	1.742			
10	17.5	1.750	d = 5 1/2 inches		
12	21.0	1.750	18	61.5	1.707
14	24.3	1.737	20	68.0	1.700
16	27.8	1.738	22	74.5	1.693
18	31.1	1.728	24	81.0	1.688
20	34.7	1.734	26	87.5	1.682
22	38.0	1.727	28	93.5	1.669
24	41.3	1.720	30	100.0	1.666
26	44.8	1.723	32	106.5	1.614
28	47.9	1.710	34	111.5	1.640
30	52.0	1.732	36	117.5	1.632

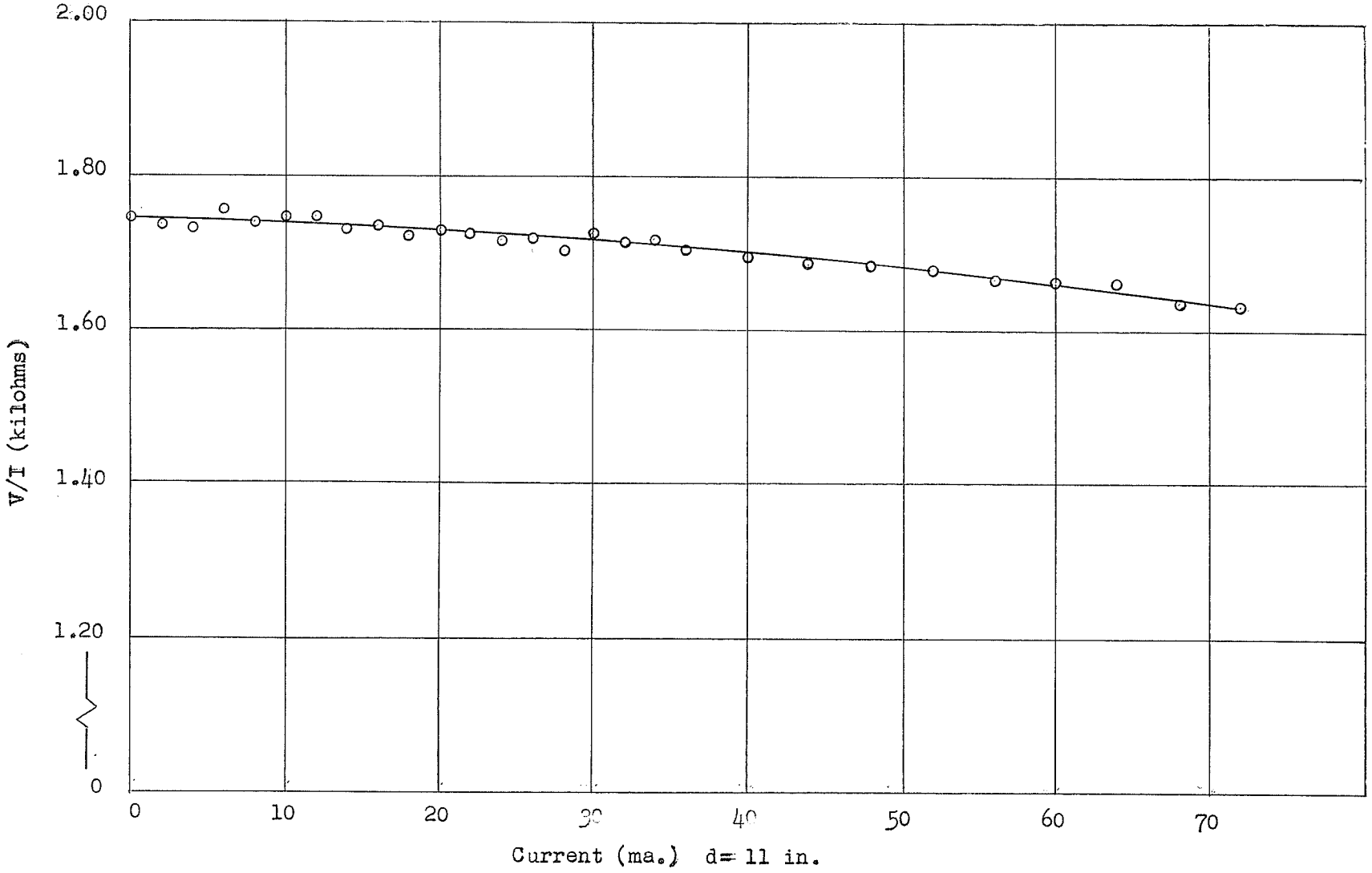

FIGURE A.4.2 CHANGE OF SHEET RESISTANCE WITH CURRENT DENSITY

APPENDIX B.1

ANALYSIS OF THE POLE-ZERO REGULATOR

A fundamental schematic diagram of the regulator unit is shown below in figure B.1.1.

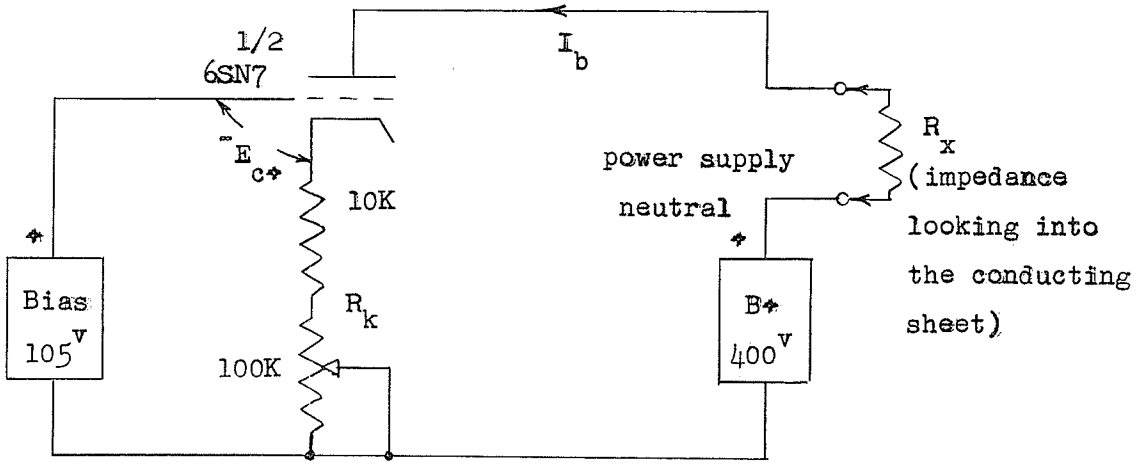

FIGURE B.1.1
FUNDAMENTAL SCHEMATIC OF A SINGLE REGULATOR UNIT

A high positive bias imposed on the tube forces operation on an almost flat bias line which may be computed from:

$$E_c = I_p R_k - 105 \qquad \text{B.1.1}$$

When the regulator unit is short-circuited ($R_x = 0$) the tube operates at some quiescent point, say Q_1. For a load of R_x the operation will be at some other point Q_2, the load lines being computed from:

$$E_b = 400 - I_b (R_k + R_x) \qquad \text{B.1.2}$$

Figure B.1.2 shows the graphical solution.

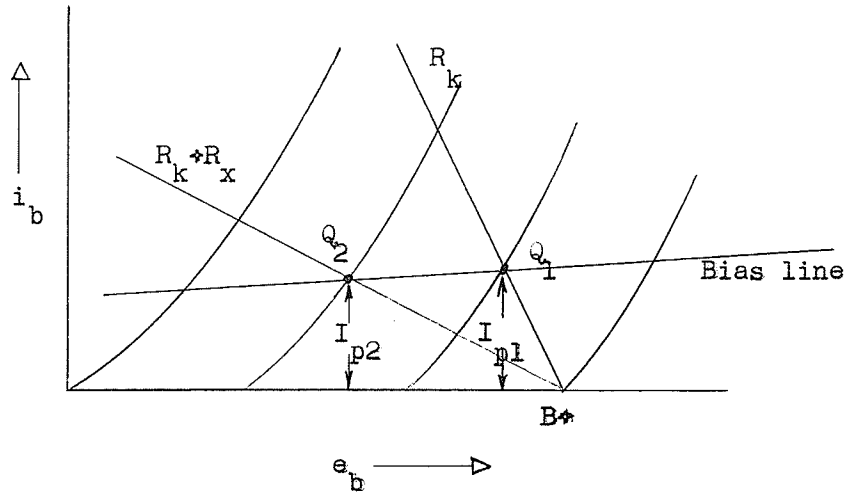

FIGURE B.1.2

A GRAPHICAL SOLUTION FOR THE REGULATOR UNIT OPERATION

The current regulation as determined from figure B.1.2 is simply:

$$\frac{I_{p1} - I_{p2}}{I_{p1}} \times 100 \text{ (percent)} \qquad \text{B.1.3}$$

An analysis of the regulator operation at a typical current value follows. We had:

$$E_c = I_b R_k - 105 \qquad \text{B.1.1}$$

and

$$E_b = 400 - I_b(R_k + R_x) \qquad \text{B.1.2}$$

Now for $R_x = 0$:

$$E_b = 400 - I_b R_k$$

and substituting for $I_b R_k$ from equation B.1.1 we have:

$$E_b = 400 - E_c - 105 = 295 - E_c \qquad \text{B.1.4}$$

or approximately $E_b = 295$ for $R_x = 0$

For an operating value of say 5 milliamperes the load line may now be drawn for $R_x = 0$ on the plate characteristic curves of figure B.1.3. At the operating point the bias is read as -12 volts and using equation B.1.1 we have:

$$12 = 5\times10^{-3} R_k - 105$$

solving $$R_k = \frac{105 + 12}{5\times10^{-3}} = 23.4K$$

The bias equation is then:

$$E_c = I_b \times 23{,}400 - 105$$

which allows the bias line to be drawn on the characteristic curves.

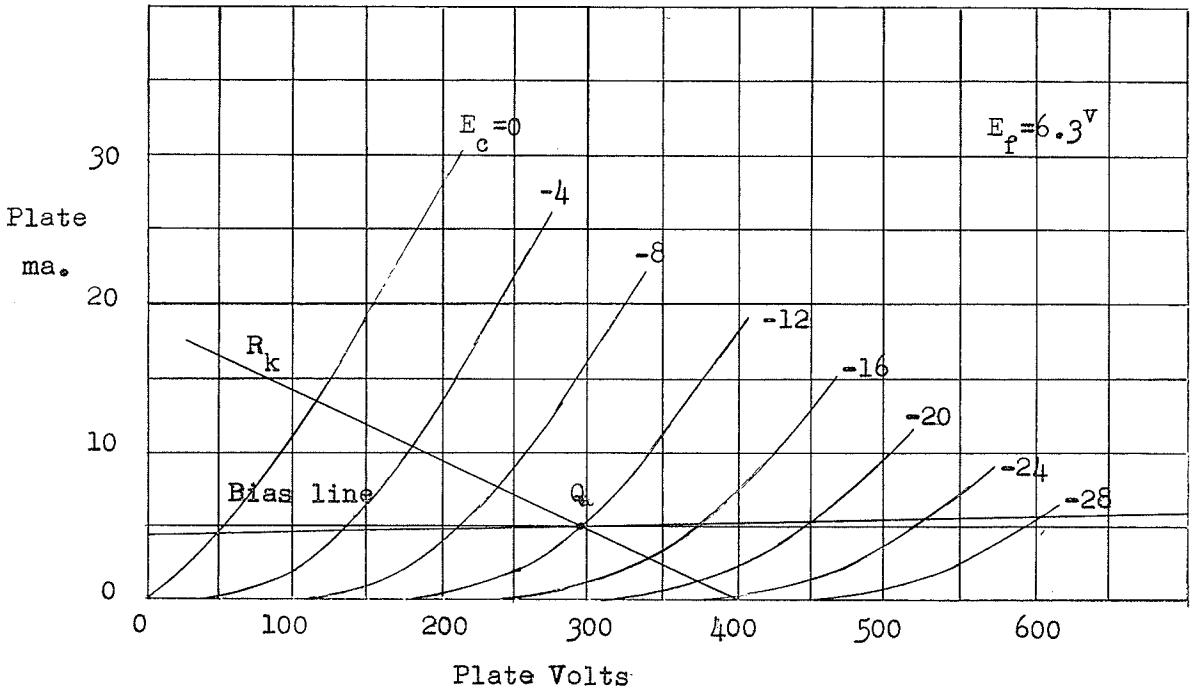

FIGURE B.1.3

AVERAGE PLATE CHARACTERISTICS FOR THE 6SN7

It should be noted that:

$$E_b = 400 - I_b R_k - I_b R_x \qquad \text{B.1.2}$$

and in particular for $R_x = 0$

$$E_{b1} = 400 - I_{b1}R_k$$

At some other point of operation

$$E_{b2} = 400 - I_{b2}R_k - I_{b2}R_x$$

However I_{b1} approximately equals I_{b2} and so:

$$E_{b2} = 400 - I_{b1}R_k - I_{b1}R_x$$

Thus $$\Delta E_b = E_{b1} - E_{b2} = I_{b1}R_x$$

that is $$R_x = \frac{\Delta E_b}{I_{b1}} \qquad \text{B.1.5}$$

From the curves of figure B.1.3 we see that:

at $E_b = 700$ volts $I_b = 5.7$ ma.

and at $E_b = 0$ volts $I_b = 4.3$ ma.

That is, the plate voltage changes by 500 volts for each milliampere of current change. For a desired regulation of 2 percent at the 5 ma. operating current the maximum current drop that can be tolerated is 0.1 ma. Thus:

$$\Delta E_b = 0.1 \times 500 = 50 \text{ volts}$$

and $$R_x = \frac{50}{5 \times 10^{-3}} = 10K$$

The impedance looking into the plane must not change by more than 10K from its initial setting. The maximum sheet resistances are always well below this value. Appendix B.2 verifies experimentally the results presented here.

APPENDIX B.2

TEST DATA FOR REGULATOR UNIT OPERATION

The regulation of the pole-zero current unit was checked by placing a series combination of a milliammeter and 10 kilohm resistance between each pole and zero output and the neutral point in the power supply. The current was adjusted with the resistance shorted and the change observed when the short was removed. The regulation was calculated and is tabulated along with the test data in table B.2.1.

TABLE B.2.1

REGULATION DATA FOR THE REGULATOR UNITS

Unit	I (ma.) R_x=0	I (ma.) R_x=10K	Regulation (percent)	Unit	I (ma.) R_x=0	I (ma.) R_x=10K	Regulation (percent)
P1	2	1.99	0.5	Z1	2	1.98	1.0
	5	4.93	1.4		5	4.91	1.8
	8	7.80	2.5		8	7.80	2.5
P2	2	1.99	0.5	Z2	2	1.98	1.0
	5	4.91	1.8		5	4.94	1.2
	8	7.80	2.5		8	7.78	2.75
P3	2	1.99	0.5	Z3	2	1.98	1.0
	5	4.91	1.8		5	4.94	1.2
	8	7.80	2.5		8	7.80	2.5
P4	2	1.99	0.5	Z4	2	1.98	1.0
	5	4.92	1.6		5	4.90	2.0
	8	7.75	3.1		8	7.80	2.5
P5	2	1.99	0.5	Z5	2	1.98	1.0
	5	4.91	1.8		5	4.91	1.0
	8	7.80	2.5		8	7.77	2.9
P6	2	1.99	0.5	Z6	2	1.98	1.0
	5	4.90	2.0		5	4.93	1.4
	8	7.80	2.5		8	7.78	2.75

APPENDIX C

THE D.C. AMPLIFIER UNIT TEST DATA

The following tests were run on the d.c. amplifier unit and monitor oscilloscope to check linearity and sensitivity.

TEST (A) ADDER CIRCUIT

The A and B inputs were both grounded and the operational switch placed in the A+B position. The adder zero-adjust was set to give zero adder output. A d.c. signal was placed at the A input and the output of the adder monitored with a VTVM. The results are given in table C.1 and a plot of the output versus the input (figure C.1) shows that the adder has a linear operating range of from -6 volts to +6 volts.

TABLE C.1

TEST DATA FOR ADDER CIRCUIT

A input volts	Adder Output volts	A input volts	Adder Output volts
-1.0	+0.36	+1.0	-0.42
-2.0	+0.74	+2.0	-0.90
-3.0	+1.15	+3.0	-1.42
-4.0	+1.55	+4.0	-1.90
-5.0	+1.88	+5.0	-2.35
-6.0	+2.25	+6.0	-2.80
-8.0	+2.70	+7.0	-2.80

TEST (B) DIFFERENCE CIRCUIT

The A and B inputs were both grounded and the operational switch placed in the A+B position. The adder output was adjusted to zero. The operational switch was next placed in the A-B position and the adder output set to zero with the inverter zero control. A d.c. signal of several volts was placed on the A and B inputs and the adder output

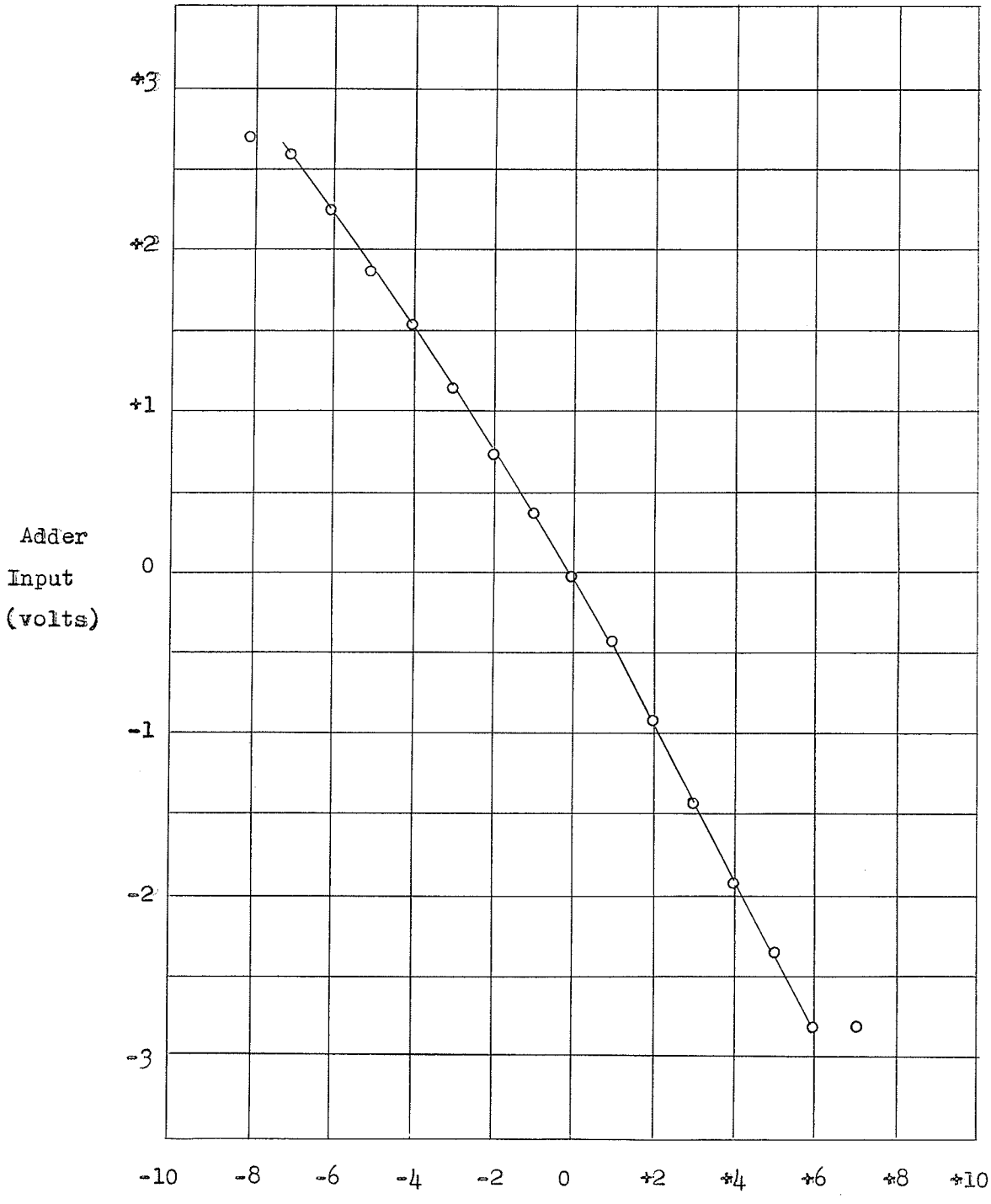

FIGURE C.1 ADDER CIRCUIT OPERATING CHARACTERISTICS

again set to zero with the inverter gain control. The output from the adder circuit was taken for a range of inputs to the A and B sections. Table C.2 gives the test results and show that the system remains linear to within 20 millivolts for a range of inputs from +7 volts to -7 volts.

TABLE C.2

TEST DATA FOR THE DIFFERENCE CIRCUIT

A and B Input (volts)	Adder Output (volts)	A and B Input (volts)	Adder Output (volts)
0.0	+0.02	0.0	+0.03
-1.0	+0.02	+1.0	+0.02
-2.0	+0.03	+2.0	+0.00
-3.0	+0.03	+3.0	-0.02
-4.0	+0.04	+4.0	-0.04
-5.0	+0.03	+5.0	-0.04
-6.0	+0.04	+6.0	-0.05
-7.0	+0.02	+7.0	-0.07
-8.0	+0.02	+8.0	-0.13

The integration circuit was not tested since the sweep system of the present unit would permit only the immittance magnitude and phase slope to be observed.

TEST (C) HORIZONTAL AND VERTICAL DEFLECTION AMPLIFIERS

A d.c. signal was supplied to the horizontal and vertical deflection amplifiers and the output potential and oscilloscope deflection measured. Table C.3 gives the test results. Figure C.2 is a plot of the response characteristics of the vertical amplifier while figure C.3 shows the characteristic of the horizontal unit. The curves show that the amplifiers are linear over a range of inputs from + 1 volt to - 1 volt (sufficient to cause full scale spot deflection).

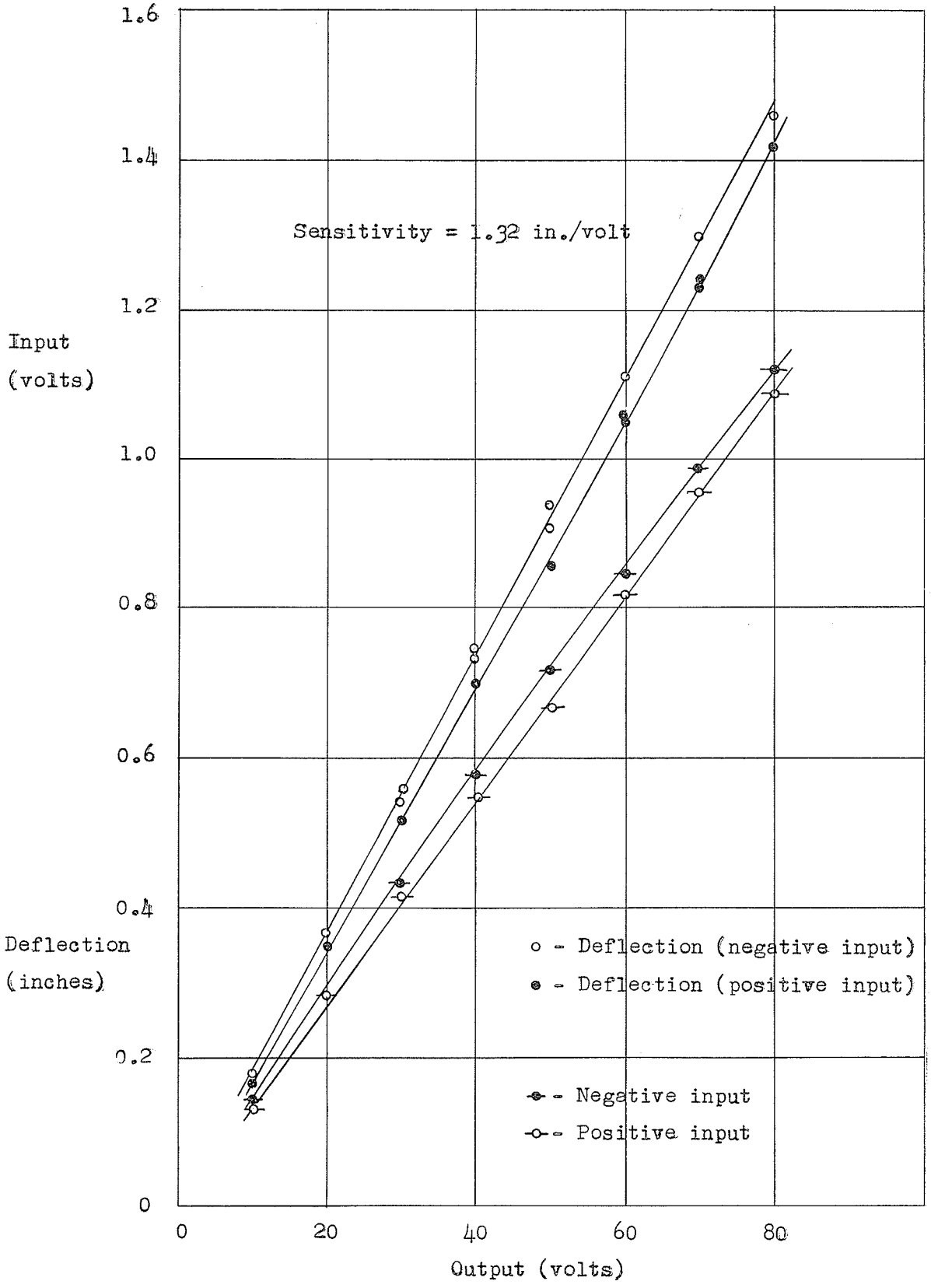

FIGURE C.2 VERTICAL DEFLECTION AMPLIFIER RESPONSE

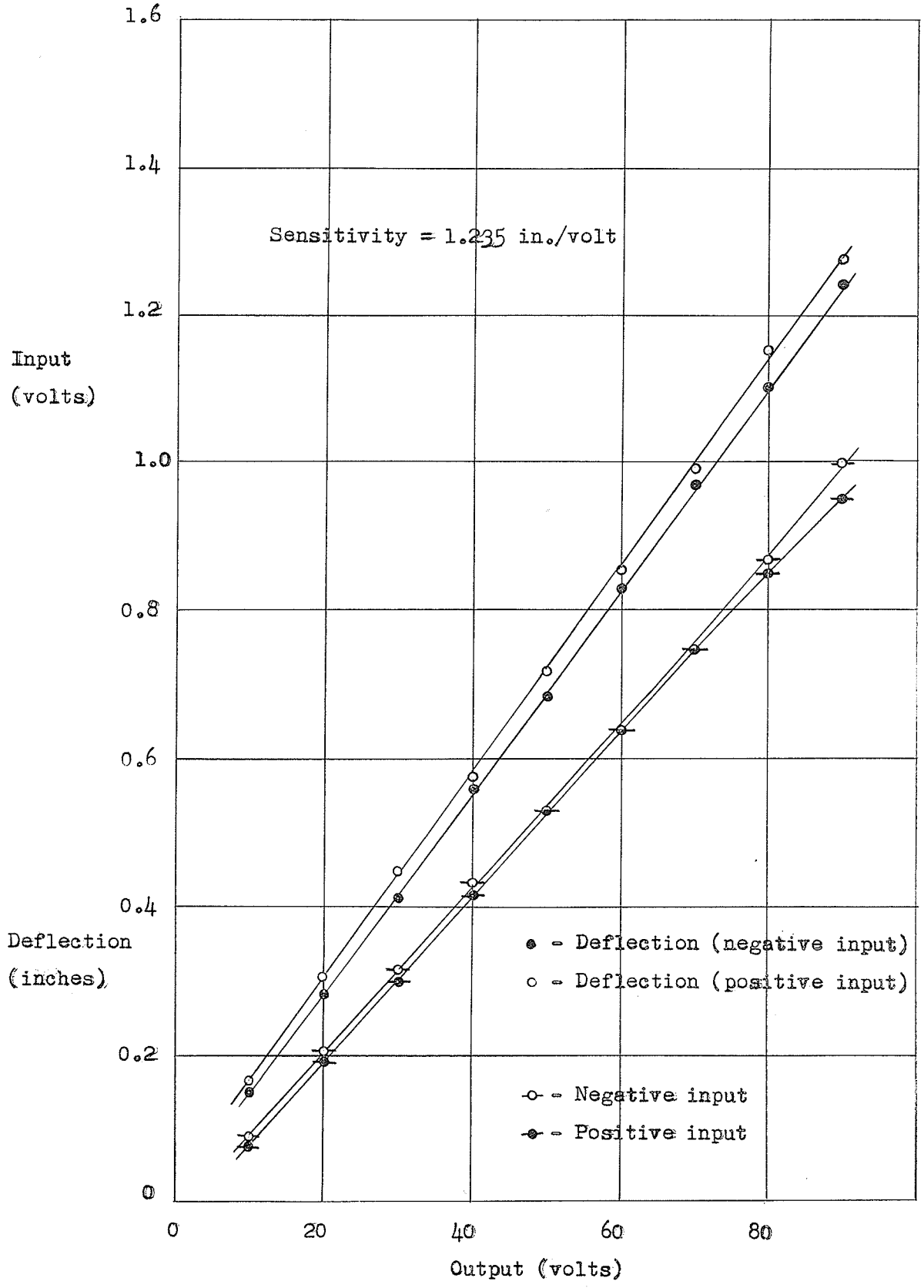

FIGURE C.3 HORIZONTAL DEFLECTION AMPLIFIER RESPONSE

TABLE C.3

TEST DATA FOR THE DEFLECTION AMPLIFIERS

VERTICAL			HORIZONTAL		
Input (volts)	Output (volts)	Deflection (inches)	Input (volts)	Output (volts)	Deflection (inches)
+0.144	10.0	0.160	+0.09	10.0	0.164
+0.283	20.0	0.350	+0.19	20.0	0.304
+0.415	30.0	0.520	+0.30	30.0	0.446
+0.550	40.0	0.700	+0.42	40.0	0.574
+0.670	50.0	0.860	+0.53	50.0	0.716
+0.820	60.0	1.060	+0.64	60.0	0.856
+0.955	70.0	1.230	+0.75	70.0	0.992
+1.085	80.0	1.420	+0.87	80.0	1.140
-0.134	10.0	0.170	+1.00	90.0	1.272
-0.288	20.0	0.370	-0.08	10.0	0.140
-0.434	30.0	0.560	-0.20	20.0	0.280
-0.580	40.0	0.750	-0.31	30.0	0.410
-0.720	50.0	0.940	-0.43	40.0	0.550
-0.850	60.0	1.110	-0.53	50.0	0.680
-0.990	70.0	1.300	-0.64	60.0	0.830
-1.120	80.0	1.460	-0.74	70.0	0.970
			-0.85	80.0	1.100
			-0.96	90.0	1.240

APPENDIX D.1

EXAMPLE OF AN INFINITY ERROR CALCULATION

Let us assume an immittance function having the form

$$F(s) = \frac{1}{s-s_1} \qquad \text{D.1.1}$$

where s_1 is a pole on the negative real axis and having a magnitude of half the distance to the infinity circle. We may write equation D.1.1 as:

$$F(s) = \frac{1}{s + \frac{R}{2}} \qquad \text{D.1.2}$$

The effect of the finite "infinity" circle is to cause an image zero to appear at $s = -2R$ which we shall call s_1'. Figure D.1.1 illustrates the pole-zero configuration in the finite "infinity" plane.

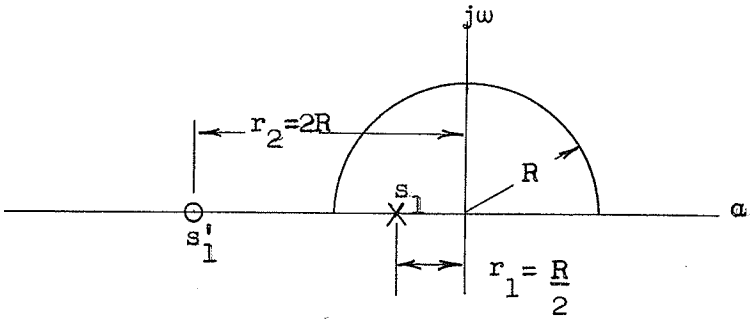

$$r_1 r_2 = R^2$$

FIGURE D.1.1

POLE-ZERO CONFIGURATION CREATED BY $F(s) = \frac{1}{s + \frac{R}{2}}$

IN THE FINITE "INFINITY" PLANE

This configuration is representative of a new immittance function

$$F'(s) = \frac{s + 2R}{s + \frac{R}{2}} \qquad \text{D.1.3}$$

In terms of the logarithm of the magnitude of F(s) we have:

$$\log |F(s)| = - \log |s-s_1| \qquad \text{D.1.4}$$

and for F'(s):

$$\log |F'(s)| = \log|s-s_1'| - \log |s-s_1| \qquad \text{D.1.5}$$

At any particular reference point the difference between these two functions may be compensated for by a d.c. bias potential.

That is:

$$\log |F'(s)| - |\log F(s)| = \log |s-s_1'| \qquad \text{D.1.6}$$

and at s_o $\qquad \log |s_o-s_1'| =$ some constant, say M $\qquad$ D.1.7

At any other frequency point, s, the error is then:

$$\mathcal{E}\,[\log |F(s)| + M\,] = \log |s - s_1'| - \log |s_o - s_1'| \qquad \text{D.1.8}$$

In particular if $s_o = 0$ and $s = j\frac{R}{2}$ then the error is:

$$\log \sqrt{(R/2)^2 + (2R)^2} - \log 2R = \log \sqrt{\frac{17/4}{2}}$$

$$= 0.01284$$

Also at $s = j\frac{R}{2}$

$$\log |F(s)| + M = - \log |s - s_1| + \log |s_o - s_1'|$$

$$= - \log \left| j\frac{R}{2} + \frac{R}{2} \right| + \log 2R$$

$$= \log 2\sqrt{2} = 0.45148$$

The percentage error is thus:

$$\frac{0.01284}{0.45148} \times 100 = 2.86 \text{ percent}$$

APPENDIX D.2

OPERATING PROCEDURE

(A) POLE-ZERO ADJUSTMENT

1) Locate the probes in the pole-zero positions.

2) Turn on the power to the pole-zero unit after checking to make sure that the switches on the distribution unit are in the OFF position.

3) After a minute warmup turn the bias units on.

4) By means of the distribution unit switch on one pole and one zero of the same current strength.

5) Switch the POLE-ZERO switch to POLE and push the appropriate button of the push button switch to insert the milliammmeter.

6) Adjust the pole current to the desired unit value by means of the corresponding potentiometer control.

7) Release the push button switch and then switch the POLE-ZERO switch to ZERO.

8) Adjust the zero current in the same manner.

9) Repeat for each pole-zero set.

10) After all the poles and zeros have been inserted the currents should be checked and a final adjustment made.

(B) MAGNITUDE OPERATION

1) Turn the d.c. power supply and d.c. amplifier unit filaments on and after a one minute warmup turn on the 400 volt and 250 volt plus and minus supplies.

2) Place the CALIBRATE-USE switch to CALIBRATE and the GROUND- ⏚ switch to GROUND.

3) Place the d.c. amplifier unit operational switch to either the A or B position.

4) Turn the oscilloscope power on and after a minute warmup adjust the spot with the INTENSITY, FOCUS and ASTIGMATISM controls.

5) Start the sweep motor and adjust the spot trace so that it is centered using the HORIZONTAL and VERTICAL CENTERING controls. The trace width is adjusted with the HORIZONTAL GAIN control.

6) Turn the CALIBRATE-USE switch to USE and increase the VERTICAL GAIN control. Then bring the start of the spot trace to the same horizontal level as was used in part (5) with the external battery reference level control.

7) Place a single pole at $s = -1$ and a d.c. marker voltage on the probe located at $\omega = 1$.

8) Adjust the VERTICAL GAIN so that the signal sag at the marker pip is 3 units below the trace reference level. The vertical deflection is now calibrated for one decibel per division of deflection. Note here that any other calibrating scale listed in table 3.1 may be used.

9) Place any desired pole-zero configuration on the conducting sheet and again adjust the plane bias so that the start of the spot trace is at the reference level. The observed waveform is the magnitude response of the immittance function represented by the pole-zero configuration in decibels with respect to the impedance magnitude at zero frequency.

(C) PHASE SLOPE OPERATION

1) Follow instructions (1) through to (5) from section (B).

2) Place the amplifier operational switch in the A + B position and adjust the ADDER ZERO control so that the oscilloscope trace returns to its center position.

3) Turn the amplifier operational switch to the A -B position and adjust the oscilloscope trace to its center position with the INVERTER ZERO.

4) Turn the GROUND - + switch to + and again adjust the oscilloscope trace to its center position with the INVERTER GAIN.

5) Place a single zero at s = -1 and a d.c. marker pip at the required probe location given in table 3.2 for the desired calibration level.

6) Turn the USE-CALIBRATE switch to USE and adjust the VERTICAL GAIN control so that the signal deflection at the marker pip is scaled to the computed time delay in table 3.2.

7) Place the required pole-zero configuration on the conducting sheet and observe the oscilloscope response. The observed waveform is the time delay response of the immittance function.

(C) PHASE RESPONSE

Note: The procedure outlined in this section is not applicable to the present unit due to the interlaced scanning system.

1) Follow instructions (1) to (4) of section (C).

2) Place the operational switch in the INTEGRATE position and adjust the spot of the oscilloscope trace to the center position with the INTEGRATOR ZERO.

3) Place a zero at s = -1 and a d.c. marker voltage at the required probe location listed in table 3.3 for the desired calibration level.

4) Turn the CALIBRATE-USE switch to USE and adjust the VERTICAL GAIN so that the signal deflection at the marker point is related to the computed phase in table 3.3.

5) Place the required pole-zero configuration on the plane and observe the calibrated phase response of the immittance function.

APPENDIX E

TABLES OF TEST DATA

TABLE E.1

COMPUTED IMPEDANCE MAGNITUDE, TIME DELAY AND PHASE RESPONSE OF THE MARK II CIRCUIT

ω radians	Magnitude ohms	Time Delay msec.	Phase degrees	ω radians	Magnitude ohms	Time Delay msec.	Phase degrees
0	68.00	+21.77	0.00	42	25.82	+87.20	+12.47
2	68.52	+20.64	+ 2.43	44	26.15	+78.99	+22.08
4	70.09	+17.27	+ 4.64	46	27.24	+67.68	+30.46
6	72.68	+11.68	+ 5.29	48	28.86	+56.22	+37.57
8	76.24	+ 3.86	+ 7.23	50	30.84	+46.12	+43.41
10	80.62	- 6.15	+ 7.10	52	33.05	+37.81	+48.25
12	85.53	-18.23	+ 5.72	54	35.39	+31.18	+51.83
14	90.37	-31.73	+ 2.82	56	37.81	+25.95	+55.43
16	94.14	-45.00	- 1.54	58	40.27	+21.84	+58.16
18	95.50	-55.00	- 7.33	60	42.76	+18.57	+60.48
20	93.30	-58.18	-13.88	62	45.24	+15.96	+62.43
22	87.32	-52.77	-20.29	64	47.72	+13.85	+64.10
24	78.57	-40.15	-25.68	66	50.19	+12.13	+65.60
26	68.62	-23.43	-29.31	68	52.64	+10.71	+66.91
28	58.84	- 5.14	-30.98	70	55.07	+ 9.53	+68.08
30	50.00	+13.54	-30.49	72	57.49	+ 8.54	+69.09
32	42.47	+32.36	-27.87	74	59.88	+ 7.69	+70.03
34	36.36	+51.08	-23.06	76	62.26	+ 6.98	+70.86
36	31.68	+68.52	-16.22	78	64.62	+ 6.36	+71.62
38	28.42	+82.15	- 7.56				
40	26.51	+88.84	+ 2.34				

TABLE E.2

HALF PLANE CALIBRATION DATA

Distance cm.	Potential volts	Distance cm.	Potential volts	Distance cm.	Potential volts
1	4.26	26	1.065	51	0.394
2	3.61	27	1.025	52	- -
3	3.20	28	0.985	53	0.352
4	2.93	29	0.955	54	0.345
5	2.72	30	0.920	55	0.321
6	2.53	31	0.880	56	0.305
7	2.39	32	0.850	57	0.287
8	2.25	33	0.820	58	0.273
9	2.11	34	0.795	59	0.257
10	2.02	35	0.770	60	- -
11	1.92	36	0.735	61	0.221
12	1.83	37	0.710	62	0.199
13	1.74	38	0.680	63	0.192
14	1.69	39	0.655	64	0.179
15	1.62	40	0.630	65	0.161
16	1.57	41	0.605	66	0.146
17	1.50	42	0.585	67	0.131
18	1.43	43	0.560	68	0.120
19	1.39	44	0.540	69	0.107
20	1.33	45	0.515	70	0.091
21	1.29	46	0.495	71	0.078
22	1.225	47	0.475	72	0.062
23	1.180	48	0.455	73	0.054
24	1.145	49	- -	74	0.053
25	1.105	50	0.415	75	0.029

Unit current strength = 3.60 ma.

Infinity used as the potential reference

TABLE E.3

HALF PLANE MARK II CIRCUIT MAGNITUDE RESPONSE (PROBE POSITIONS UNCORRECTED)

ω radians	Potential volts	Magnitude ohms	ω radians	Potential volts	Magnitude ohms
0	0.000	68.0	42	-0.915	27.2
2	+0.008	68.7	44	-0.890	27.8
4	+0.036	70.6	46	-0.840	29.2
6	+0.079	73.8	48	-0.770	31.4
8	+0.142	78.6	50	-0.695	33.8
10	+0.210	84.1	52	--	--
12	+0.281	90.4	54	-0.540	39.6
14	+0.333	95.2	56	-0.480	42.1
16	+0.400	101.9	58	-0.405	45.4
18	+0.420	103.9	60	--	--
20	+0.400	101.9	62	-0.276	51.6
22	+0.337	95.6	64	-0.215	54.8
24	+0.226	85.5	66	-0.160	58.0
26	+0.086	74.4	68	-0.105	61.3
28	-0.096	61.9	70	-0.052	64.6
30	-0.260	52.4	72	-0.002	66.8
32	-0.437	43.8	74	+0.037	70.7
34	-0.595	37.4	76	+0.101	75.4
36	-0.730	32.6	78	+0.141	78.5
38	-0.840	29.2			
40	-0.900	27.5			

Unit current strength = 3.60 ma. $K_1 = 2.288$

Origin used as reference potential

note:

$$\frac{V}{K_1} = \log \frac{|F(s)|}{|F(s_o)|} \qquad s_o = 0 \quad |F(0)| = 68.0 \text{ ohms}$$

$$|F(s)| = 68.0 \text{ antilog } \frac{V}{2.288}$$

TABLE E.4

HALF PLANE MARK II CIRCUIT MAGNITUDE RESPONSE (PROBE POSITIONS CORRECTED)

ω radians	Potential volts	Magnitude ohms	ω radians	Potential volts	Magnitude ohms
0	+0.000	68.0	42	-0.910	27.2
2	+0.009	68.7	44	-0.890	27.8
4	+0.033	70.5	46	-0.855	28.8
6	+0.072	73.2	48	-0.780	31.1
8	+0.123	77.2	50	-0.720	32.9
10	+0.184	82.0	52	-0.640	35.8
12	+0.248	87.4	54	-0.570	38.4
14	+0.293	91.6	56	-0.510	40.8
16	+0.350	96.9	58	-0.440	43.8
18	+0.361	97.9	60	--	--
20	+0.339	95.7	62	-0.315	49.6
22	+0.272	89.6	64	-0.256	52.6
24	+0.174	81.1	66	-0.200	55.7
26	+0.039	70.8	68	-0.149	58.6
28	-0.132	59.6	70	-0.097	61.8
30	-0.292	50.8	72	-0.049	64.8
32	-0.457	43.1	74	-0.031	66.0
34	-0.600	37.2	76	+0.058	72.2
36	-0.735	32.5	78	+0.099	75.3
38	-0.835	29.4			
40	-0.895	27.6			

Unit current strength = 3.60 ma. K_1 = 2.288

Origin used as the reference potential

TABLE E.5

HALF PLANE MARK II CIRCUIT TIME DELAY RESPONSE

ω	V	dØ/dω	ω	V	dØ/dω	ω	V	dØ/dω
radians	mvolts	msec.	radians	mvolts	msec.	radians	mvolts	msec.
0	+13.4	+21.9	24	-24.7	-40.4	48	+26.2	+42.8
1	+11.5	+18.8	25	-22.4	-36.6	49	+22.4	+36.6
2	+11.6	+18.9	26	-15.7	-25.7	50	+22.5	+36.8
3	+10.4	+17.0	27	-7.72	-12.6	51	+16.3	+26.6
4	+9.45	+15.5	28	-0.50	-0.82	52	+17.8	+29.1
5	+7.40	+12.1	29	-0.20	-0.33	53	+18.8	+30.7
6	+5.65	+9.24	30	+6.00	+9.81	54	+15.2	+24.9
7	+3.70	+6.05	31	+10.3	+16.8	55	+13.5	+22.0
8	0.00	0.00	32	+18.3	+29.9	56	+6.70	+11.0
9	-3.22	-5.26	33	+25.9	+42.4	57	+10.0	+16.3
10	-7.75	-12.7	34	+28.9	+47.2	58	+3.60	+5.89
11	-10.0	-16.3	35	+32.0	+52.3	59	+9.15	+15.0
12	-13.5	-22.0	36	+37.8	+61.8	60	+6.91	+11.3
13	-17.5	-28.6	37	+42.4	+69.4	61	+1.25	+2.04
14	-21.5	-35.2	38	+45.9	+75.0	62	+6.12	+10.0
15	-26.6	-43.5	39	+49.3	+80.6	63	+4.60	+7.52
16	-31.1	-50.8	40	+48.1	+78.6	64	+4.72	+7.72
17	-34.2	-55.9	41	+47.3	+77.4	65	+0.92	+1.50
18	-36.0	-58.9	42	+44.5	+72.7	66	+2.78	+4.55
19	-36.5	-59.7	43	+44.9	+73.4	67	+2.35	+3.84
20	-37.5	-61.3	44	+46.8	+76.5	68	--	--
21	-35.5	-58.0	45	+40.0	+65.4	69	+0.80	+1.31
22	-32.5	-53.1	46	+33.7	+53.5	70	+0.95	+1.55
23	-26.4	-43.2	47	+30.0	+49.0	71	+0.65	+1.06
						72	+1.08	+1.77

Unit current = 3.45 ma. K_1 = 2.22 ω= 1 cm. α= 0.635 cm.

$$\frac{d\emptyset}{d\omega} = \frac{2.303}{K_1} \Delta V \frac{\Delta \omega}{\Delta \alpha} = \frac{2.303}{0.635\, K_1} \Delta V$$

TABLE E.6

HALF PLANE MARK II CIRCUIT PHASE RESPONSE

ω radians	Area sq. in.	Phase degrees	ω radians	Area sq. in.	Phase degrees
0	0.00	0.00	36	-19.35	-22.8
2	+ 1.96	+ 2.32	38	-12.67	-15.0
4	+ 3.60	+ 4.25	40	- 4.94	- 4.18
6	+ 4.82	+ 5.70	42	+ 2.97	+ 3.51
8	+ 5.29	+ 6.25	44	+10.62	+12.6
10	+ 4.77	+ 5.64	46	+16.98	+20.1
12	+ 3.17	+ 3.75	48	+21.68	+25.6
14	+ 0.35	+ 0.42	50	+25.70	+30.4
16	- 3.87	- 4.45	52	+28.79	+34.0
18	- 9.23	-10.9	54	+31.30	+37.0
20	-15.14	-17.9	56	+33.34	+39.4
22	-20.71	-24.5	58	+34.94	+41.2
24	-25.31	-29.9	60	+36.18	+42.8
26	-28.53	-33.7	62	+37.14	+43.8
28	-30.11	-35.6	64	+37.82	+44.7
30	-29.97	-35.4	66	+38.24	+45.2
32	-28.19	-33.3	68	+38.46	+45.4
34	-24.55	-29.0			

The phase slope response was plotted on a large graph sheet using the following scales:

vertical $1'' = \frac{10 \times 10^{-3}}{0.804}$ seconds horizontal $1'' = 1\ 2/3$ radians $= \frac{180}{0.603\ \pi}$ degrees/sec.

The area under the curve was determined with a planimeter and the phase computed.

Thus $\phi = \frac{1.8}{0.804 \times 0.603\ \pi} \times$ area (sq. in.) (degrees)

TABLE E.7

CALIBRATION DATA FOR THE LOGARITHMICALLY TRANSFORMED PLANE

Distance cm.	Potential volts	Distance cm.	Potential volts
0	6.30	60	4.17
5	6.15	65	3.99
10	5.90	70	3.78
15	5.75	75	3.63
20	5.60	80	3.47
25	5.45	85	3.30
30	5.20	90	3.04
35	4.99	95	2.95
40	4.95	100	2.78
45	4.63	105	2.60
50	4.51	110	2.42
55	4.33	115	2.25
		120	2.08

Unit current = 3.45 ma. infinity reference

TABLE E.8

ANALOG RESULTS FOR THE MARK II CIRCUIT IMPEDANCE MAGNITUDE RESPONSE FROM THE LOGARITHMICALLY TRANSFORMED PLANE

ω radians	Distance cm.	Potential volts	Magnitude ohms	ω radians	Distance cm.	Potential volts	Magnitude ohms
1.00	0	+0.004	68.2	35.5	93	-0.620	34.2
1.47	10	+0.008	68.5	36.7	94	-0.700	31.3
2.15	20	+0.015	69.0	38.1	95	-0.760	29.3
3.16	30	+0.028	70.0	39.8	96	-0.810	27.7
4.15	40	+0.054	72.2	41.3	97	-0.830	27.1
6.81	50	+0.100	75.8	42.8	98	-0.835	26.9
10.0	60	+0.187	83.6	44.7	99	-0.810	27.7
12.1	65	+0.243	89.0	46.2	100	-0.775	28.8
14.7	70	+0.306	95.5	48.0	101	-0.735	30.1
15.2	71	+0.313	96.2	50.0	102	-0.680	32.0
15.8	72	+0.321	97.2	51.9	103	-0.620	34.2
16.5	73	+0.328	98.0	54.0	104	-0.565	36.3
17.1	74	+0.333	98.5	56.2	105	-0.500	39.1
17.8	75	+0.333	98.5	58.2	106	-0.445	41.5
18.5	76	+0.328	98.0	60.5	107	-0.389	44.2
19.1	77	+0.319	96.9	63.1	108	-0.327	47.3
19.9	78	+0.304	95.3	65.4	109	-0.267	50.5
20.8	79	+0.289	93.7	68.0	110	-0.215	53.5
21.5	80	+0.260	90.6	70.8	111	-0.156	57.1
22.4	81	+0.222	86.9	73.3	112	-0.102	60.7
23.3	82	+0.182	83.1	76.2	113	-0.057	63.8
24.1	83	+0.131	78.5	79.5	114	-0.002	67.8
25.1	84	+0.080	74.2	82.3	115	+0.057	72.2
26.1	85	+0.017	69.1	85.5	116	+0.104	76.2
27.0	86	-0.052	64.0	89.1	117	+0.158	81.0
28.2	87	-0.127	58.9	92.5	118	+0.208	85.5
29.2	88	-0.208	53.9	96.0	119	+0.252	90.0
30.3	89	-0.283	49.6	100.0	120	+0.294	94.1
31.6	90	-0.368	45.2				
32.7	91	-0.457	41.0				
34.0	92	-0.540	37.4				

Unit current = 3.45 ma.

K_1 = 2.08

Origin used as reference

TABLE E.9

DATA FOR MAPPING OF THE MARK II IMPEDANCE MAGNITUDE IN THE HALF PLANE

Unit current = 3.45 ma. Origin used as reference

ω rad.	Potential volts	Magnitude ohms	ω rad.	Potential volts	Magnitude ohms	ω rad.	Potential volts	Magnitude ohms
α=+70 nepers						α=-5 nepers		
0	+0.121	76.8	45	-0.398	45.8	0	-0.172	57.5
20	+0.128	77.0	50	-0.356	47.7	5	-0.068	64.0
40	+0.148	78.1	55	-0.278	51.2	10	+0.233	85.0
α=+50 nepers			60	-0.181	56.5	12	+0.388	99.5
0	+0.088	74.1	65	-0.083	62.2	15	+0.653	130.0
20	+0.079	73.5	70	+0.014	68.5	18	+0.813	160
40	+0.079	73.5	75	+0.111	75.8	20	+0.898	165
60	+0.143	77.9	α= 0 nepers			22	+0.763	144
α=+30 nepers			0	0.000	68.0	25	+0.398	101
0	+0.064	72.0	5	+0.051	71.5	27	+0.111	75.5
10	+0.052	71.2	10	+0.190	82.0	30	-0.330	49.3
20	+0.023	69.2	15	+0.335	94.0	35	-1.047	24.2
30	-0.016	67.0	17	+0.367	97.5	40	-1.537	14.8
40	-0.046	65.0	20	+0.349	95.5	45	-1.322	18.4
50	-0.030	66.0	25	+0.120	76.5	50	-0.942	26.8
60	+0.040	70.6	30	-0.266	52.0	55	-0.646	35.9
70	+0.128	77.0	35	-0.640	36.0	60	-0.420	44.7
α=+10 nepers			40	-0.860	29.0	70	-0.070	63.5
0	+0.078	73.5	45	-0.835	30.0	80	+0.150	78.5
5	+0.085	74.0	50	-0.675	35.0	α=-10 nepers		
10	+0.104	75.0	55	-0.500	41.8	0	-0.498	41.5
15	+0.105	75.1	60	-0.330	49.0	5	-0.329	49.0
20	+0.068	72.0	65	-0.179	57.0	10	+0.118	76.0
25	-0.029	66.0	70	-0.045	65.0	12	+0.365	97.0
30	-0.161	58.0	75	+0.078	73.5	15	+0.875	162
35	-0.292	50.8	80	+0.142	77.5	18	+1.80	404
40	-0.379	46.5				20	+2.99	1310

TABLE E.9 (CONTINUED)

ω	Potential	Magnitude	ω	Potential	Magnitude	ω	Potential	Magnitude
rad.	volts	ohms	rad.	volts	ohms	rad.	volts	ohms
22	+1.68	360	40	-1.79	11.6	5	-1.295	18.9
25	+0.660	131	42	-1.73	12.3	10	-0.705	33.8
27	+0.229	90.5	45	-1.40	17.0	15	-0.333	49.0
30	-0.348	48.1	50	-0.950	26.6	20	-0.162	58.0
32	-0.720	33.3	55	-0.635	36.5	25	-0.200	55.8
35	-1.330	18.2	60	-0.393	46.0	30	-0.381	46.5
37	-1.97	9.65	65	-0.198	56.0	35	-0.590	38.0
40	-3.69	1.76	75	+0.116	76.0	40	-0.710	33.7
42	-2.53	5.55	α=-20 nepers			45	-0.700	34.0
45	-1.69	12.8	0	-3.03	3.38	50	-0.580	38.2
50	-1.030	24.6	5	-1.350	17.9	55	-0.414	45.2
55	-0.680	34.5	10	-0.560	39.0	65	-0.101	61.4
60	-0.420	45.0	15	-0.052	64.0	75	+0.153	78.7
70	-0.050	64.5	18	+0.132	77.5	α=-40 nepers		
80	+0.161	79.2	20	+0.183	81.5	0	-0.580	38.2
α=-15 nepers			22	+0.158	79.5	10	-0.463	43.2
0	-1.165	21.5	25	+0.017	69.0	20	-0.321	49.2
5	-0.810	30.5	30	-0.382	46.5	30	-0.270	52.0
10	-0.192	56.1	35	-0.800	30.7	40	-0.253	52.9
15	+0.462	92.0	37	-0.935	27.0	50	-0.165	57.9
18	+0.845	157	40	-1.050	24.0	60	-0.009	67.0
20	+0.960	176	42	-1.070	23.5	70	+0.151	78.8
22	+0.820	153	45	-1.000	25.3	α=-60 nepers		
25	+0.401	101	50	-0.770	31.8	0	-0.148	58.5
27	+0.093	74.5	55	-0.545	39.6	10	-0.130	59.6
30	-0.370	47.0	65	-0.160	58.0	20	-0.089	62.0
32	-0.680	34.5	75	+0.135	76.0	30	-0.032	65.8
35	-1.140	22.0	α=-25 nepers			40	+0.028	69.5
37	-1.455	16.1	0	-1.88	10.6	50	+0.109	75.2
						α=-80 nepers		
			0	+0.117	76.0	5	+0.118	76.0
			10	+0.124	76.8	15	+0.132	77.0

BIBLIOGRAPHY

BIBLIOGRAPHY

(CH) Cherry, E.C., Electrolytic Tank Techniques, Proc. of the Symp. on Modern Network Synthesis, Polytechnic Inst. of Brooklyn, 1, 140, 1952.

(DA) Darlington, S., Potential Analogue Method of Network Synthesis, Bell System Tech. Journal, 30, 315, 1951.

(GU) Guillemin, E.A., The Mathematics of Circuit Analysis, Wiley, 1949.

(HU) Huggins, W.H., A Note on Frequency Transformations for Use with the Electrolytic Tank, Proc. IRE, 36, 421, 1948.

(SF) Stanford University, Electrical Eng. Tech. Memorandum PZM no. 12, c. 1950.

(SM) Smythe, W.R., Static and Dynamic Electricity, McGraw-Hill, p. 248, 1950.

(ST) Storer, J.E., Passive Network Synthesis, McGraw-Hill, 1957.

(VA) Van Valkenburg, M.E., Network Analysis, Prentice-Hall, 1955.

(WE) Weber, E., Electromagnetic Fields: Theory and Application, Vol. I: Mapping of Fields, Wiley, 1950.

ADDITIONAL REFERENCE MATERIAL

1. Boothroyd, A.R., Cherry, E.C., and Makar, R., An Electrolytic Tank for the Measurement of Steady-State Response and Allied Properties of Networks, IEE(1), 96, 163, May 1948.

2. Higgins, T.J., Electroanologic Methods, II App. Mech. Reviews, Feb. 1956, 49; Univ. of Wisc., Eng. Exp. Stn.; rep. no.270.

3. Tuttle, D.F., Network Synthesis, Vol. I, Wiley, 1958

note: With the aid of the last two references the bibliography may be extended to several hundreds of articles.